STUDIES ON REVERSION IN AGED ALLOYS

A Dissertation
submitted in partial fulfilment
of the requirements for the degree
of
MASTER OF ENGINEERING
in
METALLURGICAL ENGINEERING
(Physical Metallurgy)

By

S. K. SHARMA

DEPARTMENT OF METALLURGICAL ENGINEERING
UNIVERSITY OF ROORKEE
ROORKEE

August, 1972

C E R T I F I C A T E

Certified that the dissertation entitled "STUDIES ON REVERSION IN AGED ALLOYS", which is being submitted by Shri S. K. Sharma, in partial fulfilment for the award of the Degree of Master of Engineering in Metallurgical Engineering (Physical Metallurgy) of the University of Roorkee, Roorkee, is a record of his own work, carried out by him under my supervision and guidance, from 3rd January, 1972 to 8th August, 1972.

The matter embodied in this dissertation has not been submitted for the award of any other degree.

T. V. Rajan

[T. V. Rajan]
Reader
Department of Metallurgical Engg.,
University of Roorkee, Roorkee.

Roorkee.
Dated: August 12, 1972.

A C K N O W L E D G E M E N T S

I wish to express my deep sense of gratitude to Dr. T. V. Rajan, Reader in Department of Metallurgical Engineering, University of Roorkee, Roorkee , for his valuable guidance, inspiration and useful discussions during the course of this work. Without his encouragement at every stage of the work, this thesis could not have been completed.

I am also very thankful to Dr. M. N. Saxena, Professor and Head, Department of Metallurgical Engineering , University of Roorkee for providing the necessary laboratory facilities. My thanks are also due to my friends and the laboratory staff who assisted me in my work.

S. K. Sharma.

[SUNIL KUMAR SHARMA]

A B S T R A C T

'The experimental investigations presented in this thesis were undertaken to study the effects of homogenization temperature, ageing temperature, pre-ageing time followed by step ageing and / or partial reversion of G.P. zones on reageing at temperatures in the vicinity of room temperature ($0^{\circ}C$ to $30^{\circ}C$), in Aluminium-4.17 at. per cent Zinc alloys by electrical resistivity studies. A comprehensive study was undertaken by choosing judicious combinations of the above factors, so that on the basis of findings reported in this thesis, there is possibility of a better understanding of the mechanism of pre-precipitation stages in Aluminium-Zinc alloys.'

C O N T E N T S

contd..

-:-

L I T E R A T U R E - S U R V E Y

1.1 INTRODUCTION

With the beginning of the twentieth century many new phenomenon came into existence. Alfred Wilm[1,2](1903-1911) discovered a new hardening process during his work on Duralumin. He found that this alloy can be hardened quite appreciably by quenching from temperatures below it's melting point and then allowing it to stay at room temperature. The hardness is not produced by quenching alone, but increases during the period of stay at room temperature, and thus the phenomenon got the name of age-hardening. Merica[3](1930) traced it's cause to precipitation of second phase with lapse of time out of the super-saturated solid solution and called it 'precipitation hardening'.

From a metallurgical point of view, it is nucleation and growth type of transformation in which atomic re-arrangement is involved mainly by the phenomenon of diffusion, resulting in the break down of the super-saturated solid solution. These changes in the structure and constitution of the alloy during ageing, results in changes in physical, particularly mechanical properties of the alloy.

The above phenomenon has widely been used to improve the properties of various ferrous and non-ferrous alloys. Thus it has been proved very helpful in development of super high

strength light alloys essential for various industrial purposes. After steel, Aluminium alloys are the most important materials used for structural purposes, through the use of the phenomenon of precipitation hardening.

1.2 <u>HISTORICAL REVIEW</u>

As pointed out in the introduction, the earliest workers on age-hardening were Wilm[1,2] and Merica[3] who undertook detailed studies of the process.

To start with, it was assumed that the phase precipitating out from the supersaturated solid solution is the equilibrium phase. Hardening was associated with the formation of submicroscopic particles of equilibrium phase. However, resistometric studies of phase changes during precipitation, revealed an anomalous behaviour (4,5). If ageing involved simple precipitation of equilibrium phase, then there should be steady decrease in resistivity (ρ) with ageing. But it was observed that there is first an increase in ρ, followed by the expected decrease. This behaviour was explained by Gayler and Preston[6] on the basis of <u>two stage precipitation</u> process. The first stage being pre-precipitation of an intermediate or non-equilibrium phase, followed by the transformation of non-equilibrium

phase to the equilibrium phase. The internal changes in the lattice of super saturated alloy, resulted in age-hardening. Rosenhain[7] and Tammann[8] also postulated theories of two stage precipitation.

Merica[9] in 1932 suggested that the first step in precipitation is segregation of solute atoms on certain sites within solid solution and referred these regions as knots, which were associated with strain field around them, due to size difference (misfit) between the solute and the solvent atoms. Presence of such knots render the process of slip to be difficult leading to hardening. Experimental work of Jenkins and Bucknall[10] lent support to Merica's suggestions and the existence of clusters (11,12) was established at a later stage.

Application of small angle X-ray scattering (13,15) led to the discovery of zones by Guinier[16] and Preston[17], giving a major break through in the studies on ageing. It is now established (18,20) that difference between clusters and zones is only of nomenclature. The hardening mechanism associated with zones (21,23) has undergone considerable modifications from the one suggested by Merica.

With the establishment of non-equilibrium transition phase (e.g. θ' in Al-Cu alloys), the concept of coherency came into existence. Depending upon the nature of interface between

the precipitate and matrix, the precipitation is called coherent, semi-coherent or non-coherent i.e. whether all the lattice planes of the matrix and the precipitate are matching, only some are matching and the none is matching respectively. The matrix and the precipitate have different lattice constants, and hence a coherent precipitate is associated with coherency strains, resulting in hardening. Particles of non-equilibrium precipitate to start with, are fully coherent w.r.t. matrix. With growth, the elastic strain energy (24,25) associated with these increases, till a critical size is attained and coherency is lost, resulting in lowering of hardness. The credit of explaining the process of precipitation hardening including overageing goes to Mott and Nabarro[26] on the basis of coherency strains.

With this background the structural changes during ageing can be stated as follows:

Super saturated solid solution → clustering → formation of zones and their growth → precipitation of non-equilibrium transitional phase → transformation of non-equilibrium phase into equilibrium phase.

Actual number of steps involved varies from system to system, and depends on various factors, like the degree of supersaturation, which in turn depends on solute concentration. Also as ageing is by diffusional process involving solute atoms and

quench-in vacancies, the homogenisation temperature (T_H) and the ageing temperature (T_A) are most important factors governing the ageing process. Nature of interface between the matrix and the second phase is the most important parameter in controlling the structural properties of age-hardenable alloy.

1.3 PRESENT UNDERSTANDING OF THE PRECIPITATION PHENOMENON

1.3.1 Introduction

Precipitation of the stable equilibrium phase(s), out of the supersaturated solid solution, takes place in a number of intermediate steps, and their sequence is dependent on various ageing variables like the T_H, T_A, composition of alloy, and so on. The chemical free energy change, which is the driving force for precipitation depends on the degree of supersaturation and decreases as precipitation proceeds. Precipitation follows the path of minimum activational energy rather than maximum overall loss of free energy. As the primary mode of precipitation is by diffusion phenomenon, which amounts to simple interchange of atoms and excess quench-in vacancies, the factors influencing these like the T_H, quenching rate, T_A, solute concentration etc., govern the structure and sequence of precipitation. The effects of cold working, prior to ageing, reversion, step ageing, step quenching etc., can also

be satisfactorily explained on the process of annealing out of excess quench-in vacancies, diffusion of solute atoms, and the interactions between the vacancies and solute atoms.

In general the precipitation sequence can be classified into following steps, in increasing order of the activational energy:

(i) Clustering (Coherent) } Pre-precipitation
(ii) Zone formation. }

(iii) Formation of intermediate transitional phase.

(iv) Formation of non-coherent, equilibrium phase.

As the present study is mainly concerned with the earlier stages (Pre-precipitation) of ageing, we shall limit detailed discussions to clustering and zone formation only.

1.3.2 Clustering

The first stage in the process of precipitation invariably consists in the collection of solute atoms along certain preferential planes of the matrix, and as this takes place by the process of diffusion of solute atoms, the first aggregates of solute atoms are completely coherent with the matrix. The misfit, due to difference in the atomic sizes of solute and solvent atoms, must be accommodated by elastic strains to maintain coherency. Since all the f.c.c., metals have a minimum Young's Modulus along

<100>direction, the initial clusters in f.c.c., (Al) metals form as plates on {100} planes. This is also because Al. has anisotropic elasticity with $E_{\langle 100\rangle} = .99 \times 10^{12}$ dynes/cm^2 and $E_{\langle 111\rangle} = 1.14 \times 10^{12}$ dynes/cm^2.

There is low activational energy for clustering, and it is almost equal to the activational energy for migration of vacancies, and as the clustering process has no nucleation barrier, the process is of simple growth. Clusters may be formed on ageing, or possibly at T_H, or during the quenching.

The clusters constitute stable coherent regions having higher concentration of solute atoms. The elastic strains, due to difference in atomic sizes of solute and solvent, govern the form of these clusters. Nabarro[24] showed that elastic strain energy of the coherent cluster increases as it grows with time, and this energy can be reduced, due to anisotropy of elastic constants, thereby causing changes in the initial shape of clusters. Baker, Bradon and Nutting[27] explained that elastic strains in and around growing clusters may be relieved by aggregation of atoms and vacancies; atoms on most spacious planes and vacancies condense most easily on closed packed planes {111} in f.c.c., as maximum tensile strains occours in <100> direction in cubic metals.

(a) Nucleation of clusters

Turnbull[28] has shown that the kinitic law of clustering

is of the form;

$$\alpha_t = 1 - \left(\frac{1}{1 + bt} \right)^{1/3} \qquad .. \qquad (1)$$

where as, equation for sigmoidal growth i.e. nucleation of growth type of transformation is;

$$\alpha_t = 1 - \exp. (- b' t^n) \qquad .. \qquad (2)$$

Where, α_t = fraction of clustering process completed after time t

b = constant containing solute diffusion coefficient.

These are shown in Fig. C. Equation (1) shows, that there is no nucleation barrier for clustering, since the rate of clustering continuously decreases. Activational energy for clustering is low, and is equal to the activational energy for migration of solute atoms or single vacancies. Critical size of the nucleus for clustering is of the order of one atomic diameter.

(b) Growth and Kinetics of Clustering

With no nucleation barrier, the process consists of competitive growth of clusters, and then the rate of growth of a cluster is given by;

$$\frac{dr}{dt} \propto \frac{1}{r^n} \cdot \text{ where, } r \text{ is radius of cluster at time } t.$$

Abnormally high solute diffusion coefficient of solute in the solvent matrix during clustering was attributed to non-equilibrium concentration of vacancies in the quenched alloy.

The excess vacancy theory attributed to Zener[29] and Seitz[30] and developed by Federighi[31], De Sorbo, Treaftis and Turnbull[11] and recently by Herman[17] explains most of the facts concerning the kinitics of clustering, and also the effects of T_H, quenching rate, step quenching, coefficient of diffusion of solute atoms, reversion etc. The diffusion coefficient of solute (Zn) in Alluminium matrix is given by;

$$D_{Zn} = A \exp. - \left(\frac{E_F + E_M}{KT}\right)$$

where, E_F and E_M are activational energies for formation and migration of vacancies respectively.

K = boltzman's constant = 8.616×10^{-5} eV/°K.

A = another constant

Now, as diffusion is governed by a vacancy concentration which would be in equilibrium at T_H rather than T_A, and also to take into account the loss of vacancies to sinks during slow quenching, thus the retained vacancy concentration responding to some temperature value $T_{H'}$, lower to T_H, the modified equation becomes;

$$D_{Zn} = A \exp. (-E_M / KT_A) \exp. (-E_F / KT_H)$$

This equation predicts that clustering process has activational energy E_M, which is for the migration of vacancies. The second exponential of this equation is constant for the initial

stages of going but decreases as vacancies are annihilated at sinks.

Measured activational energies are slightly less than the $E_{\square}$ for pure Al, and this is explained in terms of binding energy between solute atoms and a vacancies E_{S-V}(32). Such a binding energy arises either due to elastic interaction (size factor) or electrical interaction (valency factor).

Excess vacancy theory predicts that the rate of clustering should fall while the vacancy concentration falls from $(\exp. -\frac{E_F}{KT_H})$ to $\exp. (\frac{-E_F}{KT_A})$; the equilibrium value, as the excess vacancies are annihilated at surface, grain boundaries and other sinks.

Equilibrium is reached in ^{quenched}Al (33) in about 30 min. at room temperature, and we observe that diffusion coefficient decreases fast in a short time and then remains near constant, thus dividing the clustering process into initial <u>fast reaction</u> followed by <u>slow reaction</u> (Fig. C). Cause of slow reaction was traced by Hart(34) Turnbull(12) and Herman(117) suggesting that clusters and zones <u>trap vacancies</u> due to binding energy between solute and vacancies.

If clusters and zones do contain an appreciable volume fraction of vacancies, they might be relatively mobile and migrate amoeba like and grow by <u>absorbing smaller clusters</u> or single

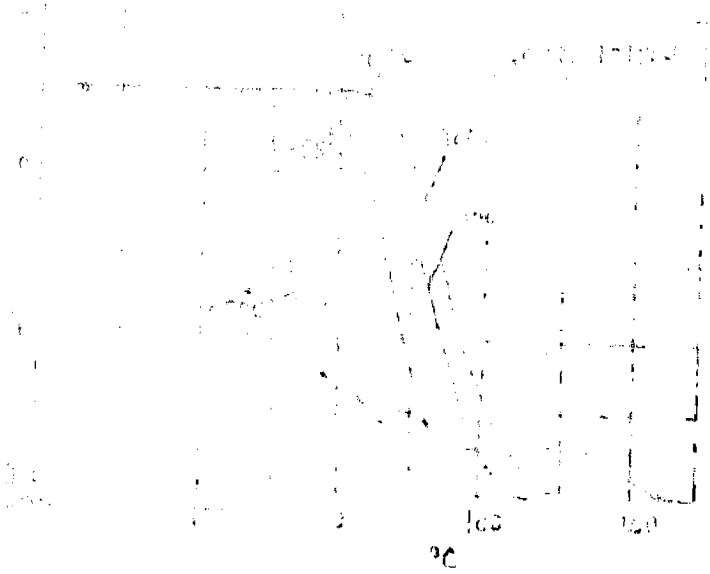

FIG. A - FRACTIONAL CHANGES IN P DURING ISOCHRONAL AGEING OF PURE Al QUENCHED FROM T_R AS INDICATED

STAGE I - 50 TO - 100°C
STAGE II 140 TO 220°C

(PENSARI FEDERIGHI [40])

FIG. B. ISOCHRONAL AGEING CURVES OF Al 10.2 wt% Zr IN THE RANGE - 80°C TO 200°C FROM T_R AS INDICATED

(PENSARI FEDERIGHI [40])

FIG. C. THE PERCENTAGE CHANGE IN ρ IN Al. 1.9% Cu ALLAY AGED AT 20°C SHOWING FAST & SLOW REACTION. DESORMO ATEL (71)

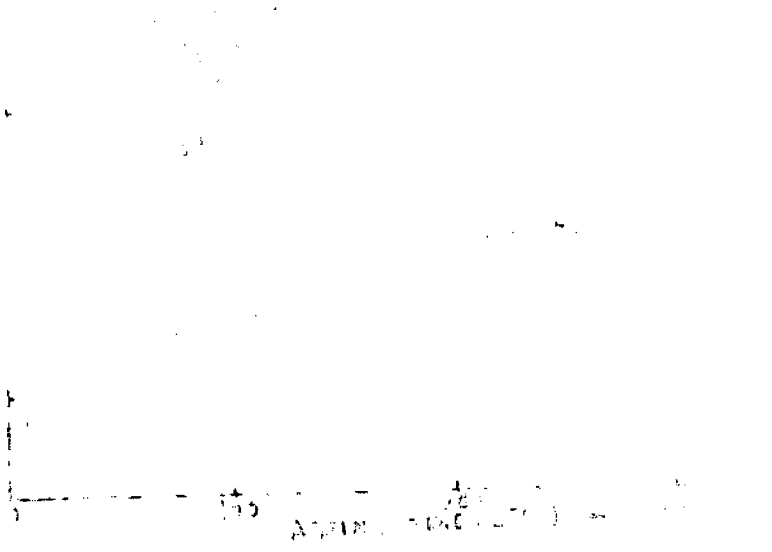

FIG. D. THE ρ CHANGES IN Al. 4 01 At% Zn AGED AT 0°C FROM T_R AS INDICATED

(PERRY [81])

FIG. E. THE ρ CHANGES IN Al 6.0Wt% Zn AGED AT 30°C FROM T_R AS INDICATED

(KAMCHANDRAN & SHRI NIWASAN [98])

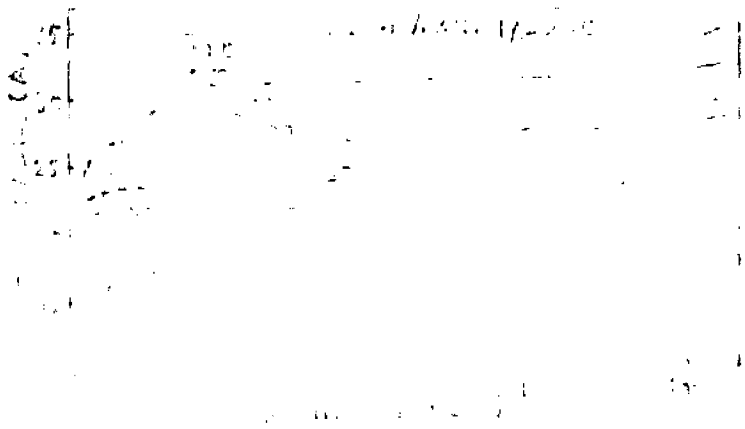

FIG. F. ZONE RADIUS AS A FUNCTION OF AGEING TIME AT ROOM TEMPERATUR FOR Al 6.8% Zn QUENCHED FROM T_R AS INDICATED

(GEROLD & SCHEWEIZIER [30])

solute atoms.

The migrational activation energy would approximate to the sum of vacancy migration activation energy and the binding energy between the vacancy and the cluster.

Federighi and Thomas[35] modified Hart's mechanism, whereby zones remain static but act as controlled emitters and absorbers of vacancies. The zones are characterised by a binding energy with vacancies. If this is small (e.g. Al - Ag, Al - Zn), the zones are poor sinks of vacancies, and there should be no slow reaction. If the binding energy is large (Al - Cu, Al-Mg-Si), the zones contain a high concentration of vacancies and slow reaction is predominant. The nature of interaction between solute and vacancy governs the ageing process by Vacancy-trap mechanism.

1.3.3 Zone formation and their growth

When the clusters attain a definite shape, they are termed as zones (20), and the difference between clusters and zones was only of nomenclature. Clustering, which is over in a short time, is followed by competitive growth of zones. Gerold and Schweizer[15,36] studied spherical zones in Al-Zn system by X-ray studies and found the radius of zones to be a function of T_H and alloy content (Fig. F). Initial rate of growth is very rapid(83), but after some time zone radius reaches almost a constant value, and these stages correspond to fast and slow reaction. Herman[117]

studied the dependence of the rate of zone growth on vacancies and found emperically;

$1 - X = \exp. - (t/\tau)^m$

Here, X = fraction of solute associated with zones at time t and is equal to $(C_o - C_t / C_o - C_f)$, C_o, C_t and C_f are concentration of solute in matrix initially, at time t, and finally.

In above equation, m is constant depending on geometry of diffusion field, and τ is relaxation time given by; $\tau = a N C_v \Gamma$, in which, N is number of growing zones and Γ is jump frequency. τ depends on sink for solute, and D_s which is given by; $D_s = d^2 C_v \Gamma$ where, d is jump distance.

Gerold and Schweizer[36] consider two models of the segregation process. Model I is a conventional distribution of precipitates in a super saturated matrix, where as Model 2 by Walker and Guinier[37] consists of clusters of solute atoms surrounded by a shell of denuded in solute with the matrix remaining supersaturated at the original composition of the alloy.

Gerold suggests that the degree of segregation is constant in model 1, whereas it should increase with ageing in model 2. Considering model 1 Gerold[36] calculated the concentration of solute inside the zones to be 69. pct. and that outside to be 1.8

per cent. He interprets these values in terms of metastability gap limits for G.P. zones at room temperature in Aluminium - Zinc alloys.

Considering the competitive growth theory, the initial rate of growth is determined by T_H, whilst the final zone radius is a function of the life time of vacancy. The maximum life time is usually obtained at some intermediate value of T_H, where the vacancy concentration is just insufficient to nucleate dislocation loops, and thereby reduce the diffusion distance of vacancies (Fig. E and F). The critical value of T_H seems to depend on quenching rate and alloy content.

The shape of the zones was determined by the atomic mismatch between the solute and the solvent atoms. Zones were found to be spherical if it was less than 3 pct. as in Al-Zn alloy and are disc like if it is greater than 3 pct. as in Al-Cu alloys.

Plastic deformation after quenching from low T_H causes an increase in the rate of zone growth but the final size is much smaller. The final structure of the alloy is largely determined by the initial stages of ageing.

1.3.4 Intermediate Precipitate

Usually the decomposition of supersaturated solid solution to equilibrium phase, takes place through one or more intermediate transition phases e.g. α' in Al-Zn and θ^* in Al-Cu system. These

phases are obtained by partial loss of coherency of usually larger zones with the matrix during ageing. Friedel[39] and Brooks[40] discovered condition for an initial coherent precipitate to become partially coherent and finally non-coherent as it grows, and according to them the precipitates become non-coherent when it is so large that the elastic strain energy due to difference in atomic volumes of matrix and precipitate becomes greater than the surface energy (γ). This criteria then predicts that a precipitate larger in radius, than $4\gamma / \delta^2 G$ will be non-coherent.

Taking $\gamma = 500$ ergs/cm^2 for a non-coherent interface, and $G = 4 \times 10^{11}$ dynes/cm^2, with $\delta = 10^{-2}$, then it predicts that precipitates larger in radius than 5000^0A will be non-coherent.

1.3.5 Equilibrium Precipitate

This is thermodynamically the most stable state which the structure ultimately attains after any ageing sequence. Thus the final microstructure constitutes the phases, predicted by the phase diagram, viz. the matrix and the second phase. The initial stages of ageing and other ageing variables, determine the morphology (size, shape and distribution) of the final structure. The appearance of intermediate phase is characterised by the peak in hardness while the appearance of equilibrium phase is characterised by a fall in hardness, thus getting the name overageing which

basically corresponds to the loss of coherency. The mode of equilibrium phase, depends on the secondary defects, usually non-coherent precipitate, appears as discontinuous and in inhomogeneous mode of precipitation.

1.3.6. The sequence of precipitation

As pointed out earlier (1.3.1) the ageing process consists of various stages. The precipitation follows initially the path of minimum activational energy rather than the maximum loss of free energy. Thus the G.P. zones are not the only precipitates formed inside the dashed line of metastable phase diagram; they are merely the most rapidly formed precipitate and subsequently they will dissolve in favour of a phase which has a lower free energy but a higher activational energy of formation.

The sequence theory by Guinier[41] argued that each stage of precipitation was associated with a definite precipitate type. According to this, the clusters develop into zones by a process of competitive growth. Some of the clusters grow to a critical size and get transformed into intermediate phase, which on further ageing is transformed to the equilibrium precipitate.

Most alloys precipitate at least one intermediate phase on ageing, and the precipitation sequence at any temperature is simply determined by the principle that the alloy decomposes

initially along the path of minimum activational energy, and the microstructure finally attains the structure predicted by the phase diagram, though the intermediate phases given by metastable phase diagram. Other ageing variables like T_H and T_A etc., may result in predominating or obscuring these successive stages.

1.3.7 Role of quench-in vacancies

Vacancy concentration 'C_V' (fraction of vacant lattice sites n, out of total sites n_o) at $T_H{}^oK$ is given by; $C_V = n / n_o = \exp.[- E_F / KT_H]$, which predicts a sharp rise in C_V with T_H, these vacancies are retained in solid solution on drastic quenching. The vacancies introduced by plastic deformation ($\sim 10^{-5}$ to 10^{-6}) are much less than that introduced by quenching ($\sim 10^{-4}$). In Al-5 pct. Zn, quenched to 20°C from 580°C and 540°C, the C_V values are~6 x 10^{-4} and~2 x 10^{-4} respectively. In a typical 1 pct. solute alloy, C_V in as quenched sample is 10^{-5}, with the ratio of solute to vacancy 10^3, thus most of the vacancies are associated with solute. In this alloy, which form zones, 10^{20} solute atoms in 1 Cu.cm. must be transported to 10^{18} zones by 10^{17} vacancies, thus each vacancy being effectively responsible for transport of at least 10^3 solute atoms in a very short time.

Emperically, vacancy decay law (117) is; $C_V = C_o \exp.-(\frac{b}{t})^n$, in which C_o and C_V are vacancy concentrations initially and at

time t, with n being number of jumps for vacancy annihilation, and b, a constant related to relaxation time. The C_V value decreased to 10^{-20} from 10^{-4} in about 30 minutes at room temperature in quenched Al. The average number of jumps n, made by a vacancy before annihilation (28) is given by;

$n = A' Z \varepsilon t \exp. (- E_M / KT_A)$,where, ε = Debye frequency, and A contains an entropy of activation and is of order 1 to 10, Z is co-ordination number of lattice and t is annealing time. They obtained, $n = 10^{10}$, indicating that vacancy sinks are approximately 5×10^{-3} cms. apart for a random walk. This indicates that not only surfaces and grain boundaries are the only sinks but dislocations introduced during quenching and formation of secondary defects like voids, vacancy clusters etc. are also effective sink of vacancies.

Pascari and Federighi(33) and others (96) studied annealing behaviour of pure Al.(Fig. A and B) and found that for T_H=470°C, the extra resistivity annealed out in one stage at room temperature with an activational energy 0.37 - 0.45 eV., and $n = 10^{-9}$-10^{10}; in good agreement with Bradshaw and Pearson(25). The process took less than 30 minutes showing the initial fast reaction followed by the slow reaction. The vacancies tending to cluster on closely packed atomic planes i.e. (111) in Al. For T_H=470°C, the annealing process took place in two stages. Stage I at room temperature,

with activational energy 0.58 eV., and $n = 10^4$, and stage II in range 140 to 200 °C with activational energy 1.3 eV. These results were interpreted in terms of clustering of vacancies by addition of single vacancies. Stage II is process of self diffusion as $E_D = 1.3$ eV. For low T_H, vacancy supersaturation is insufficient for large clusters to form and annealing is due to single vacancy and divacancies to sinks. Vacancy clusters should be unstable and might collapse to form dislocation loops. This is confirmed in pure quenched Al., which shows density of loops $\simeq 10^{15}/cm^3$, and C_V to be one in 10^4.

Turnbull et.al.[21] discussed clustering with the initial concentration of vacancies and the average life of vacancies. An equation is derived giving the number of atoms n, in the greatest cluster which could form during the vacancy decay period;

$n = C_S [C_V (T_H)]^{3/2}.(L_V/d)$. Here L_V is mean spacing for the vacancy sinks and d is atomic diameter. This equation gives, n = 10, for 1 pct. alloy quenched from 550°C and aged at room temperature; in agreement with Webb[43]. This also predicts that the cluster size will increase with increasing T_A, due to increase in L_V ; with smaller vacancy supersaturation. Turnbull[12] working on Al-Ag. deduced that final cluster size is limited for kinetic rather than thermodynamic reasons. There are limitations imposed on cluster size by, the C_V, life time of vacancies, and the diffusion coefficient which increases steadily during ageing.

Excess vacancy mechanism, is the most important one in explaining ageing processes. De Sorbo[11] studied effect of T_H, T_A, step quenching, step ageing, reversion etc., and gave explanations on the basis of role of vacancies. Step quenching gives time for vacancies to annihilate to sinks or form secondary defects and thus resulting in slow clustering. Reversion has even greater effect in reducing the rate of clustering. Turnbull[12] has shown that light cold working has little effect on rate of clustering on specimen rapidly quenched, but there is considerable effect, in enhancing, in specimen which are step quenched and then cold worked.

Addition of small concentration of solute atoms(1 pct.) increases the vacancy concentration (90) compared with pure Al. Thus the activational energy of formation of a vacancy 'E_F', is reduced, and solute atoms must increase the equilibrium concentration of vacancies at T_H. This is due to existence of binding-energy (32, 44, 45) between vacancy and solute atom , E_{S-V}. In pure Al., E_F = 0.76 eV., but in Al-Zn alloy it is 0.70 eV., thus giving E_{S-V} = 0.06 eV.(Ref.44).

Addition of large concentration of alloying element (1 to 10 pct.) generally decreases the number of vacancies which are absorbed on helices or dislocation loops. This is due to decrease in equilibrium number of vacancies at T_H, but it seems unlikely since

it would reverse the trend shown by dilute alloys. Vacancies are concluded to be the most important factor governing the various aspects of the ageing process.

1.3.8 General Conclusions on Precipitation Phenomenon

Conclusions concerning the structural changes during ageing are following:

i) Alloy decomposes during or immediately after quench, and there is formation of coherent clusters with simple growth.

ii) Clusters grow with diffusion controlled process of solute atoms and vacancies, until they attain a shape to be called zones. The shape of zone is dependent on misfit (δ) between solute and solvent atoms; being spherical if it is low, and disc or plates if it is high.

iii) Rate of growth of clusters and zones is determined by the motion of vacancies and solute atoms, which is governed by C_V and T_A.

iv) As the zones grow with ageing it is not possible to maintain coherency after attaining a critical size and thus development of transitional phase having partial coherency with the matrix.

v) Ultimately the non-coherent equilibrium phase is developed out of the transition phase.

vi) Sequence of precipitation can be described by a series of metastable phases in the phase diagram.

vii) The matrix-precipitate interface energy is probably the single parameter of greatest importance in controlling both the microstructural and mechanical properties of the alloy.

Conclusions concerning ageing variables are following:

i) Concentration of vacancies in an alloy at T_H, their distribution and annihilation controls the low temperature ageing. The T_H and quenching rate determine the quench-in vacancy concentration and the life time of vacancy is important in determining the final size of zones on prolonged ageing. There is an optimum T_H, giving fastest rate of precipitation and the maximum zone size is attained with largest vacancy concentration causing no nucleation of new vacancy sinks. Nature of secondary defects is also closely related to the role of vacancies.

ii) As pre-precipitation stages involve interchange of solute atoms and vacancies, which are diffusional processes, the T_A, is the other most important variable. Usually with high T_A, ageing is faster, but the maximum hardening is obtained at some critical ageing temperature.

iii) The ageing temperature determines the degree of supersaturation and is directly related to equilibrium number of zones with a critical size thermodynamically stable at this temperature.

iv) Effects of quenching rate, step-quenching, cold working prior to ageing and reversion etc. could be satisfactorily explained on the basis of excess vacancy annihilation mechanism.

v) Kinetics of different stages of ageing, is also dependent on the binding energy terms, such as, that between a vacancy and a vacancy E_{V-V}, between solute atom and vacancy E_{S-V}, and between a solute and a solute E_{S-S}.

vi) Effects due to other variables like the specimen size, concentration of solute etc., are also explainable in terms of C_V and their annihilation mechanism.

We conclude that there are many inter-dependent factors which govern the thermodynamics and the kinetics of ageing process. The nature of interface between the precipitate and the matrix, is most important in governing the mechanical properties, while the role of excess quench-in vacancies being the primary one in governing the structural and morphological changes(kinetics and sequence) during ageing.

1.4 Techniques Employed for Precipitation Studies

Changes in various physical and mechanical properties during ageing must correspond to some quite as definite changes in the structure and constitution of the alloy, conversely, they

can be employed for following the ageing process.

Hardness measurements and X-ray techniques with optical metallography were long before used for deducing precipitate structure and the process. Later on the electron diffraction and microscopic studies were used to reveal details about the pre-precipitation. These were of great advantage as they give information on the number, size, shape and distribution of precipitates. Whereas X-ray diffraction studies showed the existence of G.P. zones, the electrical resistivity measurements being very sensitive to the atomic rearrangement, helped in detection and studies of clusters. Small-angle X-ray diffraction techniques are best proved for the studies of crystal structure of individual particles. Thus the X-ray and electron diffraction studies with electrical resistivity studies are extensively employed for pre-precipitation stages, while the hardness and optical metallographic studies for later stages. Sometimes, other techniques such as yield stress, magnetic properties and calorimetric measurements are also found useful.

In the present study, which mainly deals with pre-precipitation stage, the electrical resistivity measurements were employed for following the ageing process.

1.5 Discussion on Resistometric Studies for Precipitation

1.5.1 Theory

The electrical resistivity (ρ) of a metal or single phase alloy (82,86,99) is a sensitive function of the total number and distribution of point defects, dislocations and solute atoms. The technique therefore offers a powerful method for studying decomposition during ageing, since resistivity changes can be attributed to clustering of solute atoms, which basically involves redistribution of solute atoms and vacancies. Introduction of solute atoms and structural defects in a solvent matrix increases resistivity. The resistivity of quenched pure Al., is greater than a well annealed sample by an amount, $\Delta\rho_o$, given by:

$\Delta\rho_o = A.\exp.[-E_F / K T_H]$. Where, E_F is the activational energy for formation of defect which is responsible for resistivity increase (this is of vacancy type), and a A is a constant, with K being Boltzman's constant.

In Al-Cu system, resistivity of a single vacancy and a cluster of one hundred vacancies has been found to be as 1.0 and 0.69 μohms cms/ atomic pct., of vacancies respectively, while the resistivity of an array of dislocation, density N lines/cm^2 is approximately 1.1×10^{-14} N-μohm cms. Therefore resistivity changes $\Delta\rho$. of the order of 10^{-2} μohms cms., are expected on annealing a pure metal after quenching or cold working.

Herman[117] pointed out that 'ρ' of an alloy containing spherical zones is sum of two terms:

a). Volume term (ρ_V):- This is a positive term and is a function of the volume fraction of zones (V_z), resistivity of precipitate (ρ_z), and the resistivity of matrix (ρ_M).

b). Surface term(ρ_S):- This is a negative term and is function of the integrated interfacial area between zone and matrix (A), and the scattering power per unit area of interface (K). Thus we have the following equation for resistivity, $\rho = \rho_V + \rho_S = \varphi(V_z, \rho_z, \rho_S) + K A$.

Contribution of spherical zones to 'ρ' was studied by Pensari and Federighi[44], taking unit volume, let $\Delta\rho_z(r)$ and $\Delta\rho_S$ to be the contribution of one zone of radius r, and that of an isolated solute atom to resistivity, the total contribution $\bar{\Delta\rho}$ of these two at any instant t, is given by;

$$\bar{\Delta\rho}(t) = N_S \Delta\rho_S + N_z[\Delta\rho_z(r) - \frac{16\pi n}{3}(r/a)^3 \Delta\rho_S].$$

Where N_z and N_S being number of zones and solute atoms respectively, with 'a' being the lattice parameter. Fraction of solutes inside zones (taken constant) is n. Since, $\Delta\rho_S . N_S$ is a constant, the experimental variation of $\Delta\rho$ is simply given by;

$\Delta\rho(t) = N[\Delta\rho_z(r) - \frac{16\pi n}{3}(r/a)^3 \Delta\rho_S] \equiv N.\varphi(r)$. Where, function $\varphi(r)$ is contribution of 'ρ', of a zone of radius r, computed for

depletion of matrix. The $\varphi(r)$, increases with r, till a critical value, $r_1 = 11^0A$ is reached and is zero for $r_2 = 39^0A$.

Resistivity increase during preprecipitation in (Al-Zn, Al-Ag) has been attributed by Mott[46] to critical scattering by very small zones and by Geisler[47] and Fine[48] to coherency strains and interface dislocations, respectively. There is good experimental evidence of Mott's theory, while cause of coherency strains was ruled out after studying Al-Zn and Al-Ag systems.

The rate of change and the total change of resistivity with usual peak behaviour observed during precipitation is extremely sensitive to the ageing variables viz. T_H, quenching rate, and T_A. The great advantage of electrical resistivity measurements is that continuous measurements are possible starting as soon as 5 seconds after quenching.

1.5.2 Resistivity increase and the ρ maximum.

As introduction of defects like the solute atoms, vacancies, dislocations etc., in the ordered solute matrix causes resistivity increase, it is expected that there is an overall increase in ρ, in the alloy, just after quenching, keeping in view that the concentration of solute atoms is much higher compared to the concentration of quench-in vacancies. The appearance of a peak in resistivity during pre-precipitation was treated by Labusch[49] who gave

the expression for resistivity as:

$\rho = 1/N\ e\ \mu = m^{\circ}/N\ e^{2}\ \tau$, where, N and m° are the concentration and the effective mass of the charge carrier whose charge is e. τ is relaxation time for scattering and μ is carrier mobility which is equal to $[e\ \tau\ /\ m^{\circ}]$.

Labush[c] showed, that τ passes through a minimum as solute clustering increases in size, and corresponding to this minimum in τ ,there is a maximum in ρ at the cluster size of $8^{\circ}A$. Thus with increasing clustering there is initial decrease in τ producing an increase in ρ , giving minimum τ for a wavelength of approximately $8^{\circ}A$, following the equation; $d\rho = -\rho.(d\tau / \tau.)$ Hence scattering efficiency was largest for this size of clusters.

It has been proposed (44) that, ρ maximum.,corresponds to a definite state in the alloy, which is independent of T_H and T_A. Thus the <u>position and amplitude</u> of resistivity maximum can be used to make important deductions about the structure of alloy. According to them the maximum change in resistivity ($\Delta\rho_{Max.}$) in Al-10 wt. pct. Zn. alloy is given by, $\Delta\rho_{Max.} = 388\ [1 - 61.2\ \exp.\ (-0.13\ /\ K\ T_A)]$.

There are three <u>theories concerning the nature of resistivity maximum</u>, due to Mott[46], Geisler[47] and Fine[48] respectively.

Mott suggested that maximum occurred,when the cluster size reached a critical value, equal to the wavelength of conduction

electrons, to produce strongest scattering. Labusch predicted this to be 8°A, and Matyes[50] as 7°A which was also confirmed by Herman and Cohen[20]. This was further confirmed by Pensari and Pedrighi[44], and was found to be 10°A for Al-5.3 atomic pct., Zn alloy.

Geisler's suggestion explaining, ρ maximum, in terms of coherency strains occurring during G.P. zones stage was ruled out after studies on Al-Zn and Al-Ag., system.

Fine suggested the 'ρ' increase due to the presence of a large number of dislocations around G.P. zones. But again resistivity peaks in Al-Zn where the misfit with the matrix is low, led to rejection of this theory.

1.5.3 Conclusions from resistivity studies.

The resistivity changes ($\Delta\rho$) in the quenched alloy during ageing is the sum of following effects;

a). An increase caused by growth of G.P.zones. Since maximum in 'ρ' occurs in alloys where zones are spheres(117), plates (11 and 12) and needles (51), it is logical to suppose that Mott's theory is most plausible giving a maximum in 'ρ' at a critical zone size, signifying strongest scattering.

b). A decrease due to fall of solute concentration in the matrix. Factors (a) and (b) are interdependent.

c). A decrease arising from the annihilation of excess quenching vacancies at sinks.

d). Possibly a decrease in resistivity from the association of vacancies (di-vacancies and voids) and solute atoms.

e). Rate of resistivity increase is controlled by the rate of clustering and zone growth, and shows initial fast and slow reactions. But as zone growth is diffusion controlled, the rate of ρ increase also becomes dependent on T_A.

f). The height of resistivity peak is proportional to the number of zones.

g). Resistivity peak corresponds to a definite structure during ageing and is independent of T_H and T_A, hence its position and amplitude can be used to deduce important deductions like the evaluation of E_p, E_M, and the kinitics of structural changes during pre-precipitation.

We conclude that, $\rho_{maximum}$, is not yet completely understood, but there is evidence to show that it corresponds to a definite state of structure of the alloy.

1.6 Aluminium-Zinc System

Extensive studies on ageing in this system have been done by many workers (69, 80, 87, 91, 93, 105, 116). We have evidence of following sequence of precipitation in Al-12 and 15 atomic pct., Zn samples aged at 175°C and 225°C by Simerska and Syneck[52].

Spherical G.P. zones → ellipsoidal G.P. zones → rhombohedral transition phase (R-phase) → α' cubic transition phase → Zn rich stable precipitate.

1)6 Spherical G.P. zones:- The early stages of precipitation consists of formation of Zn rich, coherent spherical G.P. zones, because of misfit between Al and Zn atoms being low (-1.9 pct.). The average size of zones progressively increases with ageing, while solute concentration, c_s, within the zones remains constant, and therefore the molar volume of the zones, remains constant during the growth of the zones. This leads to progressive increase of coherency strains. In an 9.4 pct. Zn alloy (53), with T_H=470°C, after ageing at room temperature for 8 days the zone diameter is approximately 50°A and the density of precipitates 5 x 10^{16} zones/cm³.

ii) Ellipsoidal G.P.zones:- Progressive increase in the coherency strains during the growth of spherical zones, results in the change of shape towards ellipsoidal ones for the larger zones. Simerska, found that the change of shape from spherical to

ellipsoidal,occurred if the zones exceeded the diameter of about 30°A. It has been reported (23) that in Al-Zn alloys surface energy between coherent boundary between zones and matrix is about 300 ergs/cm² and this value is exceeded by the elastic strain energy terms when zone reaches a diameter of approximately 30°A. It is suggested that the anisotropy of strain field around the spherical G.P.zones, changes their shape to ellipsoids, with their short axis parallel to <111> direction of matrix, and the distance between the closed packed planes (111) within the zones becomes smaller. This mechanism finally results in rhombohedral distortion of matrix, as will be discussed in the next stage.

iii) Rhombohedral Transition Phase(R-phase):- The development of R-phase on ageing the quenched Al-12.2 $\overset{at.}{\wedge}$ pct. Zn. samples at 150°C, was studied by Simerska and Syneck[52], and was also confirmed by Garf and Lenormand[54], while ageing this alloy at 275°C. They suggested the mechanism for the R-phase formation. Anisotropy of coherency strains around spherical G.P.zones, causing them to become ellipsoidal ones, with further ageing, leads to the contraction of spacing along one of the <111> direction inside the zones. This internal rhombohedral lattice deformation, combined with the loss of coherency of zones with α-matrix except in (111) habit plane leads to the development of transitional rhombohedral phase. This mechanism was also confirmed (55), on ageing 12 pct. Zn alloy

they observed that the lattice parameter of R-phase were; $a = 3.992^{\circ}A$ with $\alpha_R = 91^{\circ}36'$. He estimated it's Zn content to be about 63 atomic pct. from unit cell volume. The larger interatomic distance between the neighbouring atoms lying in the same atomic plane (111) was found to be $2.862^{\circ}A$, whereas a much shorter average distance of $2.783^{\circ}A$ exists between closest neighbours in two successive (111) atomic planes. The first of these distance is almost equal to the average inter-atomic distance in α-matrix, equal to $2.858^{\circ}A$, suggesting that at least a partial coherency of R-phase with the matrix in (111) plane maintains for a long time.

iv) <u>α-transition Phase</u>:- This phase is developed by breaking down of the partial coherency of the R-phase in the (111) habit plane also. Garwood[56] was first to detect this f.c.c., transition phase by X-ray techniques in Al-25 pct. Zn alloy aged at $200^{\circ}C$. The smaller unit cell of this transition phase compared to that of parent f.c.c., (α) phase indicated that it corresponds to α' conjugate solid solution. This Zn rich α' phase was also observed by Garf[57] and Geisler, Barett and Mehl[58] in Al-30 pct., alloys aged between 175-225°C. Literature shows that α' phase is f.c.c., with lattice parameter $a_0 = 3.985^{\circ}A$ (that of Al. is $4.04^{\circ}A$). For Al-9.4 pct., Zn with $T_H = 540^{\circ}C$, and ageing for 8 days at room temperature, followed by ageing at $100^{\circ}C$ for 1 day, small precipitates of α', parallel to {111} planes were detected. These α'

precipitates were about 25°A thick, and about 300°A in diameter, with density of precipitates being $10^{16}/cm^3$. The same specimen, if aged at 100°C for 5 days, shows weak streaks, which are slightly displaced from f.c.c. matrix spots in electron diffraction studies. The displacement was only 2 pct. in [111] direction perpendicular to the plane of precipitate phase and about 0.5 pct. in the direction in the plane. This was detected by Garwood(56) to be elastically distorted f.c.c. with a_o = 3.98°A, and was doubtless the intermediate α' phase showing granular appearance in optical micrographs. This α' is probably quite stable upto a thickness of 100°A, before leading to it's transformation to the equilibrium c.p.h. Zn precipitate. Although G.P.zones can be obtained even below room temperature , a temperature of 100°C or more is required for α'.

v) Equilibrium Precipitate(c.p.h.Zn):- The stable Zn rich precipitates are formed by continuous precipitation from α'-phase with their basal planes parallel to {111} planes of the matrix. [$\{111\}_{\alpha'}$ // $(0001)_{Zn}$]. Equilibrium precipitate is also found to be observed by discontinuous mode of precipitation at the defects and at grain boundaries in polycrystalline samples, predominantly at quite low temperatures.

The sequence and mechanism of precipitation in Al-Zn alloys can be concluded to be as following:

i) The early stage is the segregation of Zn atoms into

(a).

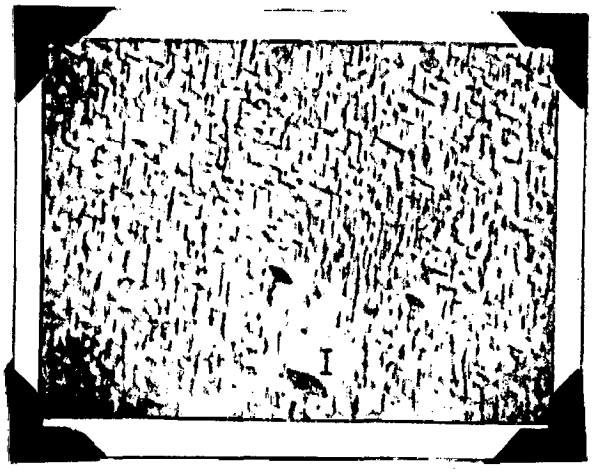

(b)

Micrographs of Al-9.4 pct. Zn alloys water quenched from 540°C and aged at room temperature (a) for one day and (b) for five days.
(Ref.44)

(c).

(d)

Micrographs of Al-25 pct. Zn alloys directly quenched to 200°C and aged
(c) for one hour and
(d) for four hours.
(Ref.111).

ophorical G.P. zones, coherent with α-matrix.

ii) Anisotropy of coherency strains around G.P. zones which increases with growing of zones, leads to the contraction of spacing along one of the <111> direction inside the zones, and thus rhombohedral deformation of lattice, resulting in the change of G.P. zones from spherical to ellipsoidal ones.

iii) The partial loss of coherency of the zones with the α-matrix except in {111} habit plane, leads to the development of transitional rhombohedral phase.

iv) The breaking down of the partial coherency of the R-phase in the (111) habit plane as well, leads to the development of known non-coherent transitional α'-phase.

v) The Zn stable precipitates, are formed by continuous precipitation from α'-phase, with epitaxial growth of hexagonal Zn precipitates, with their basal planes parallel to {111} planes of α-matrix. Also the discontinuous precipitation of Zn on grain boundaries and defects, was found in polycrystalline samples.

Here it is to be noted that the process is successive and that the intermediate phases are not nucleated independently, as has been observed in Al-Cu system.

1.7 Observations on resistometric studies on Al-Zn precipitation

Pansari and Pedorighi[44] made thorough investigation of clustering in Al-4.5 at. pct. Zn alloy. They found that the initial ρ, measured just after the quench was greater than the value expected for the super-saturated solid solution. Since the magnitude of discrepancy increases with increasing T_H, and decreased with increased quenching rate, the effect was attributed to clustering of Zn atoms during quenching. Other observations are:

i) On ageing, the ρ first increased and then decreased to some constant value, which was dependent on T_H.

ii) Time to reach maximum in ρ was less for higher T_H and T_A, as is expected because the clustering is caused by vacancy diffusion.

iii) The height of ρ maximum, was almost independent of T_H but strongly dependent on T_A, being high for low T_A.

iv) $\rho_{max.}$, occurred when mean zone diameter has attained a critical value (10^0A), which is independent of T_H or T_A.

v) The magnitude of resistivity maximum is then proportional to the number of zones, which is dependent on T_A.

vi) Initial number of zones depends on T_A and that the number remains constant with time or decreases with the same time law at different temperatures. But since there is no nucleation barrier for clustering this theory is not

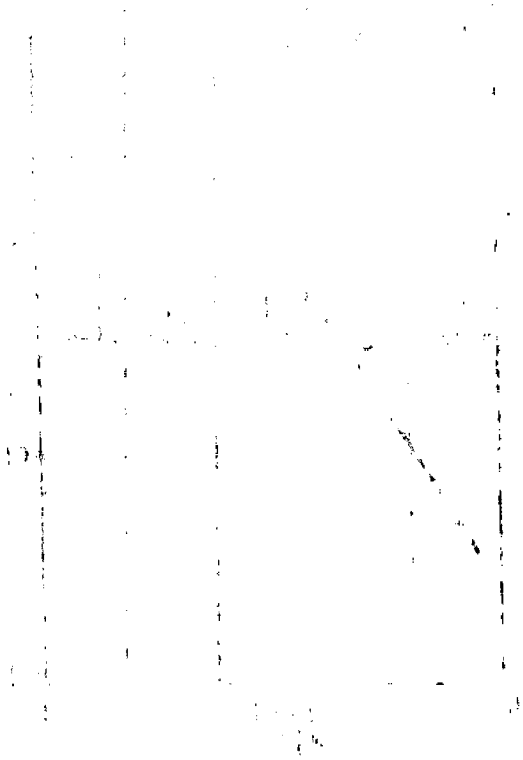

FIG. 6. SHOWING INITIAL INCREASE IN ρ WITH CUTTINGS & NO AGEING VERSUS T_H IN Al 10.2 Wt% Zn

(PENSARI & FEDERIGHI[44])

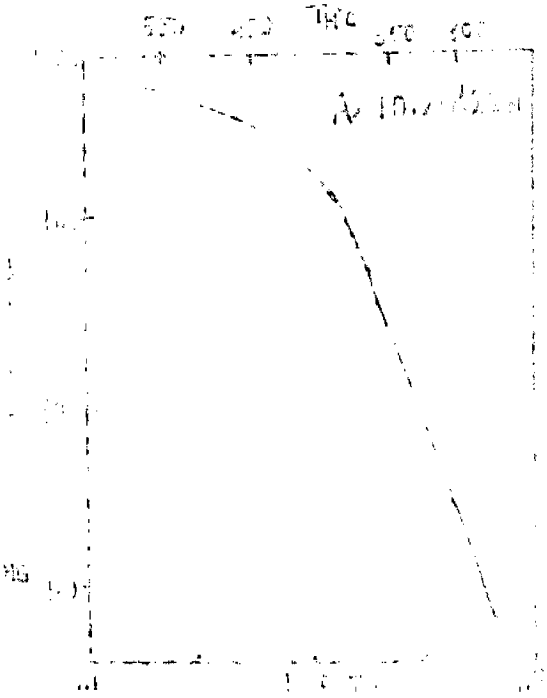

FIG. 8. INFLUENCE OF T_H ON TIME TO REACH PEAK IN RESISTIVITY IN Al 10.2 Wt% Zn

(PENSARI & FEDERIGHI[44])

FIG. 7. INFLUENCE OF T_H ON AGEING Al 10.2 Wt% Zn AT 20°C (MARKS INDICATE ρ CHANGES WITH CUTTINGS)

(PENSARI & FEDERIGHI[44])

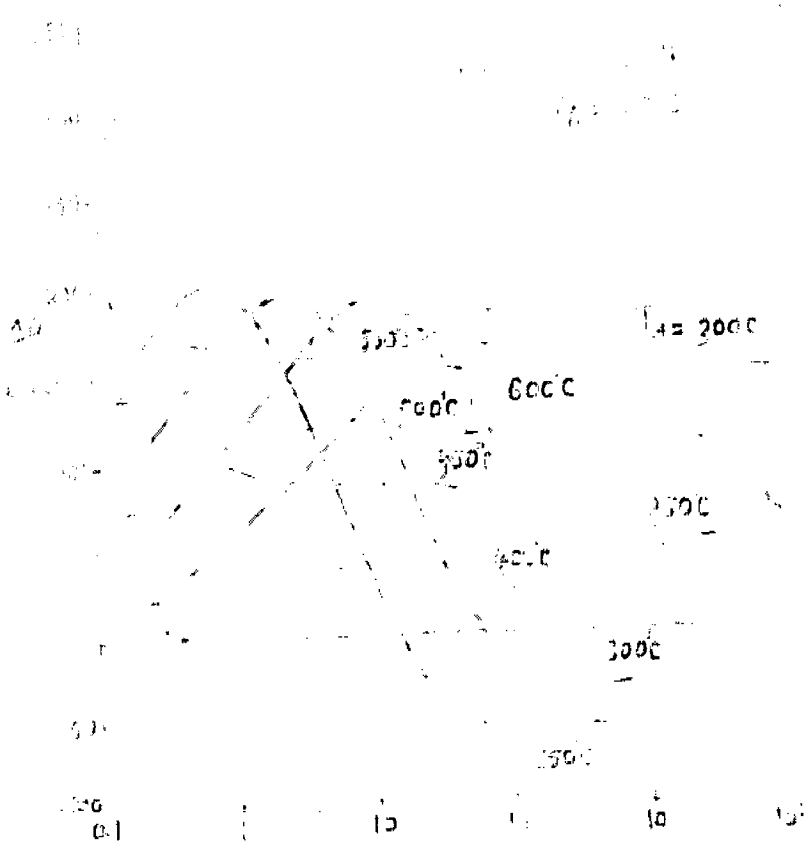

FIG J. RESISTIVITY CHANGES FOR INDICATED T_A VALUES IN Al - 4.5 At% Zn ALLAY AGED AT 44°C DASHES INDICATE ρ CHANGES WITH QUENCHING

(PENSARI & FEDERIGHI[41])

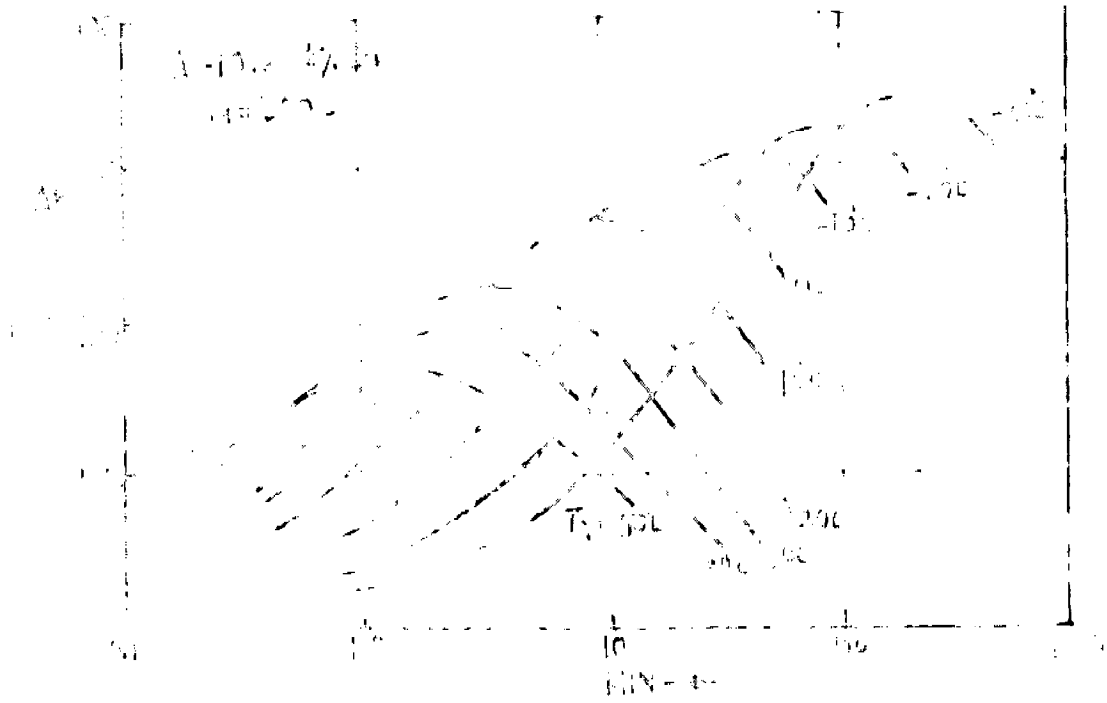

FIG. K. EFFECT OF AGEING TEMPERATURE ON Al. 12.2 Wt% Zn ALLAY HONOGRISED AT 300°C QUENCHED AND AGED.

plausible. The number of nuclii would then depend on the degree of supersaturation.

vii) Pensari and Federighi's results can be explained on the basis of Gerold's[58-60] theory, suggesting the dependence of the degree of segregation simply on the position of metastable miscibility gap, e.g. in Al-4.5%Zn, the phase boundary occurs at 180°C, whereas the solubility limit for G.P.zones is at 94°C, thus giving the equilibrium number of zones (Nz), zero at this temperature. The supersaturation of Zn, and hence the number of Zn atoms available for segregation will be small at temperatures in the range of 50 to 80°C, but will become larger at lower temperatures. Assuming the model of competitive growth for clustering and supposing that the ρ, is a function of the degree of segregation of the alloy, and hence the number of zones, we would expect the magnitude of resistivity maximum to be small at high T_A and large at low T_A. By simply changing the degree of segregation one is simply causing the clusters to grow or dissolve, and this explains the reversion treatments.

viii) On prolonged isothermal ageing, the final value was only dependent on the kinetics of clustering, and the largest zones were obtained at T_H = 350°C. This was explained in terms of concentration of vacancies and their life time.

1.8 Reversion and Metastable Phase Diagram(Al-Zn).

1.8.1 Metastable phase diagram

The whole sequence of precipitation during ageing can be described by a metastable phase diagram (Fig. M) showing the solvus line for the coherent (G.P.zones) and the non-coherent precipitates (transitional phases). The solvus line for zones and intermediate precipitate is always displaced towards lower temperature and higher solute concentration compared with equilibrium precipitate, because of the respective activational energy terms for these processes.

Metastable phase diagram can be used to explain formation of G.P. zones, intermediate precipitate and the phenomenon of reversion. Gerold[15,36] obtained solvus for G.P.zones by merely extrapolating the high temperature α-α' miscibility gap to lower region, with the limits being 1.8 and 69.0 atomic pct. Zn at room temperature. This view was confirmed by many others (39, 59-63). Dash and Fine[64] found no G.P.zones in 1.65 at.pct. Zn alloy aged at room temperature. Pensari and Federighi[44] and Garf[38] found, that zones were not stable in Al-4.5 at.pct.Zn alloy above 100°C (Gerold gave it to be 110°C). Borelius[66], Johnson[67] and Strongin[68] indicate the solvus for R-phase some 25°C below the monotectoid temperature (275°C) as shown in fig. M. They indicate that whereas G.P. zones can be formed at even below room temperature , a temperature of 100°C or more is required to obtain α'-phase.

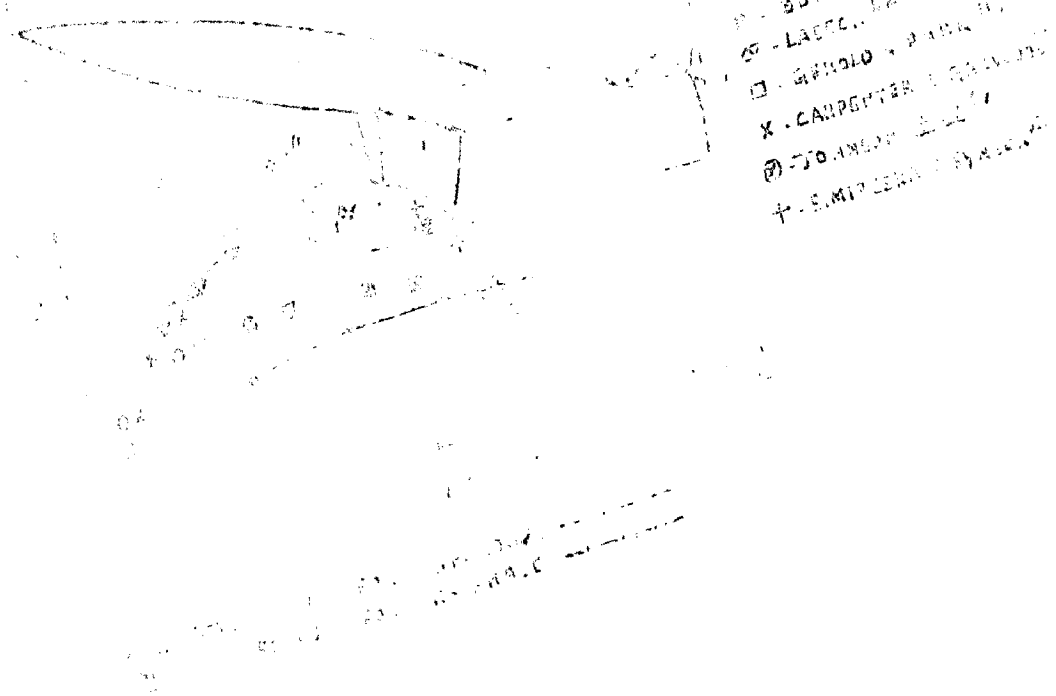

A study by Wahi and Anantharaman[69], on Al. 10-30 pct.Zn alloys also reveal the presence of R-phase on ageing in the range 200-310°C, and the appearance of R-phase was preceeded by a considerable fall in hardness. They also foundthat discontinuous precipitation at Grain Boundaries was major mode of decomposition in 10 and 20 at.pct.Zn alloys at and below 170°C. Sequential transformation of zones to equilibrium Zn, through intermediate precipitate was found to be negligible or absent in this temperature range. Calculation of Zn concentrations by Ellwood's[71] data for lattice parameter of Al-Zn alloy, in the matrix and transition phase, give rise to a second metastable miscibility gap, extended well into high temperature α-α' miscibility gap, hence suggesting two miscibility gaps in Al-Zn system.

First extending from lower temperatures to about 220°C representing metastable equilibrium between zones and the matrix, and is confirmed by other workers (36, 44, 67).

Second extending into high temperature α-α' miscibility gap, and represents metastable equilibrium between R-phase and the matrix. This was in partial agreement with conclusion of many other workers (61, 62, 72, 73).

The two loops overlap around 170-220°C, further complicating the precipitation in this range.

Metastable phase diagram gives clear explanation of

reversion, and determines the stability of transient precipitates.

1.8.2 Reversion (or Retrogression)

The phenomenon discovered by Gaylor[74] consists of the dissolution of the earlier formed, low temperature ageing products like the G.P.zones or intermediate phase, when the alloy is subjected to a reageing (reversion) treatment at higher temperature given by the solubility limits in the metastable phase diagram. Thus it may be further diversified as reversion of G.P.zones or reversion of intermediate phase, and a partial reversion treatment of any of these. Dehlinger and Knapp[75] were first to suggest that reversion was governed by the metastable phase diagram, and this has been confirmed by Silcock et.al[76]. Thus we can consider the reversion of G.P. zones and intermediate precipitate at the metastable phase boundary as completely analogous to the dissolution of the equilibrium phase at the solvus line. Reversion involve up-hill diffusion of solute from the zones to the matrix.

On re-heating alloys, which are quenched and aged to produce G.P.zones, some of the zones get dissolved in accordance with the G.P.zones solvus line, and the remaining zones grow further and are able to nucleate the transition phase in accordance with the metastable equilibrium line. In Gerold's view, the degree of segregation of an alloy containing clusters or zones is simply

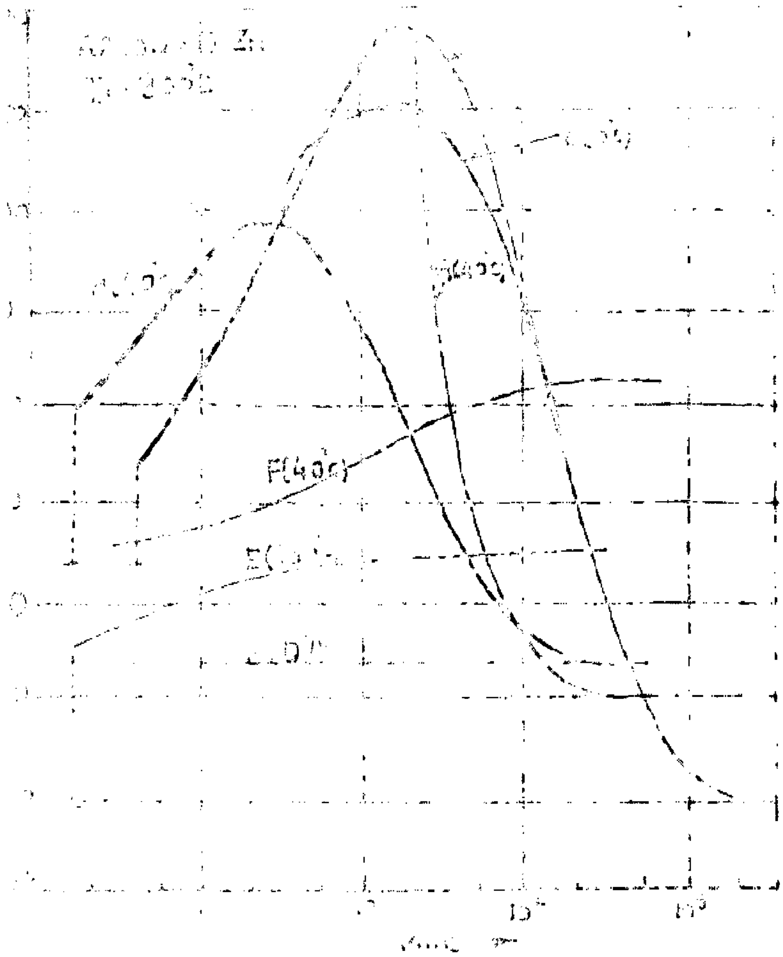

Fig. [illegible]
Curve A - [illegible]
[illegible]
[illegible] B - Ageing then continued at [illegible]
Curve [illegible] - New quench, aged at [illegible] till peak & then ageing at [illegible]
Curve D - Extended ageing at [illegible] T_H=300°C. Finally sample again aged at 40°C (curve [illegible])
Curve [illegible] - New quench, aged at 0°C to peak, then reageing [illegible] at 40°C.
For B, E [illegible] take 2590 [illegible] beginning of ageing.
(Pentam & Ferguson[37])

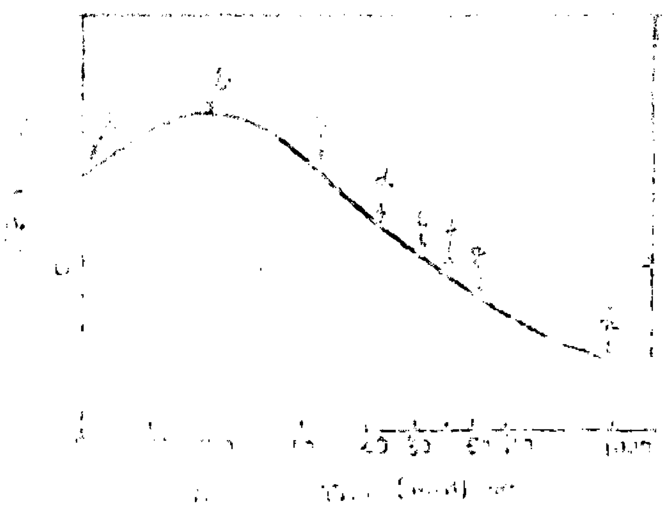

[illegible]

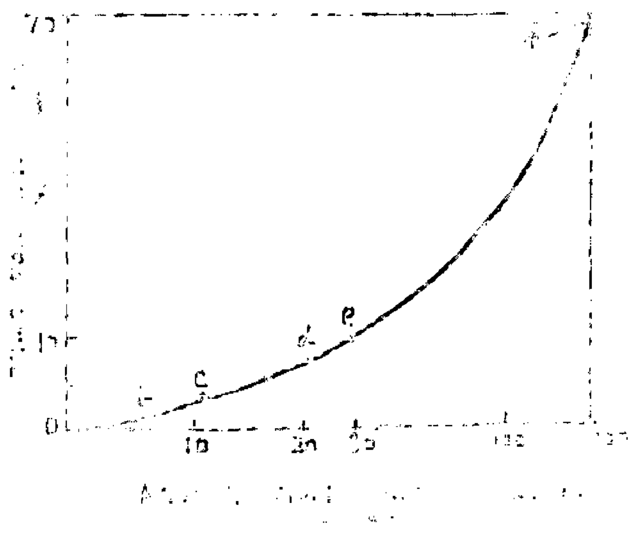

Fig. [illegible] [illegible] at 40°C, of [illegible] to point a, b, c, [illegible] in previous figure

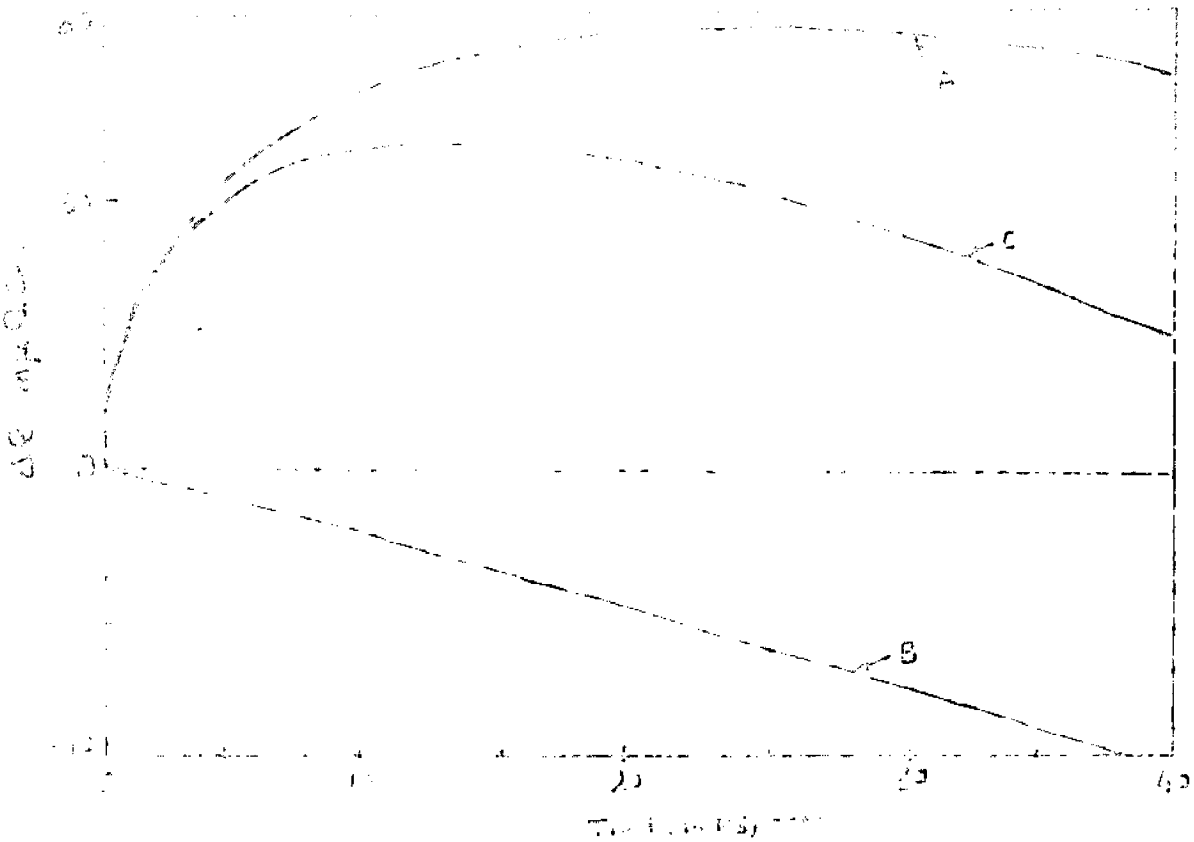
A
C
B

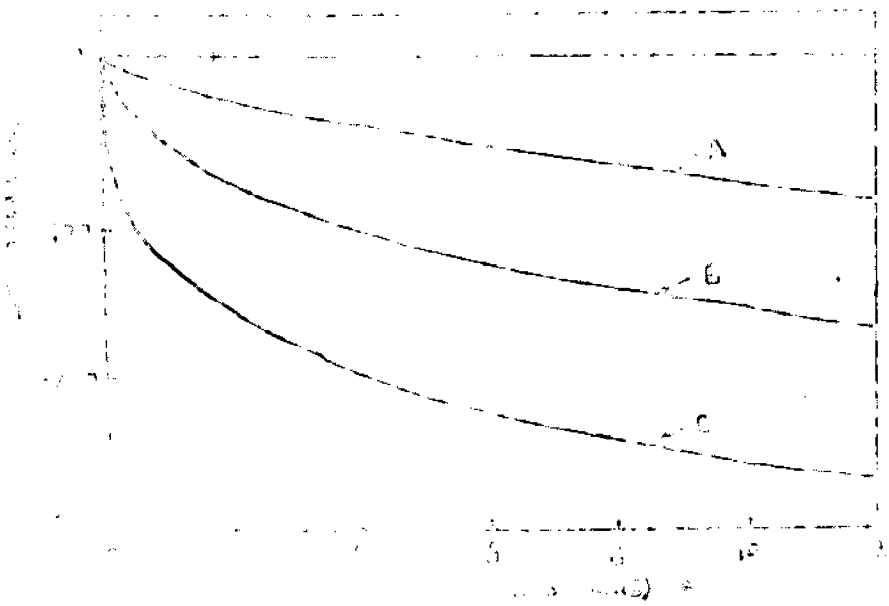
A
B
C

determined by the position of metastable solubility line. The number of zones is dependent on T_A. While simply changing the T_A, above or below the solvus line for G.P.zones, one is simply causing the zones to dissolve or grow. There is a critical size of zones[77] which is dependent on T_A; the zones smaller than this dissolve, while others grow at this reversion treatment. This study could be termed as partial reversion of zones. The minimum reversion temperature, is that given by the metastable solvus for that phase.

In Garf's[78] view true reversion is that in which the low temperature precipitate should not act as nucleus for more stable phase. This would allow simultaneous precipitation of a new phase and dissolution of the intermediate phase, and hence the true reverted state. The process of reversion involves sufficient time to allow the loss of a high concentration of vacancies, and the process of reversion is very slow.

Reversion techniques were originally employed by Beton et.al. to determine G.P.zone solvus for Al-Cu, and has been, since then, applied by many for the determination of metastable phase boundaries. Reversion studies also help in better understanding of the mechanism of various stages of precipitation, involving the formation and dissolution of the phase under consideration.

EXPERIMENTAL

PROCEDURE

the wire specimen were quenched to water at room temperature. Many such specimen were kept in stock to be used for the reageing studies after necessary heat treatments. Heat treatments were carried out in a vertical homogenization furnace with temperature controlled to $\pm$ 5°C. The homogenized specimen could be dropped out of this furnace through the removable bottom, into the quenching medium, kept directly below the furnace. From here the specimen was quickly transferred for resistivity measurements.

2.2 Resistivity Measurements

2.2.1 Description of Apparatus:- Potentiometric system was employed for following the resistivity changes in the wire specimen, during various ageing and reageing processes. The wire specimen and a standard resistance were connected in series, across an accumulator of 2.1 volts, with a variable resistor in the circuit. The specimen was kept in the ageing beaker, whose temperature was closely controlled through out the experiment by placing it in a bigger bath, fitted with a thermostat. A constant current of nearly 45mA. was made to flow through the circuit, and the potential drops across the wire specimen (E_X) and that across the standard resistance (R_S) was measured alternately by balancing this potential drop over a Vernier Portable Potentiometer(Model V-1, Toshniwal). The range of 18 mV. for the full scale deflection and with a least count of ·01 mV. was selected for this purpose.

2.1 Preparation of Alloy, and the Specimen

2.1.1 Melting and Casting:- The master alloy was prepared from high purity aluminium (99.99 %pure) and high purity zinc (99.9 %pure). Weighed quantities of Al. was melted in a graphite cruscible, placed in an electrical resistance,muffled furnace. Required amount of zinc (to account volatilisation losses,taken 10 pct. excess) wrapped in Al-foil was added to liquid aluminium and stirred. The molten alloy was homogenized for lo mins,before pouring into cylindrical cast iron molds of dia. 7/8" and length 6".

2.1.2 Hot forging and wire drawing:- The ingots were hot forged and hot drawn to long wires of 1 mm. diameter,thus removing the microinhomogenity and breaking down of the cast structure. Thereafter a stress relief treatment was given. Fine turnings of the alloy were used for composition estimations.

2.1.3 Specimen preparation for resistivity measurements:- To obtain uniform and smooth wires, they were cold drawn through a fine orifice of a steel die of diameter 0.70 mm. A 55 cms. length of this uniform wire was cut out, and marks were made at 50 cms. length, leaving 2.5 cms. on each end, for clamping. This wire was wound in the form of a coil to be used as specimen for resistivity measurements.

2.1.4 Heat treatment:- All wire specimen were given an initial homogenization treatment at 400°C, for 15 hrs. After this treatment

the wire specimen were quenched to water at room temperature. Many such specimen were kept in stock to be used for the reageing studies after necessary heat treatments. Heat treatments were carried out in a vertical homogenization furnace with temperature controlled to $\pm$ 5°C. The homogenized specimen could be dropped out of this furnace through the removable bottom, into the quenching medium, kept directly below the furnace. From here the specimen was quickly transferred for resistivity measurements.

2.2 Resistivity Measurements

2.2.1 Description of Apparatus:- Potentiometric system was employed for following the resistivity changes in the wire specimen, during various ageing and reageing processes. The wire specimen and a standard resistance were connected in series, across an accumulator of 2.1 volts, with a variable resistor in the circuit. The specimen was kept in the ageing beaker, whose temperature was closely controlled through out the experiment by placing it in a bigger bath, fitted with a thermostat. A constant current of nearly 45mA. was made to flow through the circuit, and the potential drops across the wire specimen (E_X) and that across the standard resistance (R_S) was measured alternately by balancing this potential drop over a Vernier Portable Potentiometer(Model V-1, Toshniwal). The range of 18 mV. for the full scale deflection and with a least count of ·01 mV. was selected for this purpose.

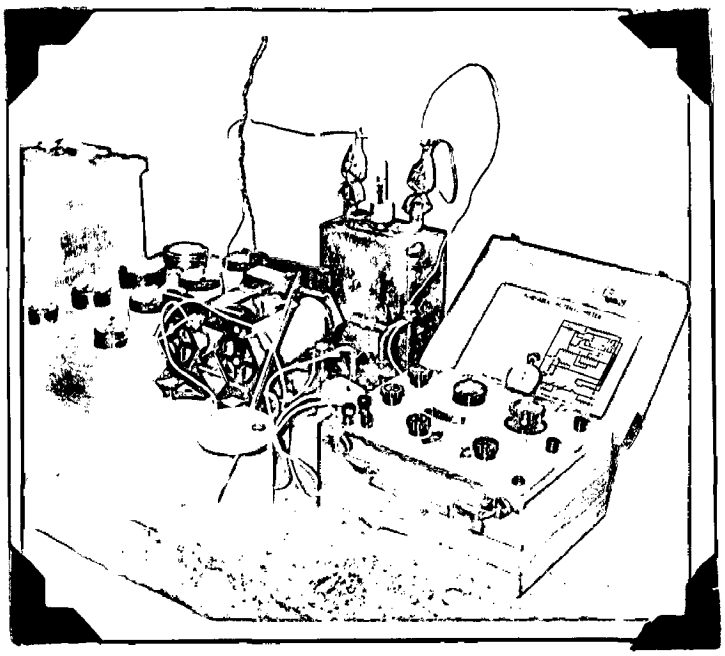

The lapse of time during ageing and reversion process was measured by a sensitive stop watch.

2.2.2 Calculation of Resistance (R_X) and Resistivity(ρ_w):- If the potential drop at any instant during ageing, across the wire specimen be E_X and that across the standard resistance be E_S, when the same constant current flows through both of them, then the resistance of the wire specimen (R_X) can be obtained by :

$$R_X = E_X \cdot R_S / E_S \text{ ohms.}$$

And the resistivity (ρ_X) of the wire of length L cms. and radius r cms. can be obtained by another equation given below :

$$\rho_X = R_X \cdot \pi \cdot r^2/L \text{ ohms. cms.}$$

In our case L = 50 cms. and r = ·035 cms.

2.2.3 Mathematical Extrapolation of initial quench resistivity:-

On the findings of Borelius[79], and De Sorbo et.al.[11], the rate of change of resistance R; (dR / dt) during the clustering and zone formation follows the following relation :

$$dR / dt = 1 / (a + bt) \qquad .. \qquad 1.$$

This is analogous to an equation of a straight line in dt/dR and t, with intercept 'a' and slope 'b'. Parameter 1/a is dR/dt at t=0., and is assumed to be proportional to the initial rate of zone growth. Values of 1/a were deduced from the value of R and t measured during isothermal ageing as follows; $(\Delta t / \Delta R)$, the

quotient of time increase and resistance increment between successive measurements, was set equal to $(dR/dt)^{-1}$. This gave data for a plot of $(dR/dt)^{-1}$ against t, and the values of the intercept 'a' and slope 'b' of the line that best fitted the experimental points was computed, using the method of least squares. R_o - the value of the resistance of the specimen immediately after quench was calculated by substituting the measured values of R and t in turn in the integrated form of equation (1).

$$R - R_o = 1/b \log (1 + bt/a). \qquad .. \qquad 2.$$

This gave a number of values of R_o equal to the number of measured values of R and the mean of all these values was quoted as R_o. With R_o known, the corresponding resistivity ρ_o, was calculated. A similar method was used by Perry[81].

2.2.4 Calculation of $\Delta\rho$ and the Thermal Coefficient of Electrical Resistivity ($\ddot{\alpha}$) of the alloy :- The change in resistivity ($\Delta\rho$) was obtained by the equation, $\Delta\rho = \rho_t(T) - \rho_o(T)$, where, $\rho_o(T)$ and $\rho_t(T)$ are resistivities just after quench and after ageing for time t at T^oC, respectively.

To account for slight changes in resistivity, due to temperature variations, the correction was employed according to the equation, $\rho_t(T) = \rho_t(0)\,[1 + \ddot{\alpha}T]$. The value of $\ddot{\alpha}$ was calculated from resistivity data at different temperatures of annealed samples.

2.3 Experimental scheme for the present study:- To obtain sufficient time for pre-precipitation processes in the selected Al-4.17 at. pct. Zn alloy, three low T_H values were selected. From each T_H value, after quenching to $T_Q{}^oC$, the ageing was carried out at various temperatures in the vicinity of room temperature as proposed in table I.

After ageing the specimen at T_A for different values of times called the pre-ageing time (t_{PA}) which are given by times required for a certain percentage of the maximum in resistivity change ($\%\,\Delta\rho_{Max.}$) to occur and then the specimen was immediately reaged for 30 mins. at a lower or higher temperature than T_A, thus constituting the process of stop ageing or partial reversion of zones respectively. Table II lists, the required pre-ageing times for different cases, employed in the present study.

Table III summarizes the different ageing and reageing operations employed in the present investigation. The figures in this table indicate the figure numbers given to denote different operations of reageing. These figure numbers were in a special code as interpreted below :

Nomenclature of Figures:- A special three digit code number was assigned to each figure obtained on reageing operation, according to scheme of Table III giving scheme for ageing and reageing temperature. If the figure number is e.g. Fig. X. YZ, then it is inter-

protod as follows:

i) First digit 'X' roprosonts tho T_H valuo which is oqual to 300°C, 350°C or 400°C for X = 1, 2 or 3 rospoctivoly.

ii) Socond digit i.o. 'Y' with a zoro placod aftor it, givos the tomporaturo of agoing (T_A) usod prior to any roagoing. Thus Y = 0,1,2 or 3 moans agoing at 0,10,20 or 30°C, rospoctivoly.

iii) Third digit i.o. 'Z' with a noro placod aftor it, givos the roagoing tomporaturo uood aftor agoing at T_A. Thus Z = 0,1,2 or 3 mean roaging at 0,10,20 or 30 dogroos contogrado, rospoctivoly.

It is ovidont that tho variouo roagoing procossos in the procont study can bo broadly clanoifiod into two catogorios.

(a) Stop Agoing:- Whon tho agoing tomporaturo was higher than the roagoing tomporaturo and in such a caso roagoing tomporaturo was donotod as T_{RA}. So wo havo the roquirod condition as $T_{RA} < T_A$, signifying $Y > Z$.

(b) Partial Rovorsion of Zonos:- When agoing tomporaturo was lowor than the roagoing tomporaturo, with roagoing tomporaturo donotod as T_R in this caso . So wo havo the roquirod condition as $T_R > T_A$, signifying $Y < Z$.

For a cortain roagingp procoss, the difforont valuos of roagoing timos as givon in Tablo II was rocordod on roopoctivo ourvos in the figuros as 20, 40, 60, 80, and 100 pot. valuos, rospoctivoly.

3.0 Results

The results of primary ageing as proposed in Table I, have been plotted in terms of resistivity changes ($\Delta\rho$) versus the ageing time, in figures 1.0, 2.0 and 3.0, corresponding to T_H = 300, 350 and 400 degree centegrade, respectively.

Table II gives the various pre-ageing times and the corresponding resistivity values, $\rho t(T_A)$, for various combinations of T_H and T_A. These values were used for different ageing and reageing operations in the present study.

The results of various reageing processes as proposed in Table III have been plotted in terms of changes in resistivity($\Delta\rho$) versus the reageing time on different figures, which has been classified into two categories (step ageing and partial reversion of zones) and are listed systematically in Table III giving the corresponding figure numbers, for these respective operations.

TABLE - I

T_H°C value	Value of Ageing temperature (T_A°C)				Corresponding figure number
300	0	10	20	30	1.0
350	0	10	20	30	2.0
400	0	10	20	30	3.0

TABLE - III

T_H°C	T_A°C	Reageing temperature (T_R or T_{RA})			
		0°C	10°C	20°C	30°C
300	0	-	1.01	1.02	1.03
	10	1.10	-	1.12	1.13
	20	1.20	1.21	-	1.23
	30	1.30	1.31	1.32	-
350	0	-	2.01	2.02	2.03
	10	2.10	-	2.12	2.13
	20	2.20	2.21	-	2.23
	30	2.30	2.31	2.32	-
400	0	-	3.01	3.02	3.03
	10	3.10	-	3.12	3.13
	20	3.20	3.21	-	3.23
	30	3.30	3.31	3.32	-

TABLE - II

T_A °C	% $\Delta\rho_{max}$	T_H °C					
		300°C		350°C		400°C	
		t_A	$\rho_t(T_A)$	t_A	$\rho_t(T_A)$	t_A	$\rho_t(T_A)$
0	0	0 -00	4.932	0 -00	4.972	0 -00	4.932
	20	4 -10	4.979	2 -08	5.012	4 -10	4.979
	40	8 -00	5.026	4 -00	5.052	8 -00	5.026
	60	12 -00	5.073	6 -12	5.092	12 -00	5.073
	80	15 -30	5.120	8 -30	5.132	15 -30	5.120
	100	25 -00	5.167	12 -00	5.172	25 -00	5.167
10	0	0 -00	4.920	0 -00	4.962	0 -00	4.920
	20	2 -10	4.963	1 -00	5.998	2 -10	4.963
	40	4 -40	5.006	2 -28	5.034	4 -40	5.006
	60	7 -30	5.049	3 -52	5.070	7 -30	5.049
	80	10 -25	5.092	5 -12	5.106	10 -25	5.092
	100	14 -00	5.135	7 -00	5.142	14 -00	5.135
20	0	0 -00	4.910	0 -00	4.952	0 -00	4.910
	20	1 -20	4.949	0 -32	4.984	1 -20	4.949
	40	3 -00	3.988	1 -20	5.016	3 -00	4.988
	60	4 -16	5.027	2 -12	5.048	4 -16	5.027
	80	6 -00	5.066	3 -16	5.080	6 -00	5.066
	100	9 -00	5.105	5 -00	5.112	9 -00	5.105
30	0	0 -00	4.900	0 -00	4.942	0 -00	4.900
	20	1 -00	4.935	0 -24	4.970	1 -00	4.935
	40	2 -08	4.970	0 -44	4.998	2 -08	4.970
	60	2 -48	5.005	1 -12	5.026	2 -48	5.005
	80	3 -36	5.040	1 -40	5.054	3 -36	5.040
	100	5 -30	5.075	2 -30	5.082	5 -30	5.075

Note: In this table, t_A, is the ageing time given as mins - seconds with, $\rho_t(T_A)$, being the corresponding resistivity value in μ -ohm-cms.

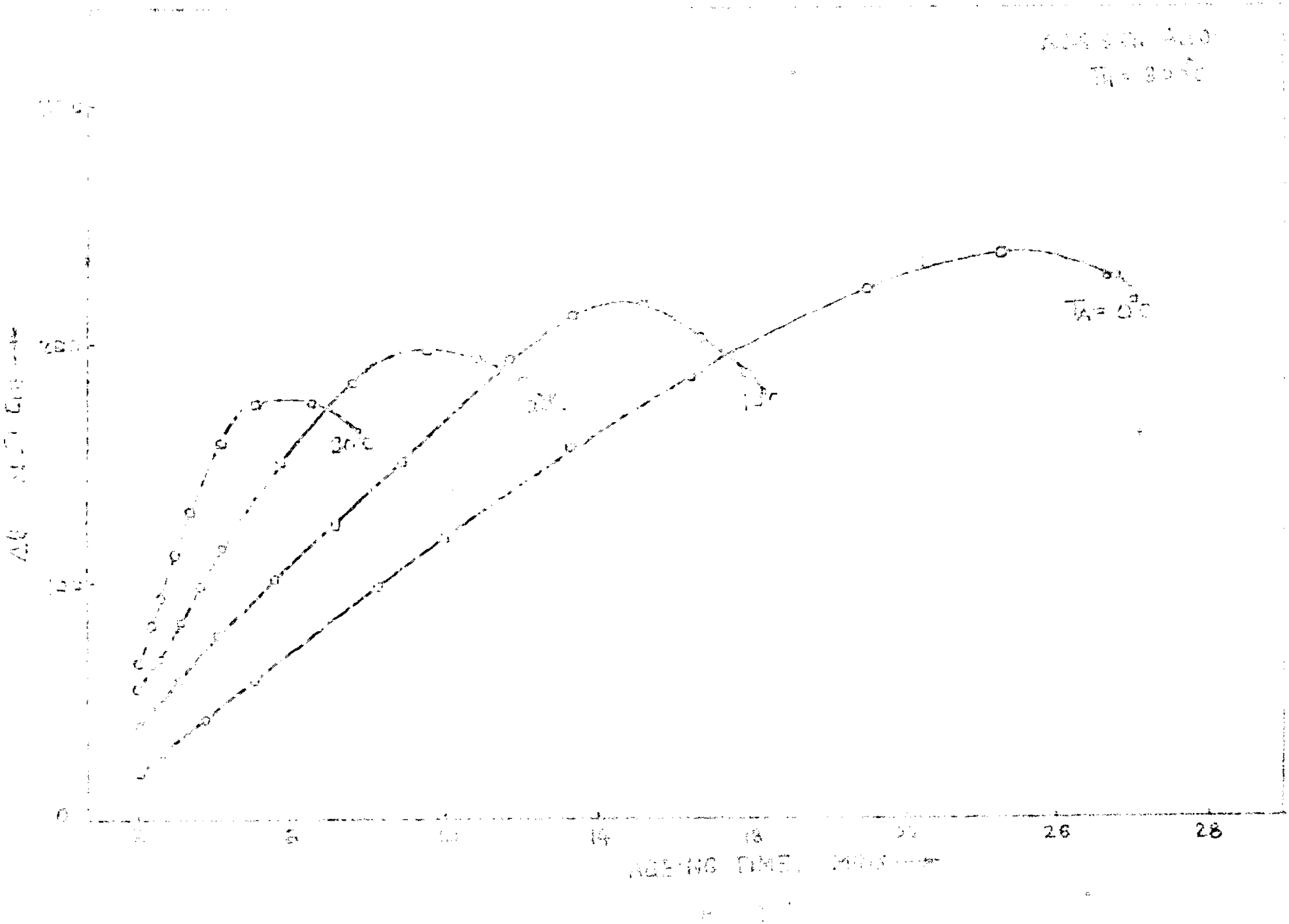
26
28
AGEING TIME,

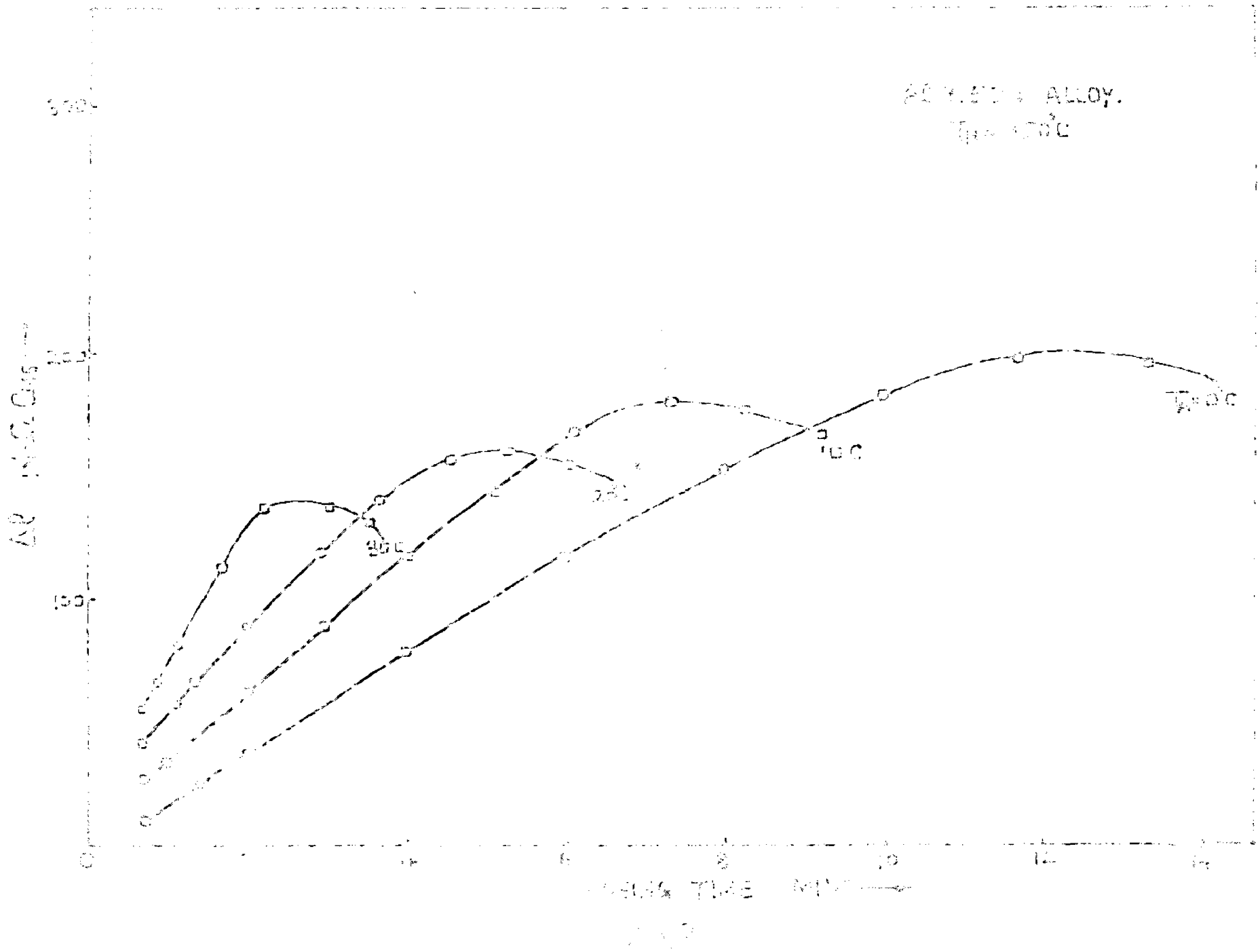
ALLOY.
400°C
450°C
500°C
550°C
TIME

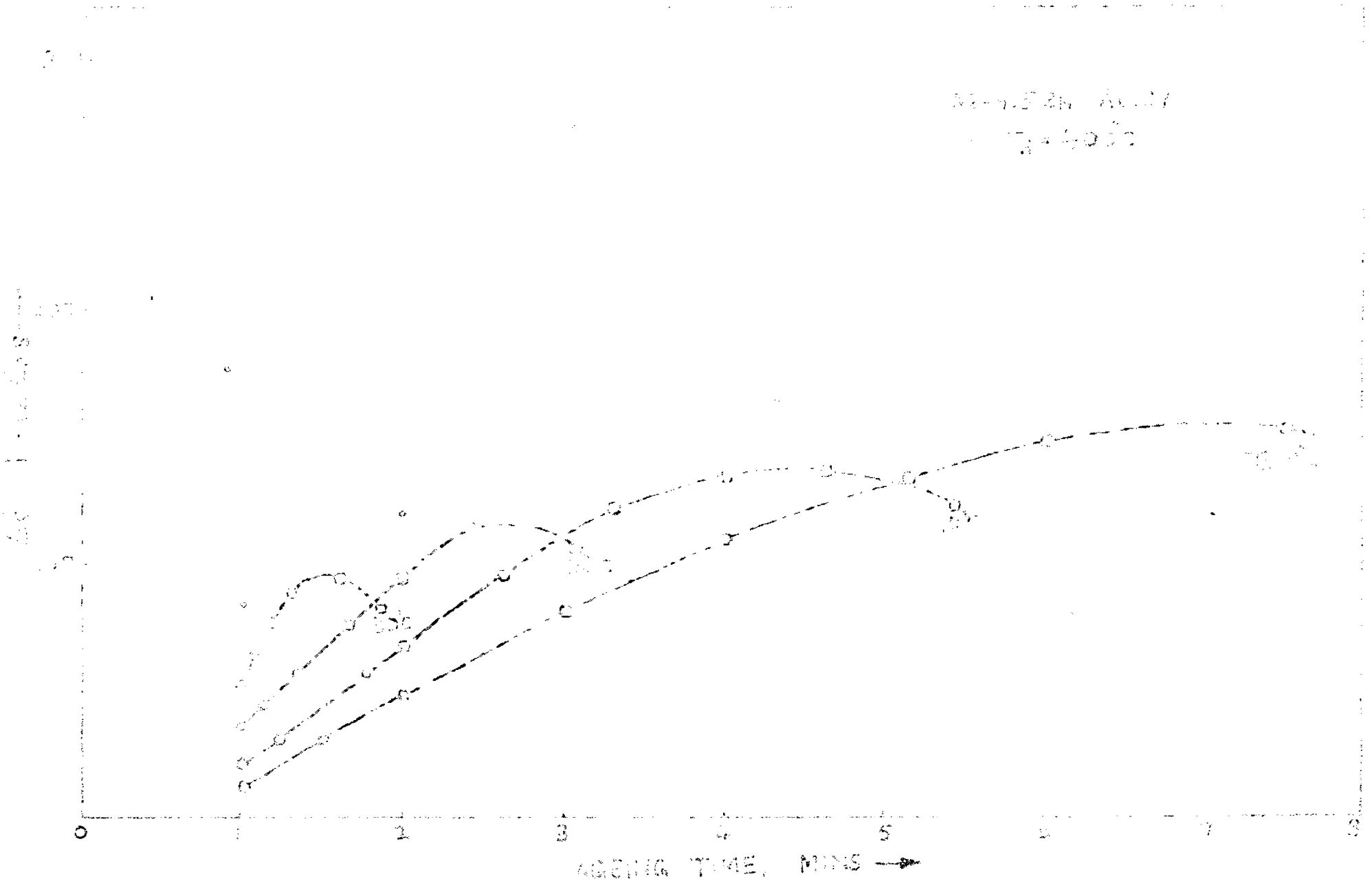

FIG. 3.9

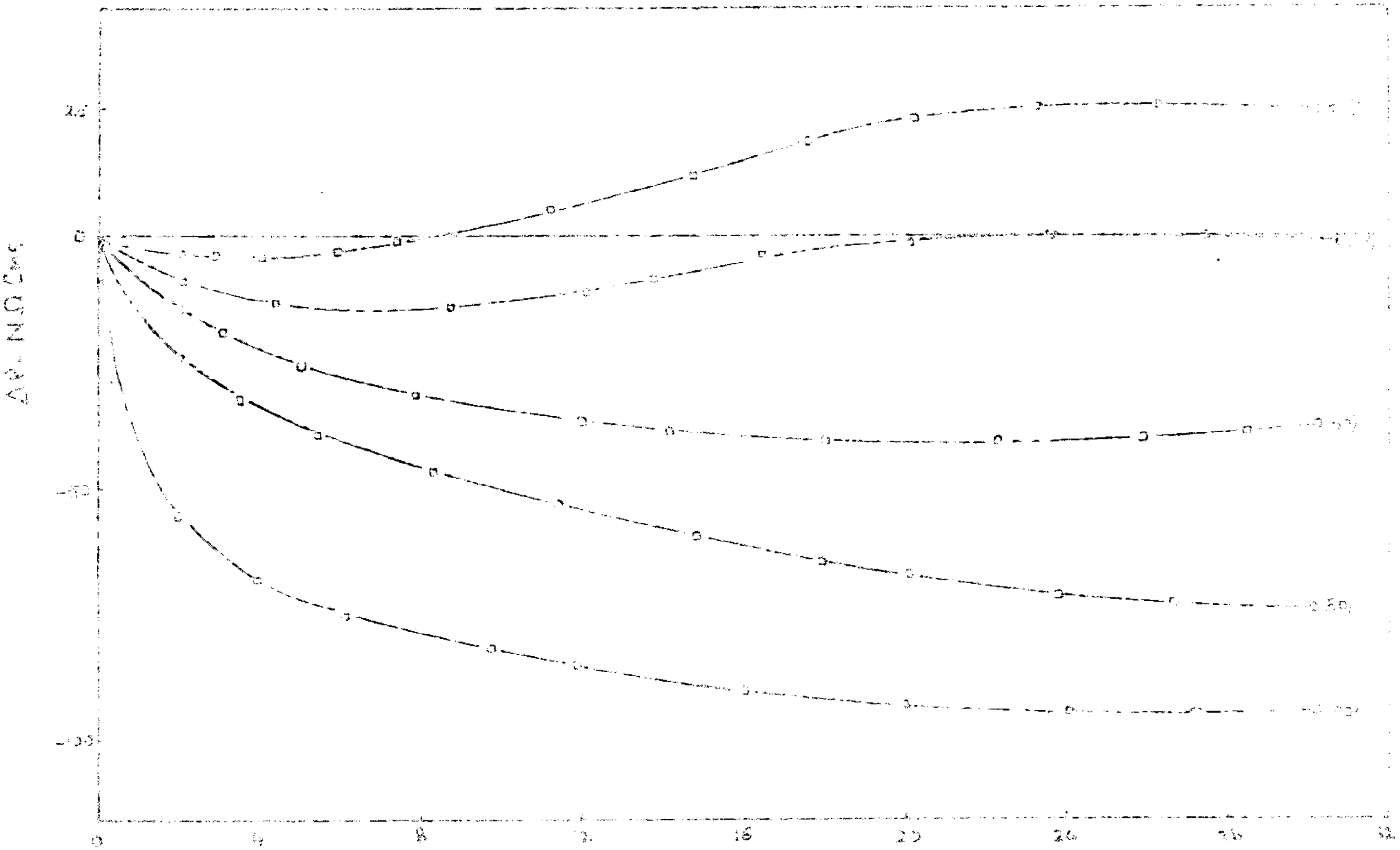

Fig.

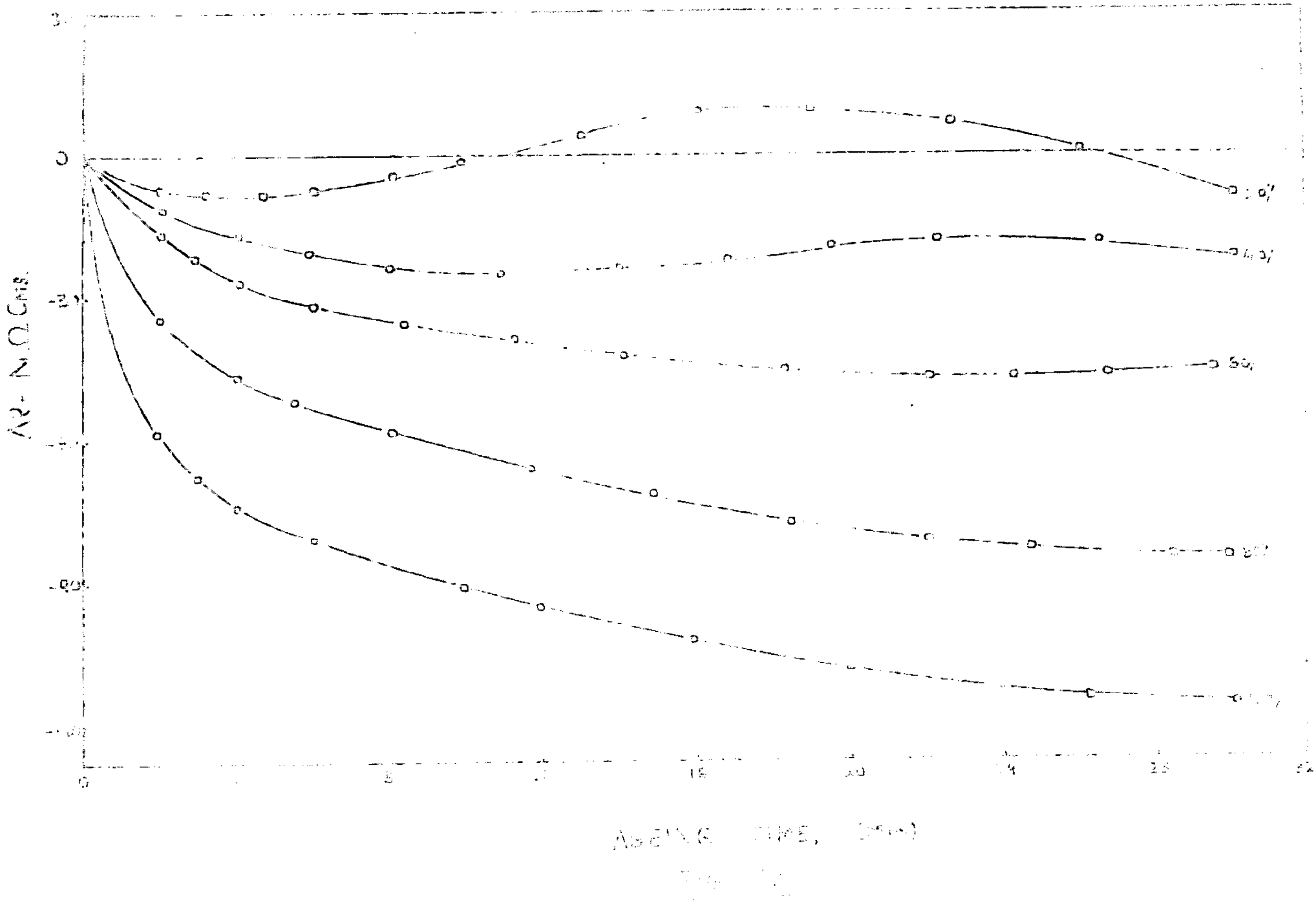
0
5
10
15
20
25
50%

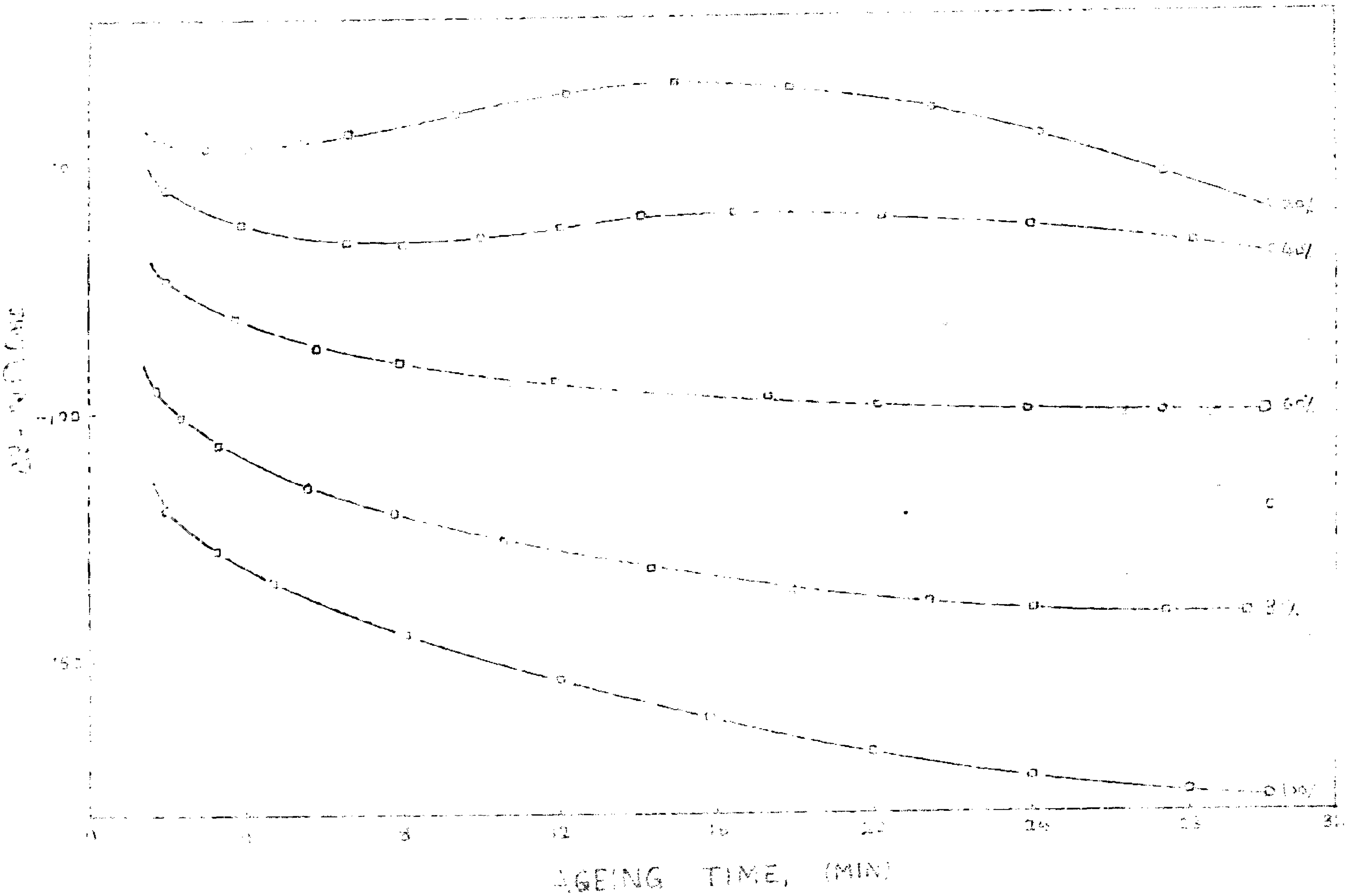

Fig 1.08

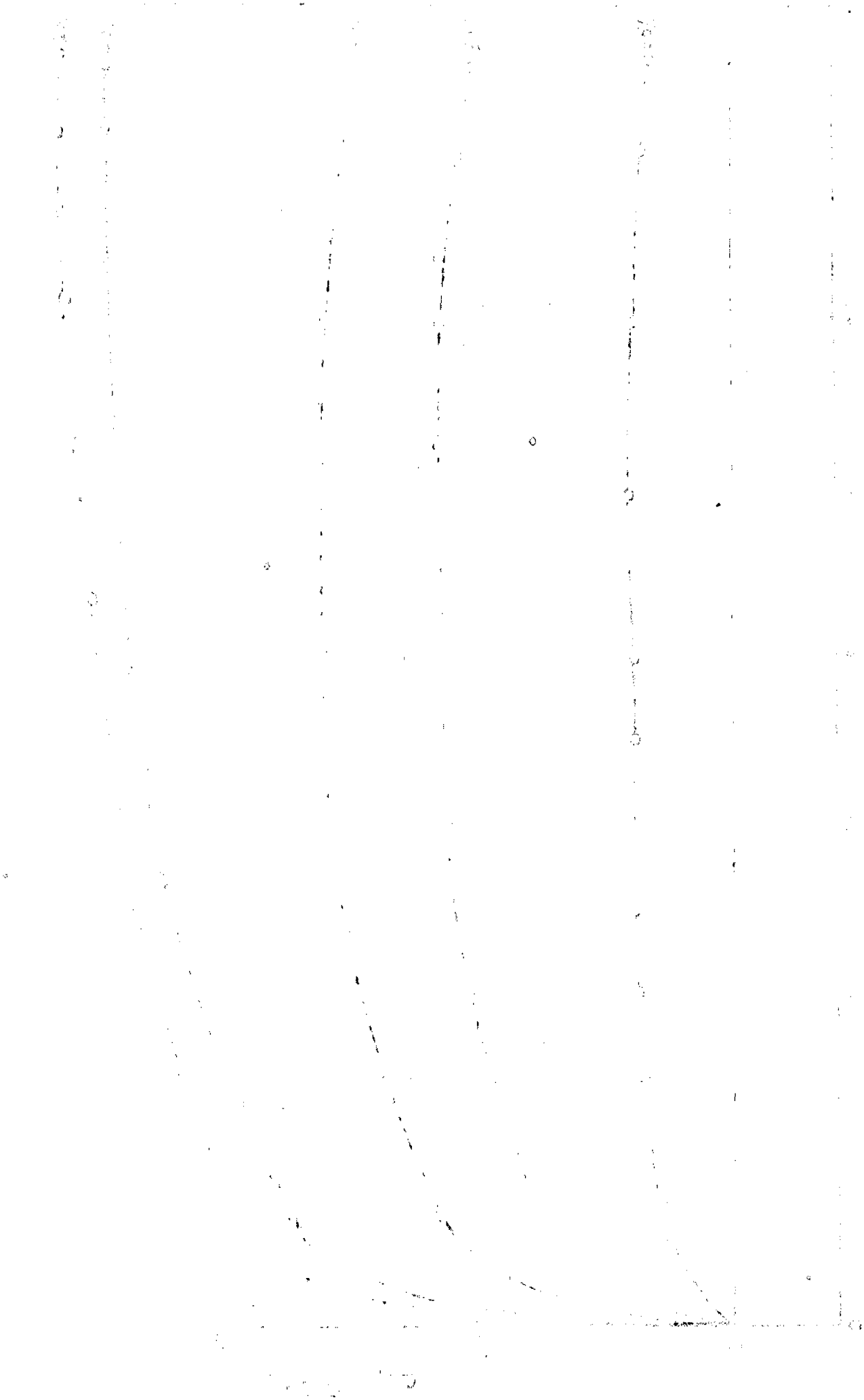

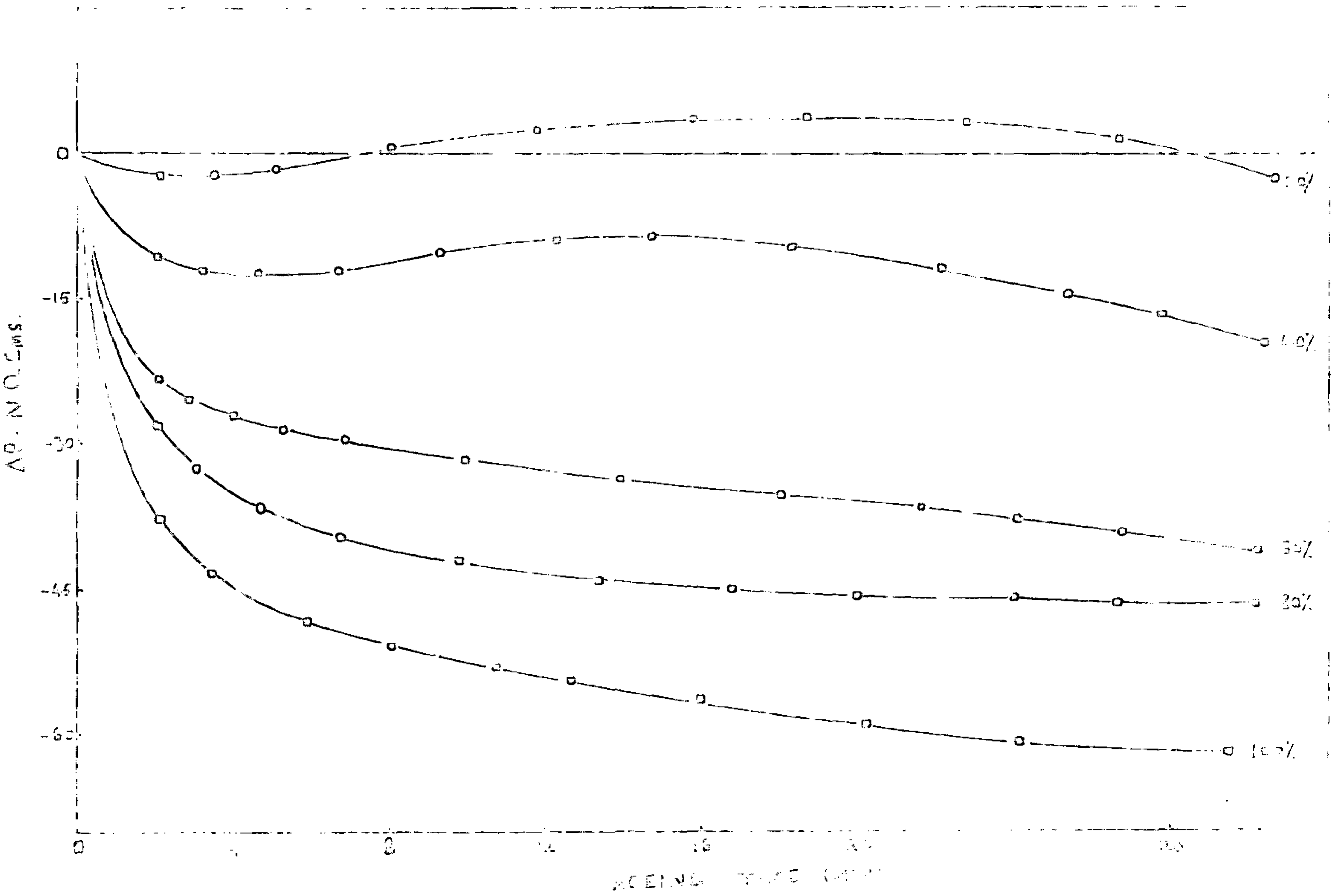
0
-15
-45
0
8
16

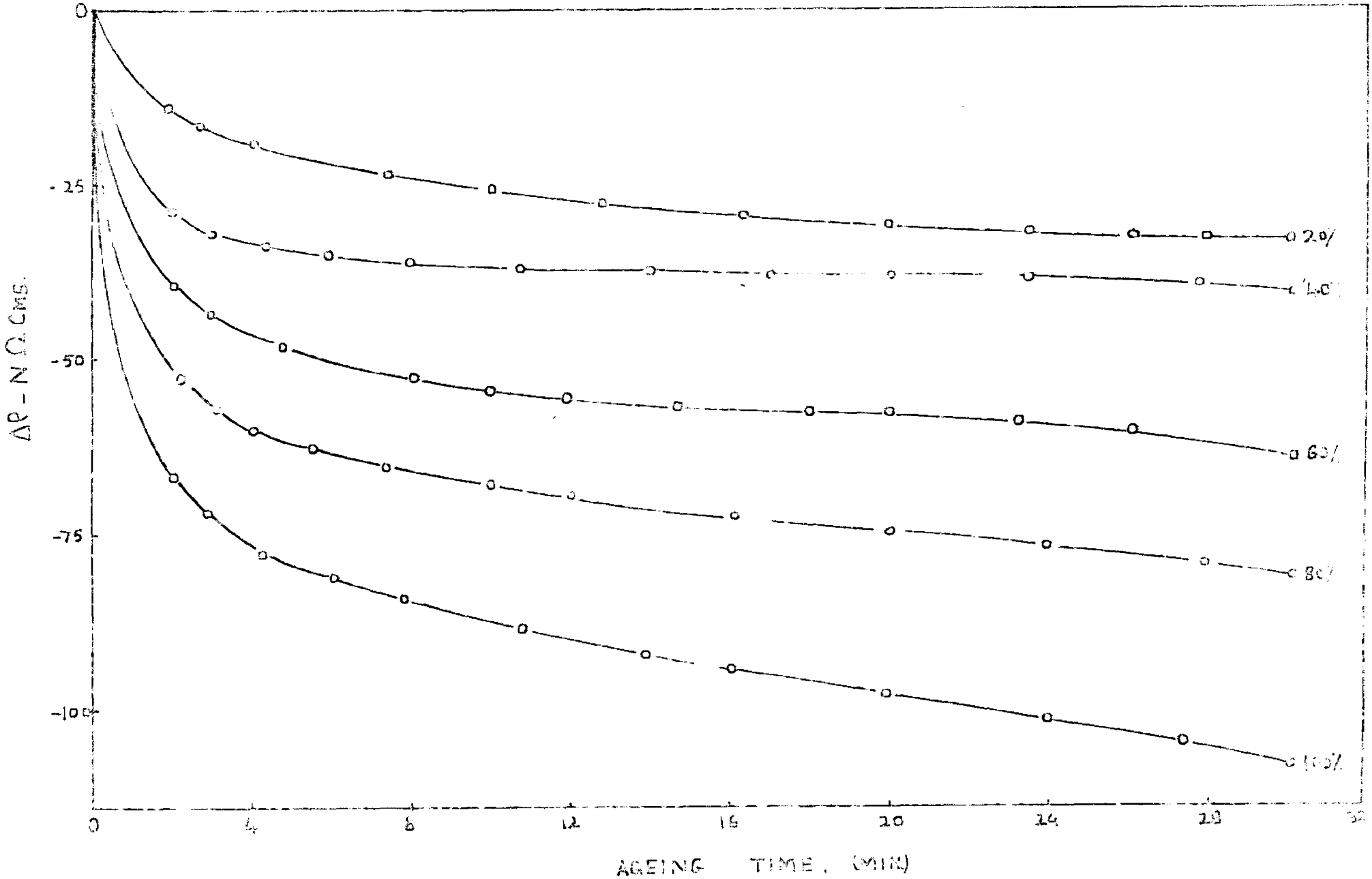
0
-25
-50
-75
-100
Δρ - N Ω. Cms.
0
4
8
12
16
20
24
28
32
AGEING TIME. (MIN)
20%
40%
60%
80%
100%

Fig. 1.2

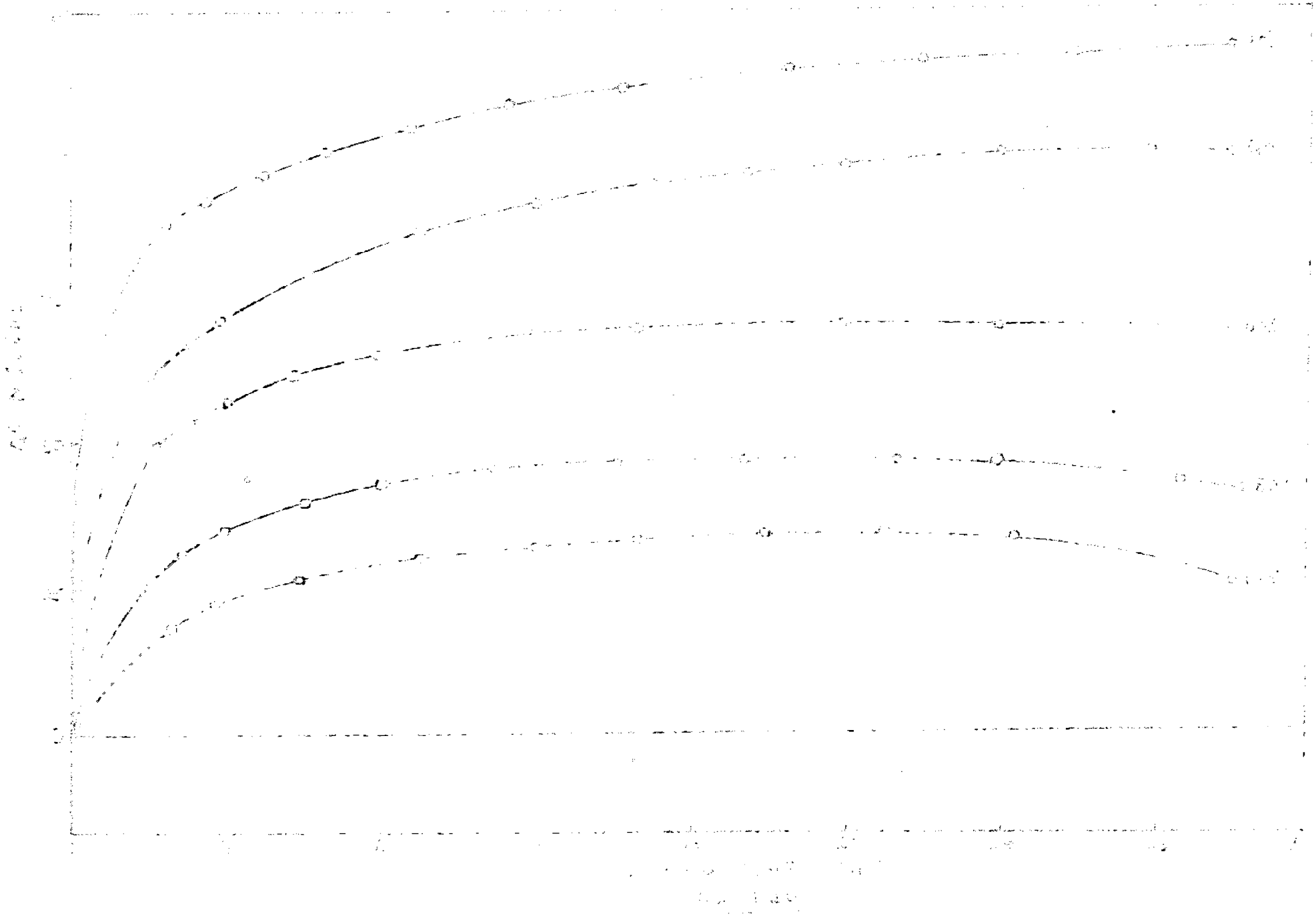

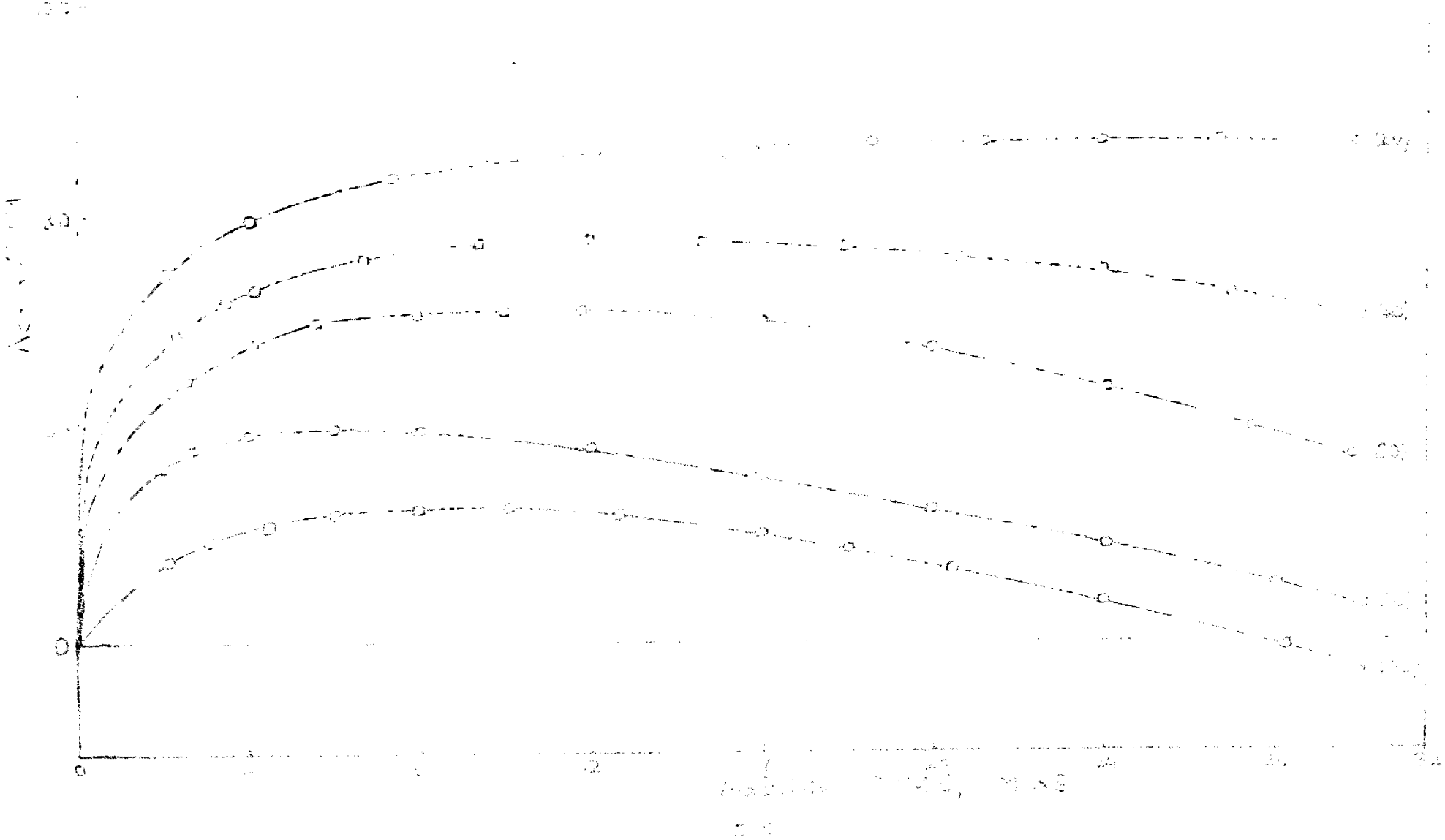

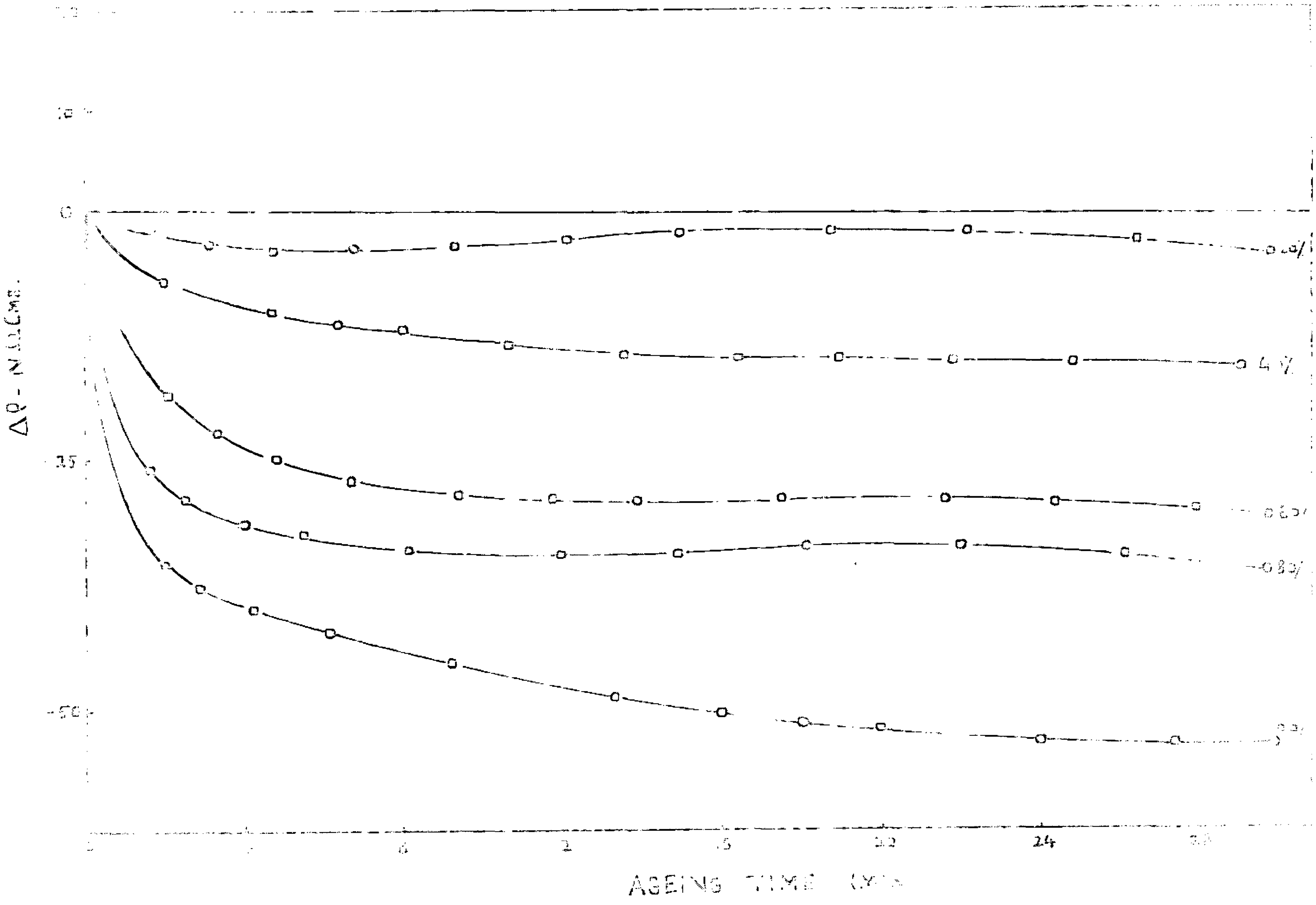

0
4 %
-25
-50
24
AGEING TIME

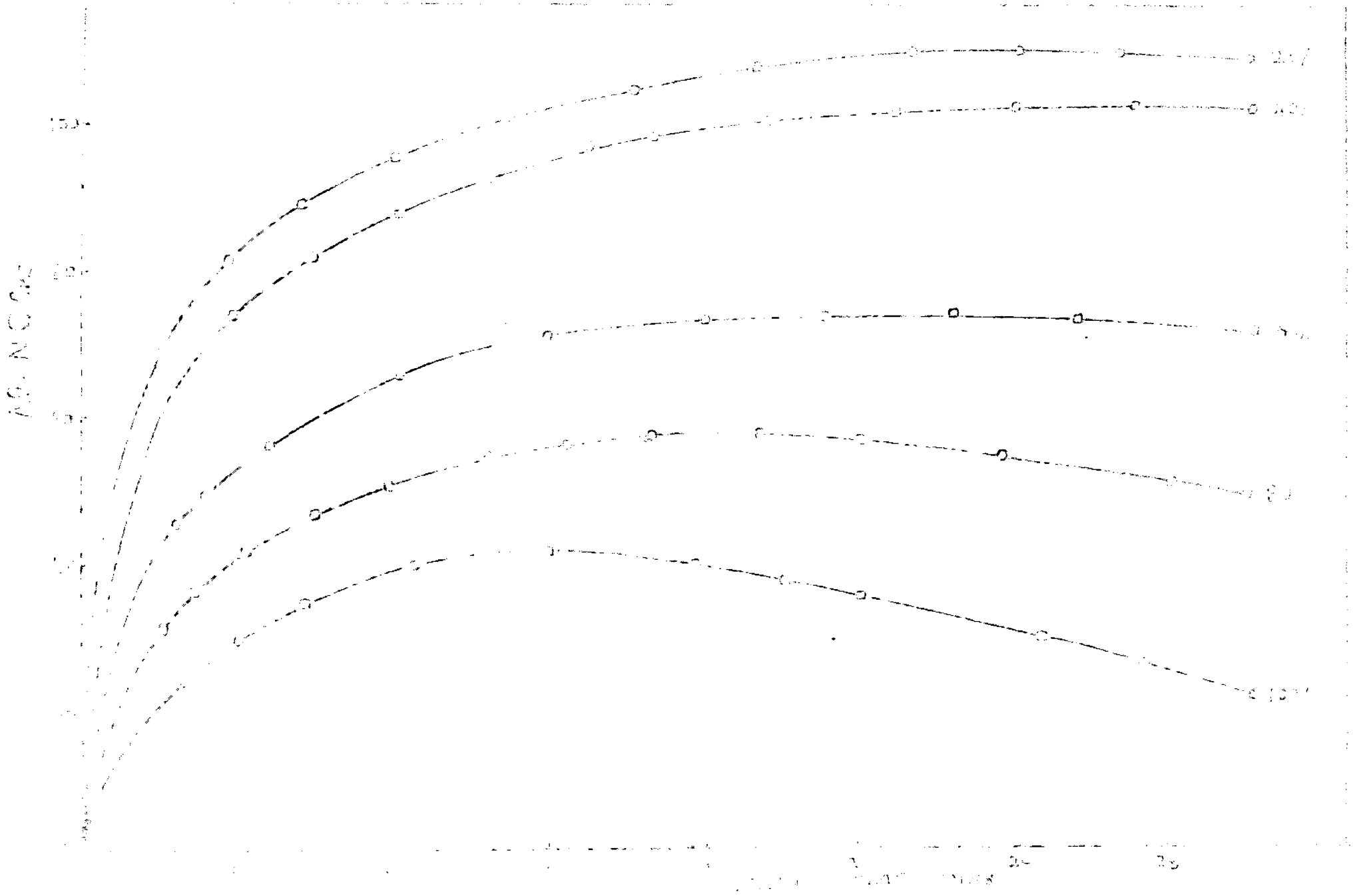

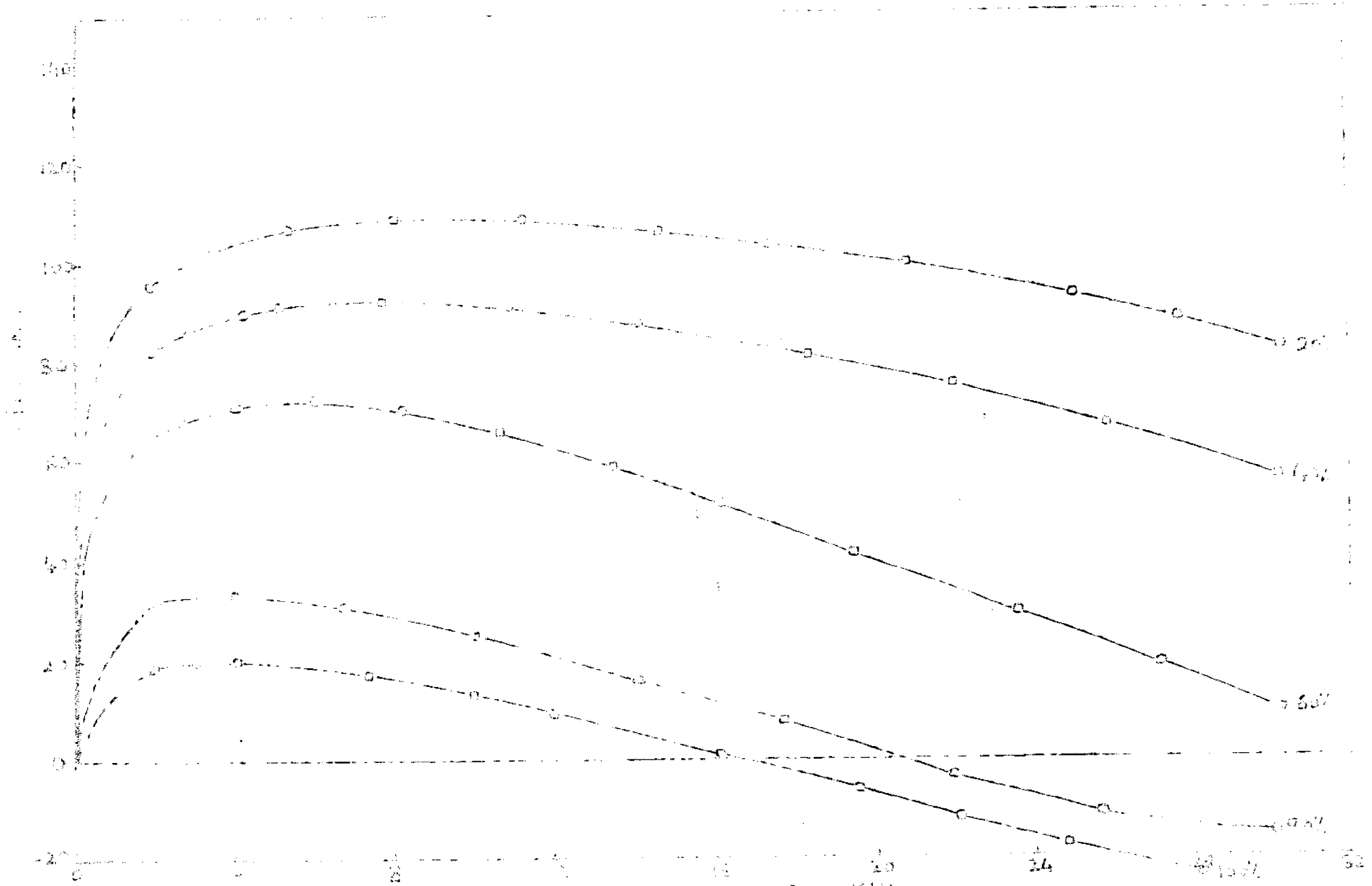

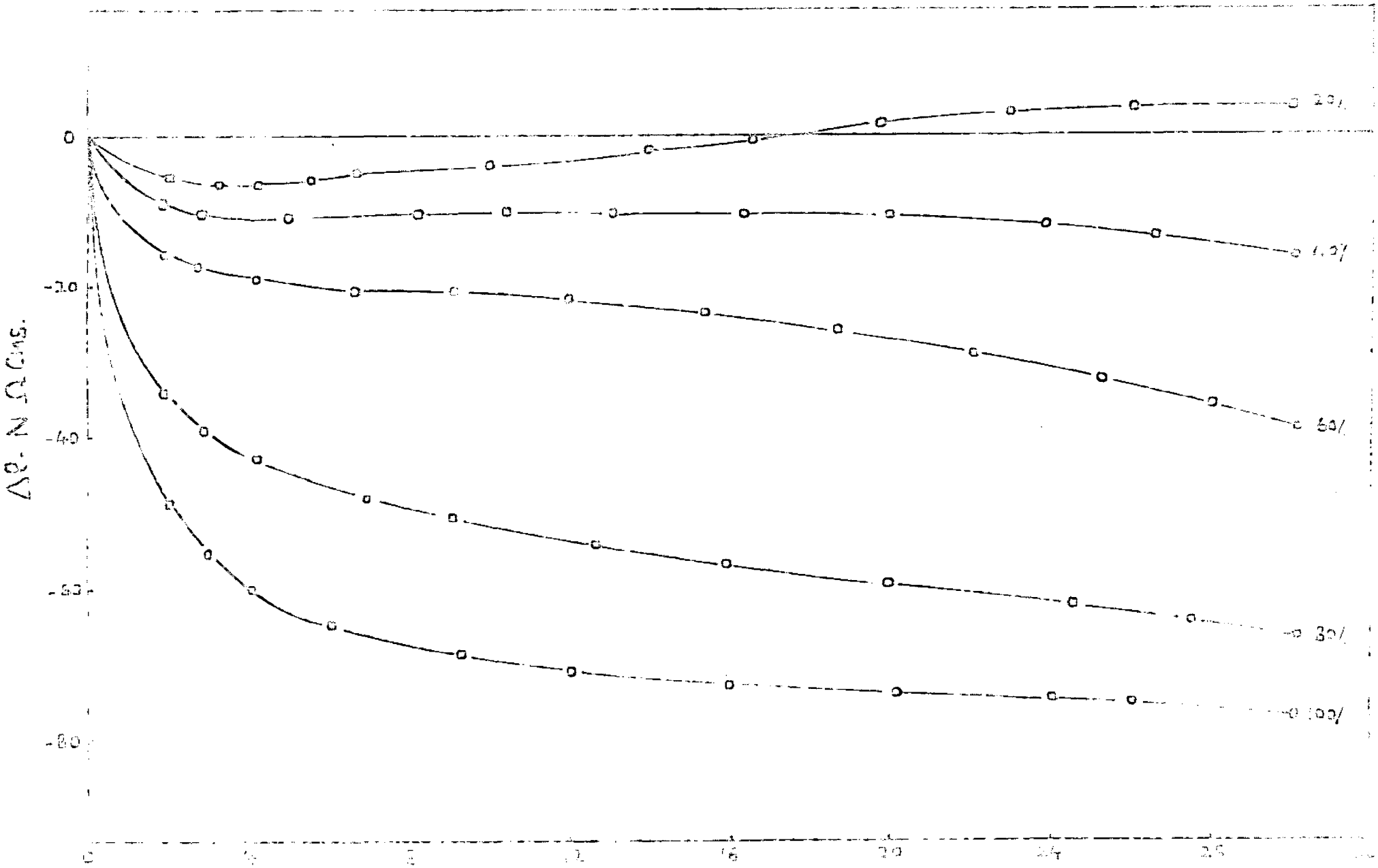
0
-20
-40
-60
-80
ΔR. N Ω Cms.
20%
10%
60%
30%
100%
AGEING TIME, (HRS)

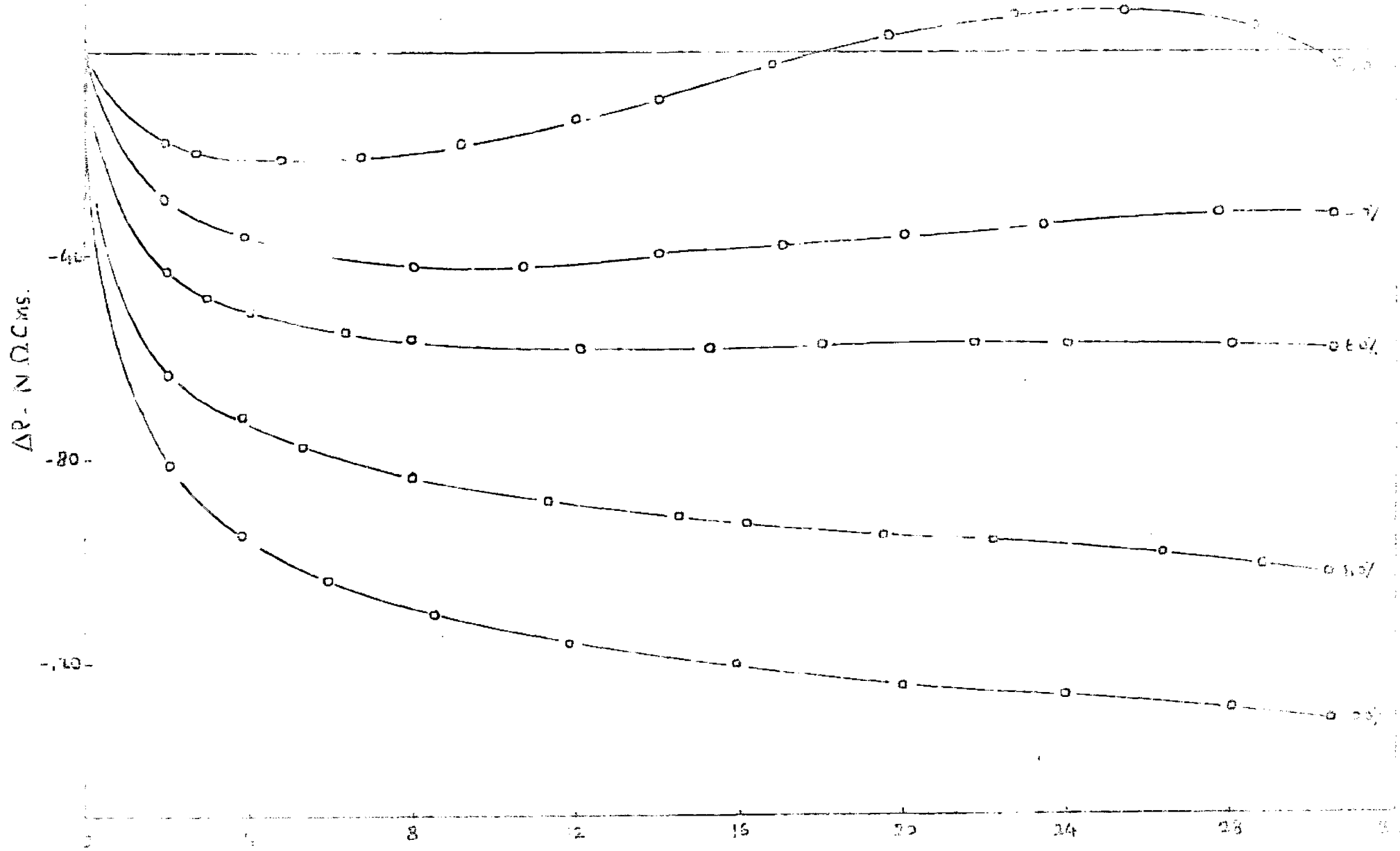
ΔP - IN Ω.Cms.
-40
-80
-120
8
16
24
AGEING TIME, (MIN)

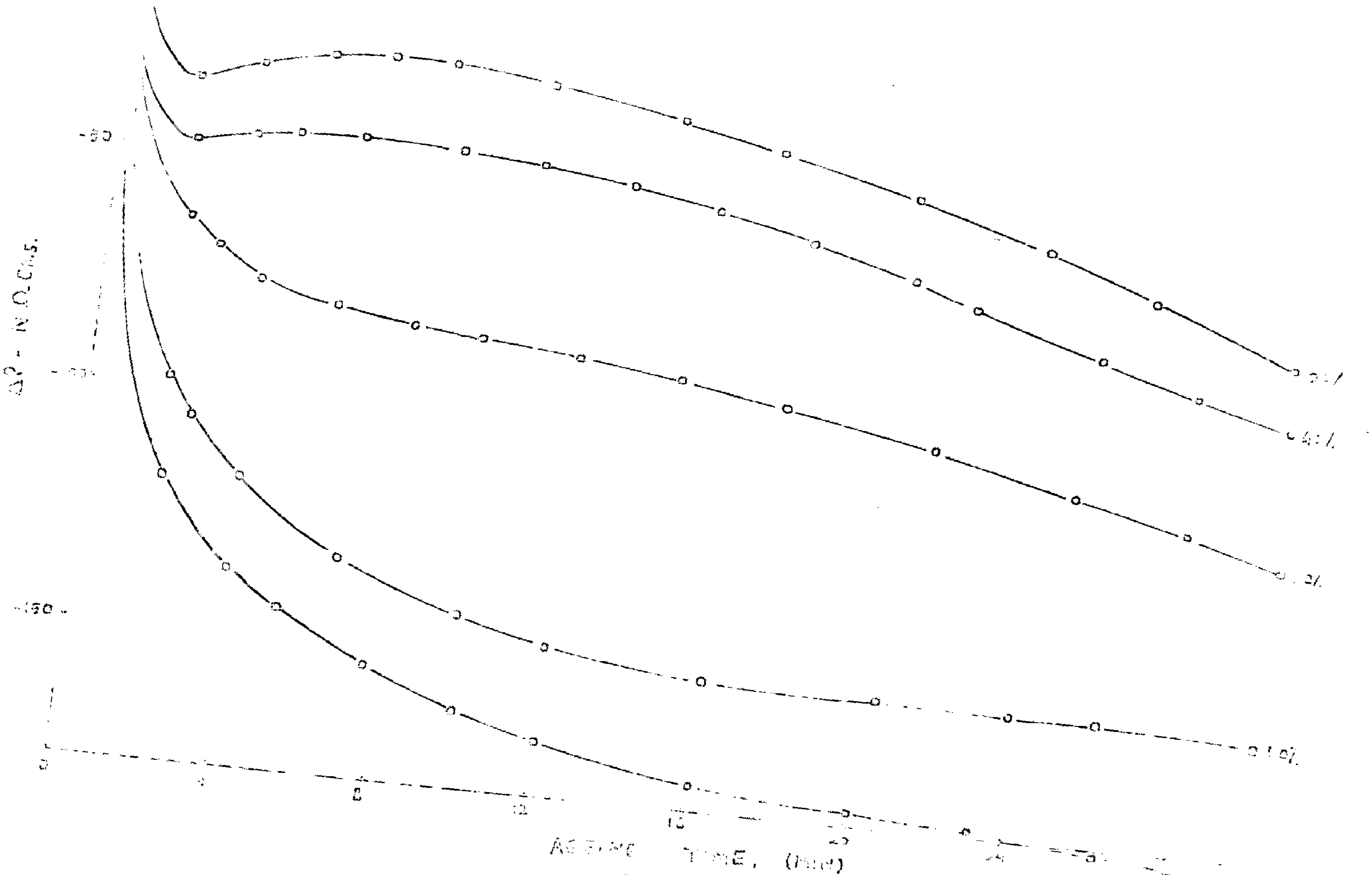
-50
-150
Δρ - N Ω.cms.
AGEING TIME, (hrs)
2%
1%
0.1%

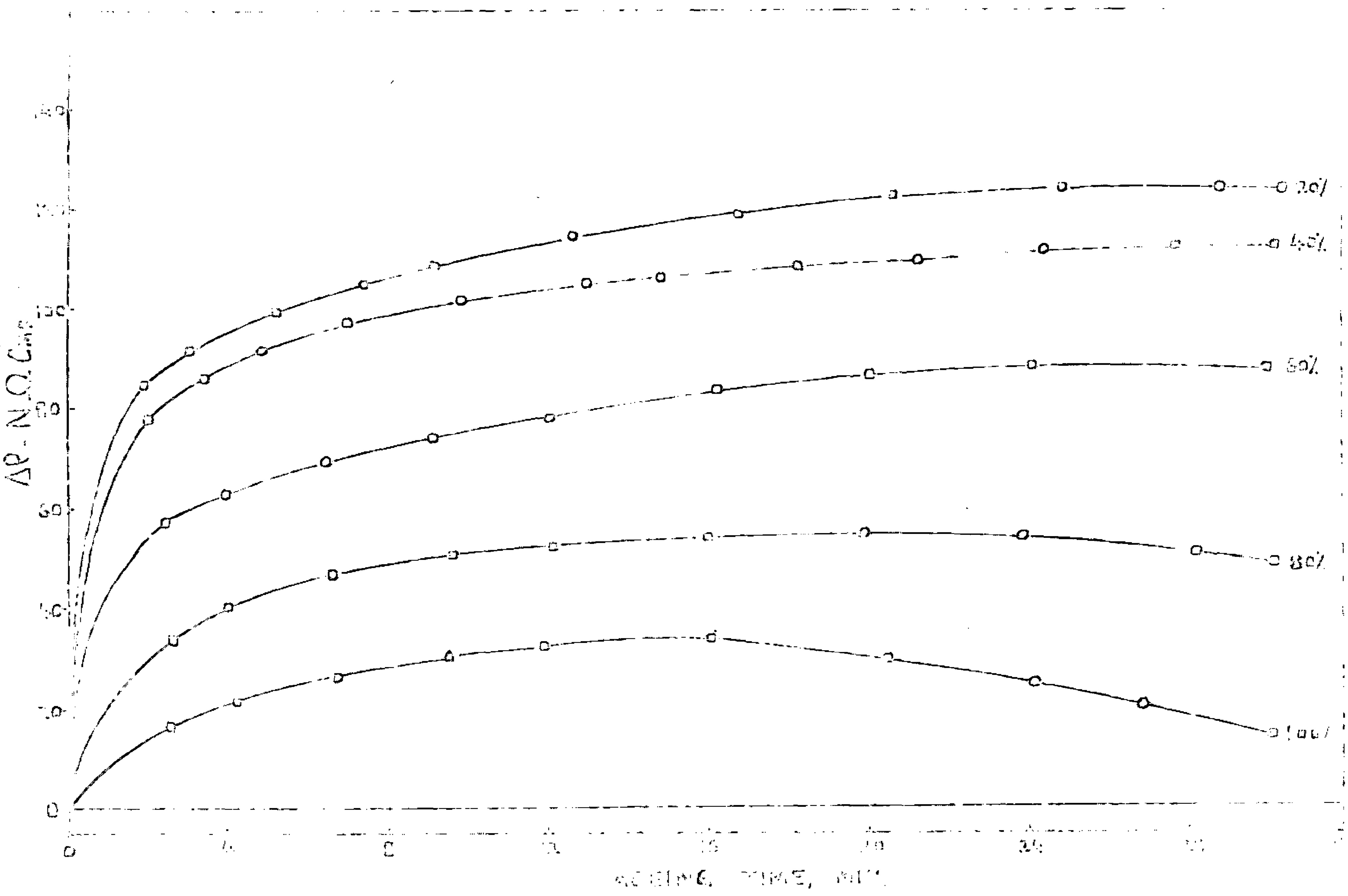

FIG. [illegible]

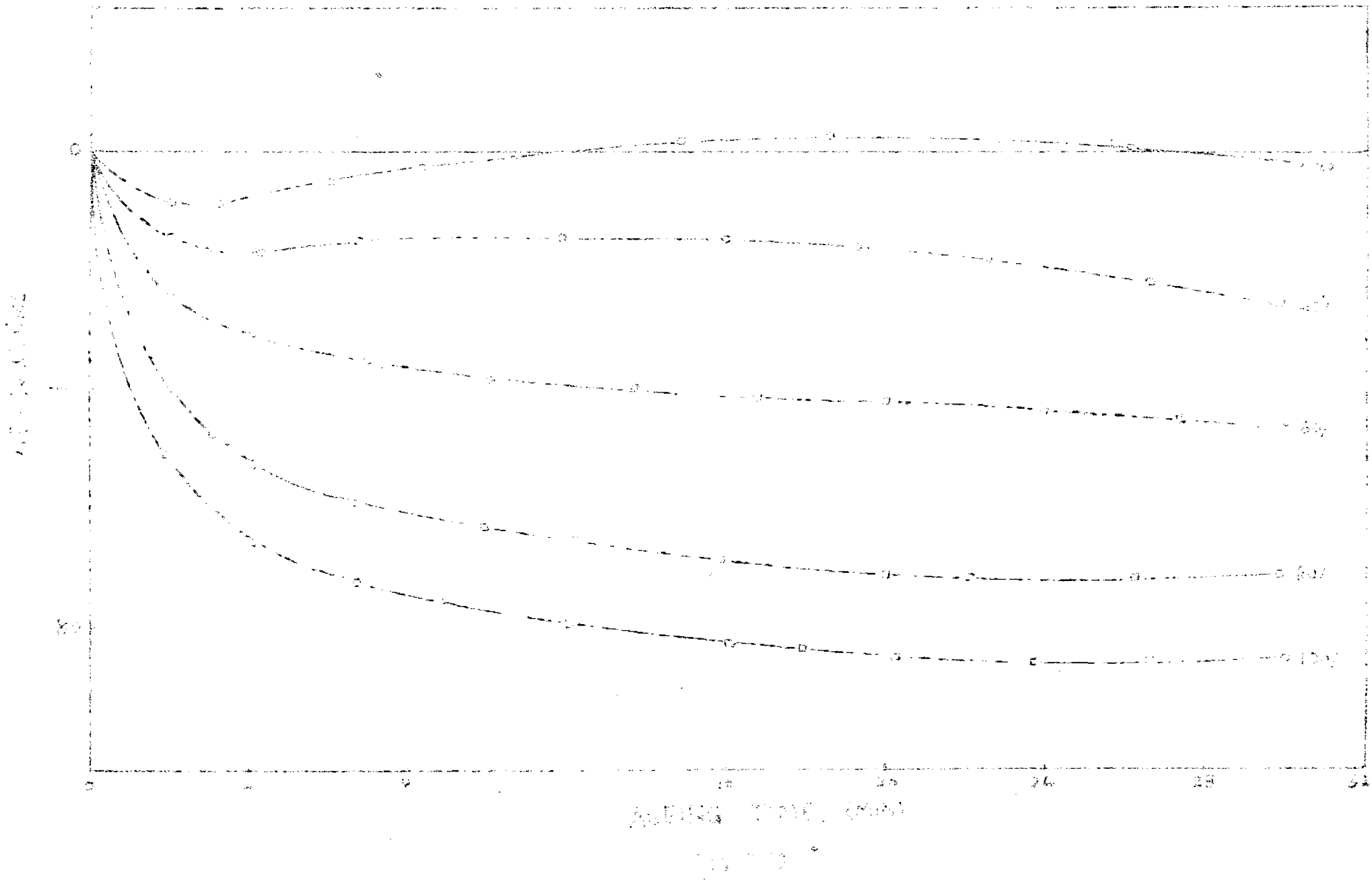

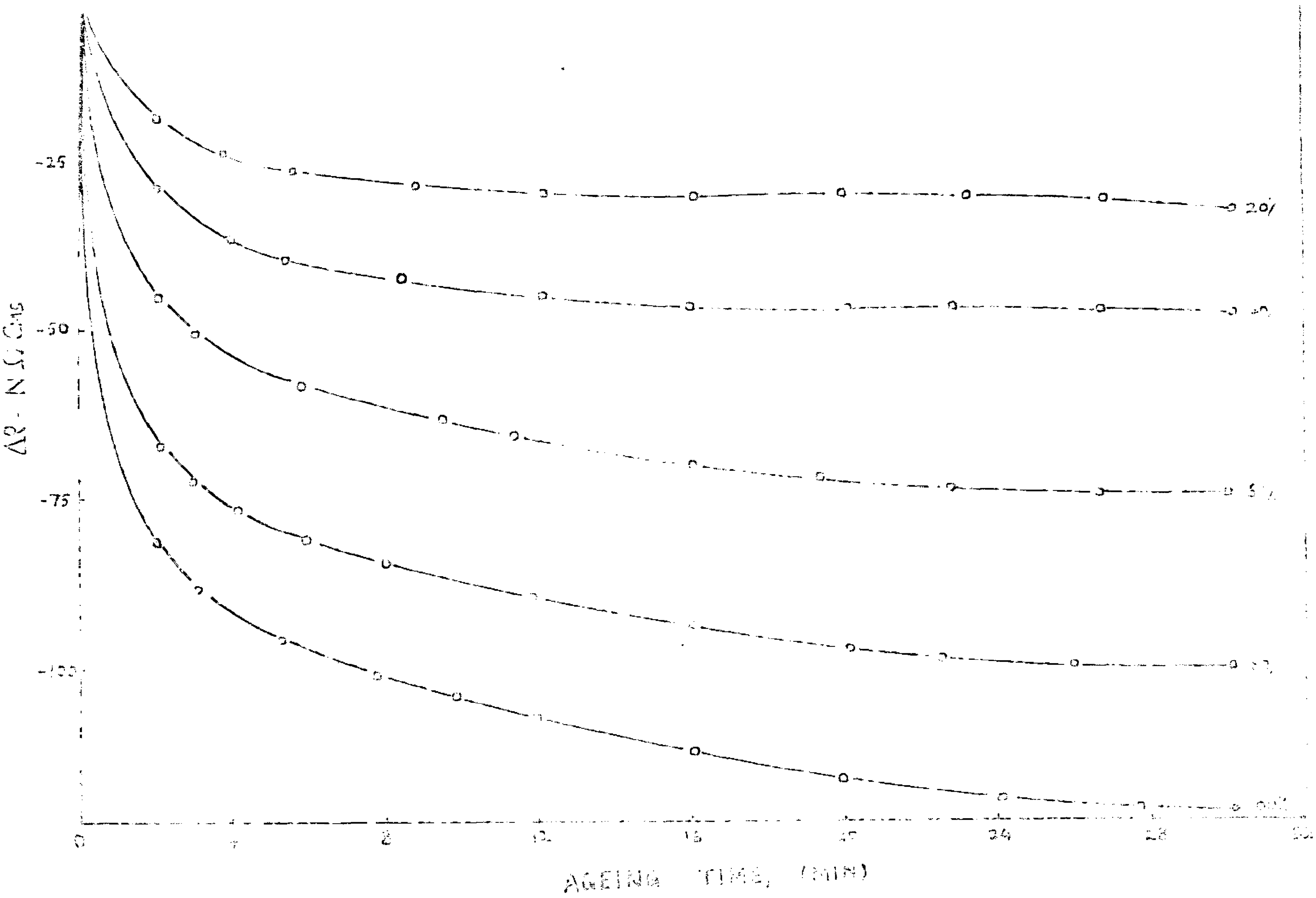

FIG. [illegible]

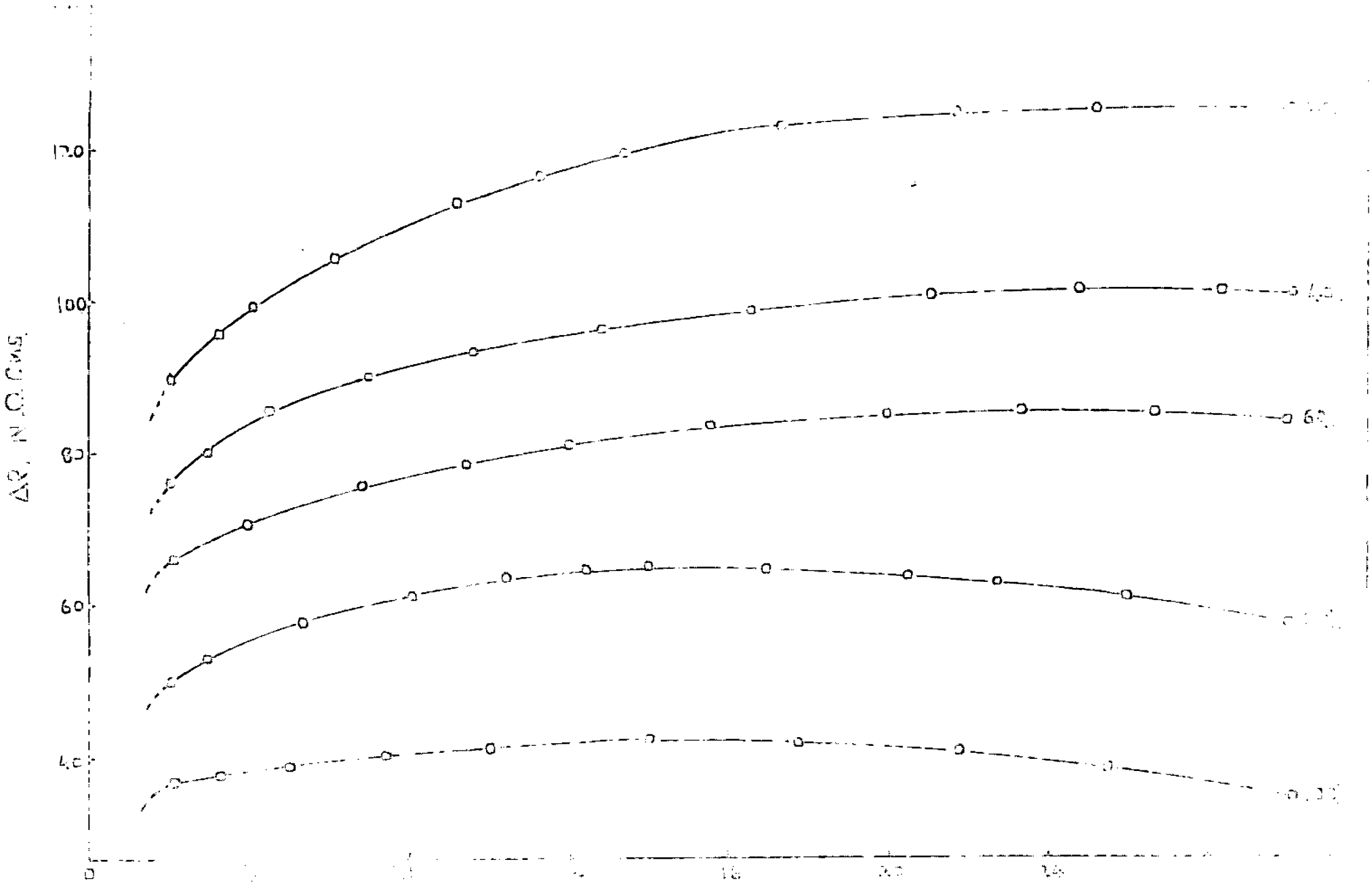

FIG. 2.2.

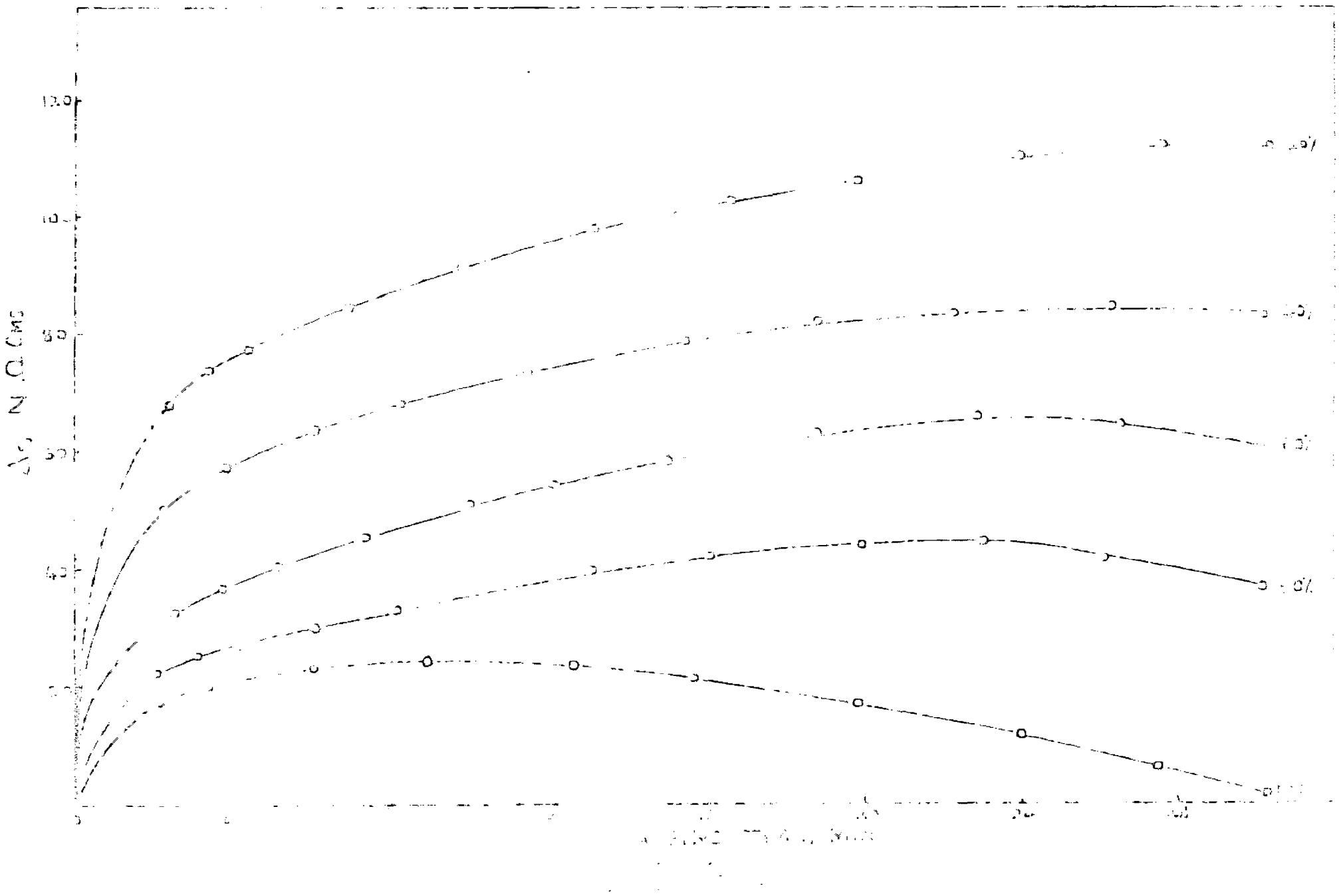

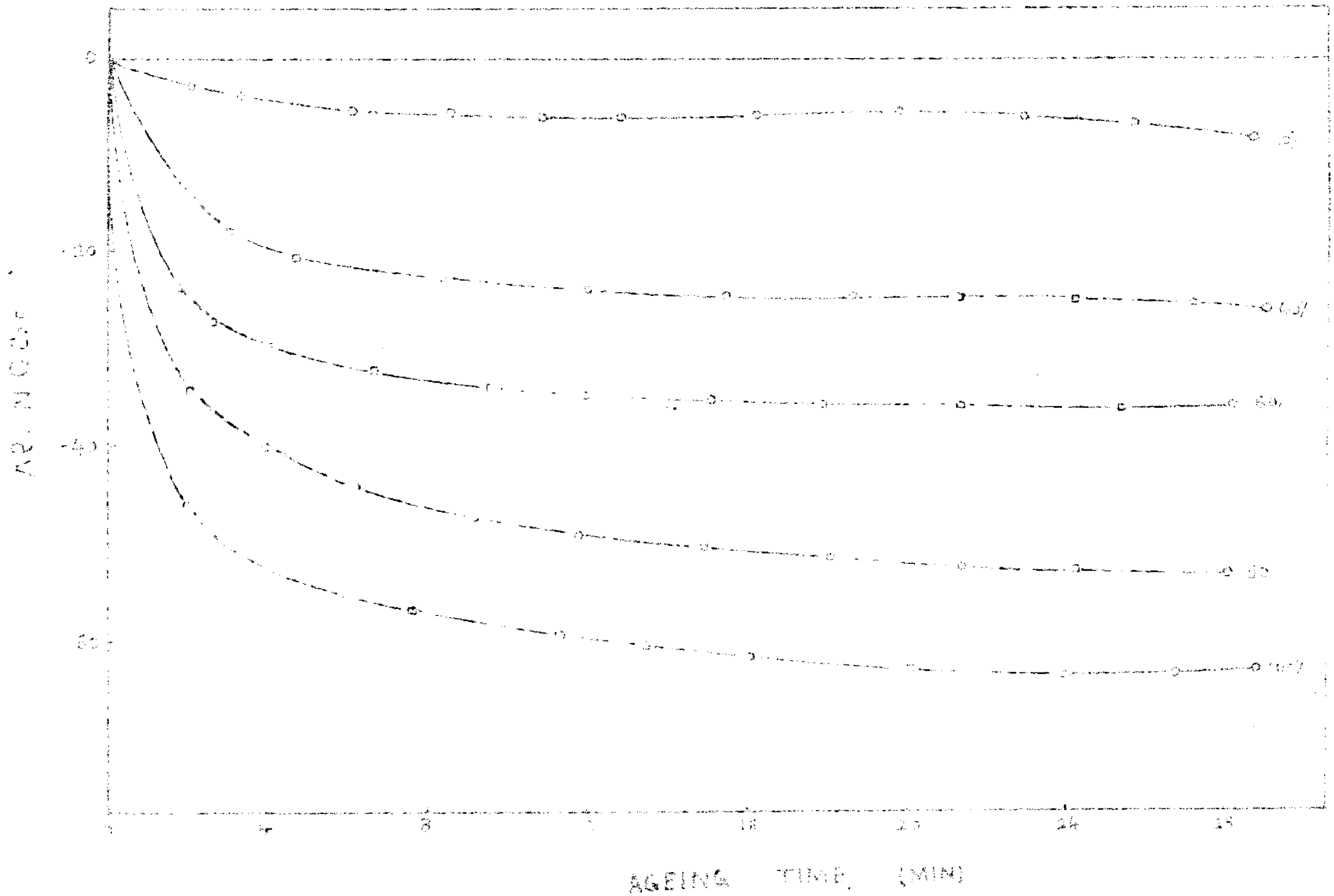

FIG 2.23

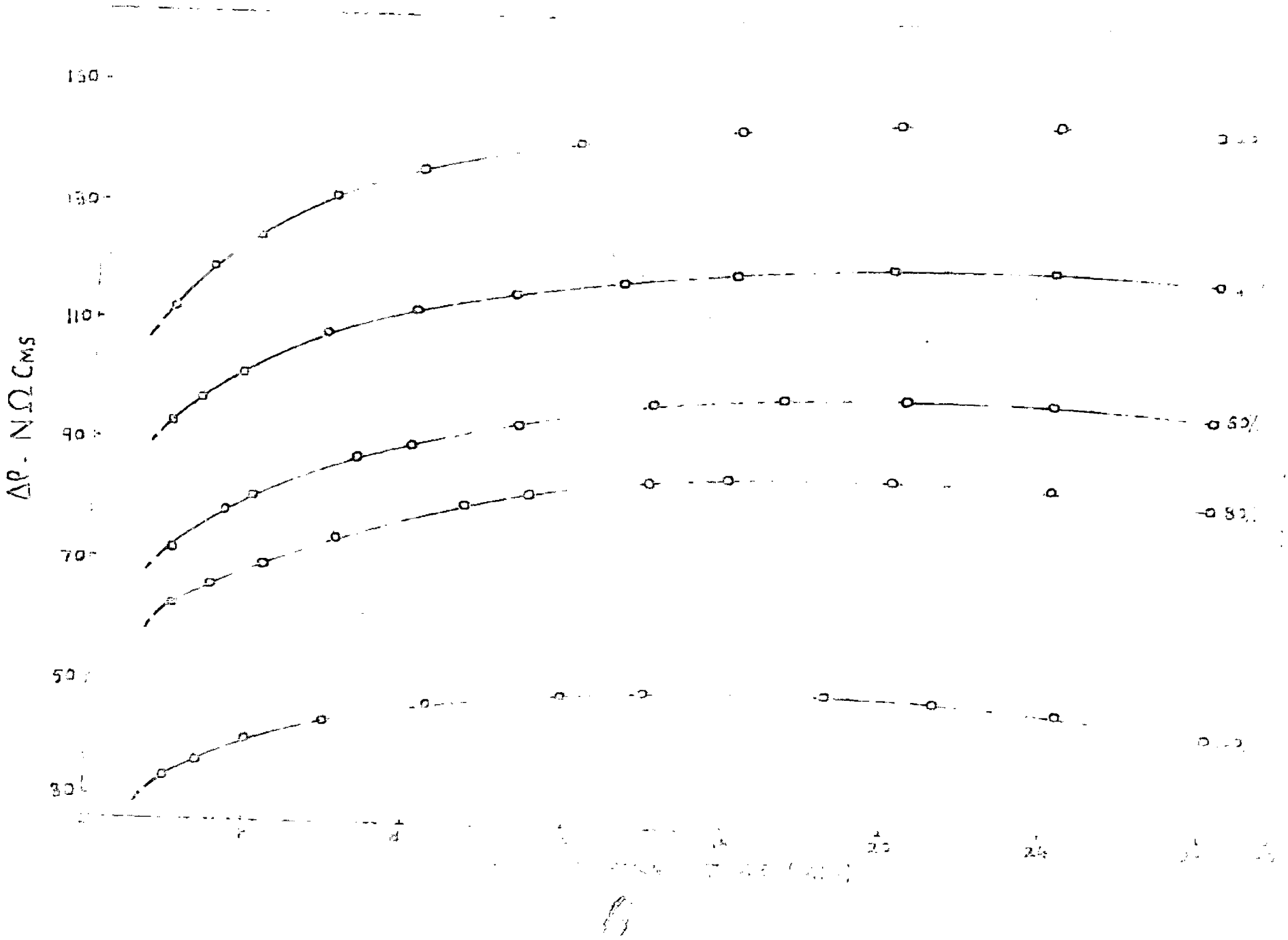
150
130
110
90
70
50
30
ΔP - NΩ CMS
50%
50%

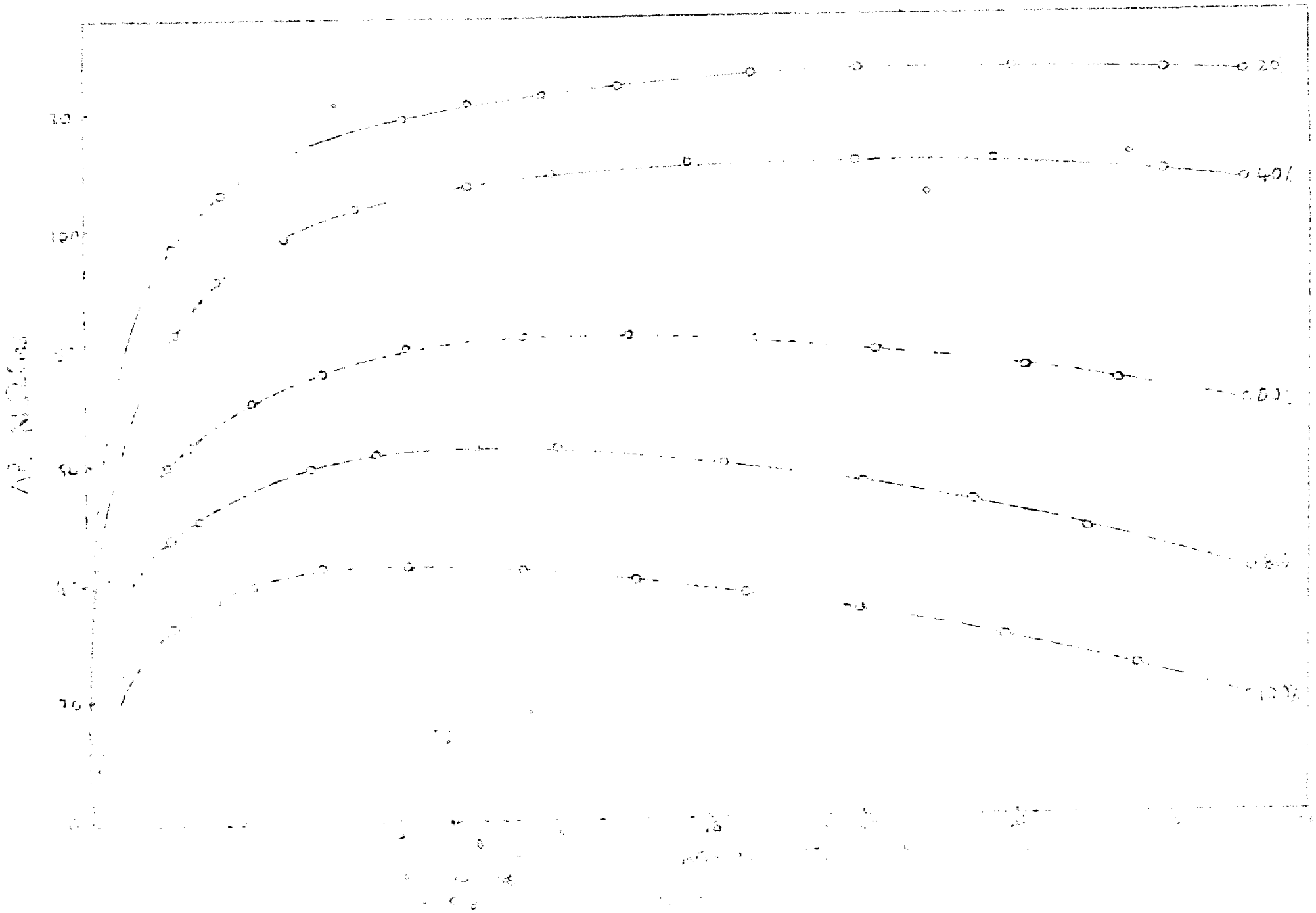

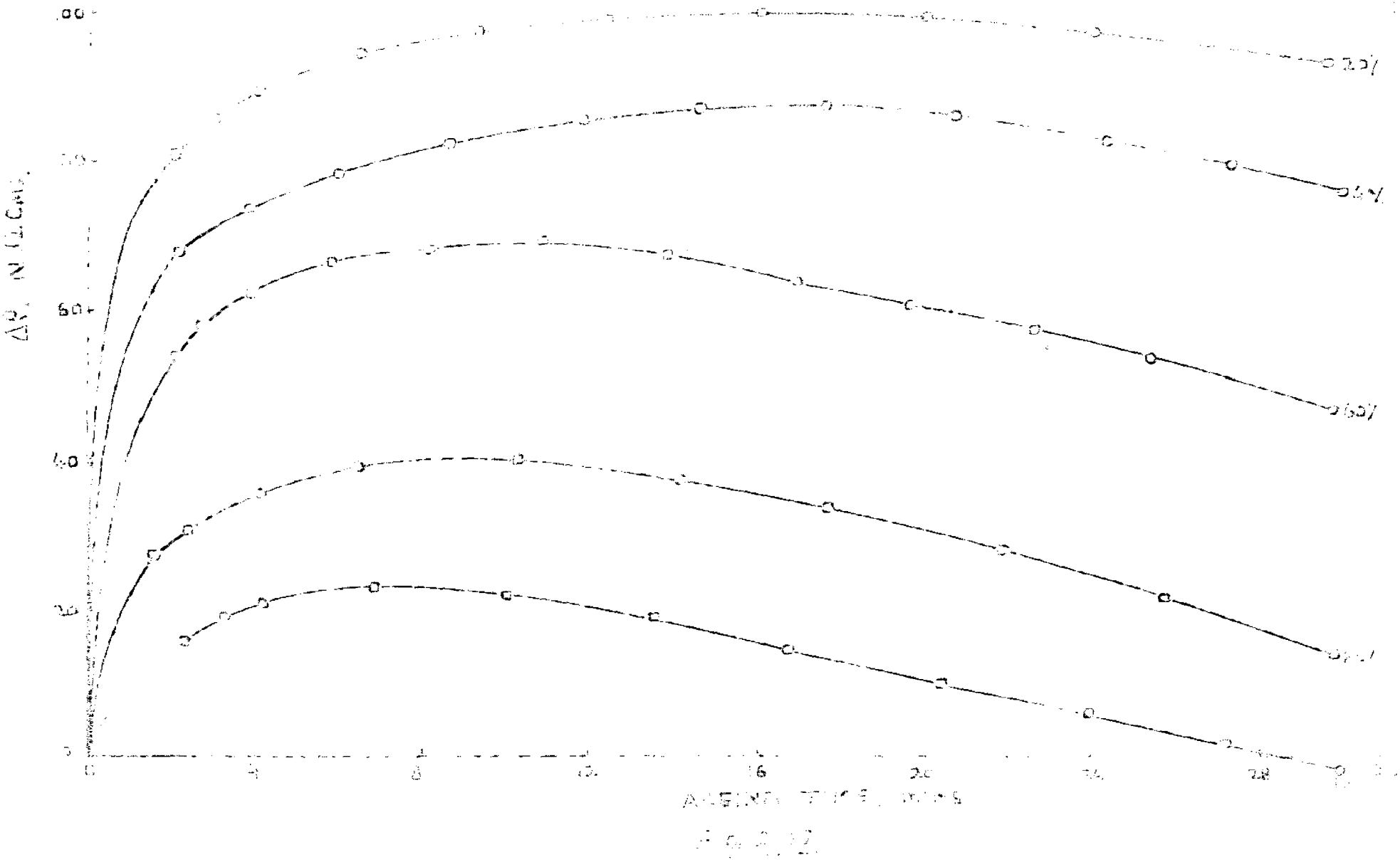

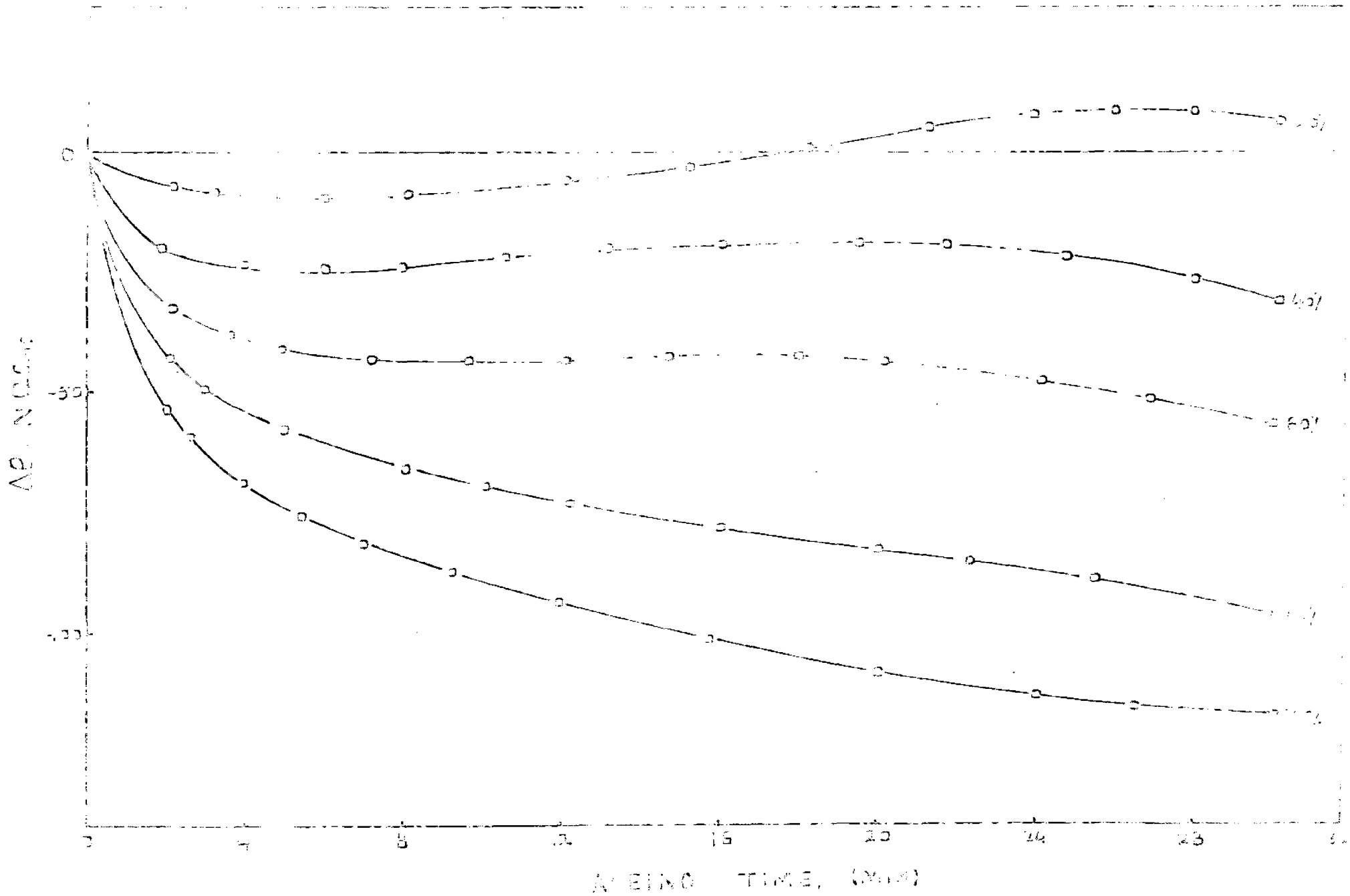
0
-50
-100
60'
40'
20'
10'
5'
0
5
10
15
20
25
30
TIME, (MIN)

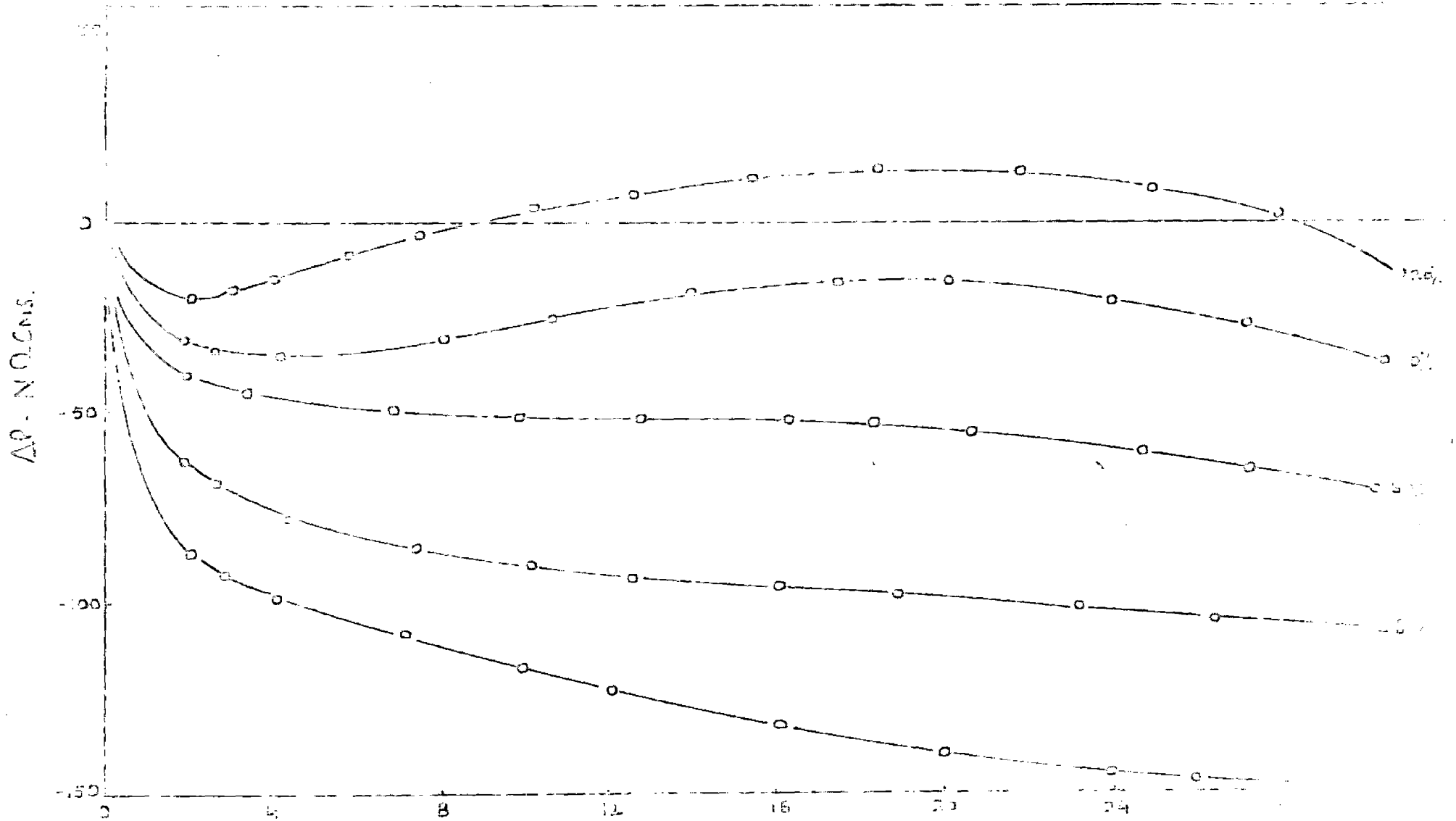

FIG 2

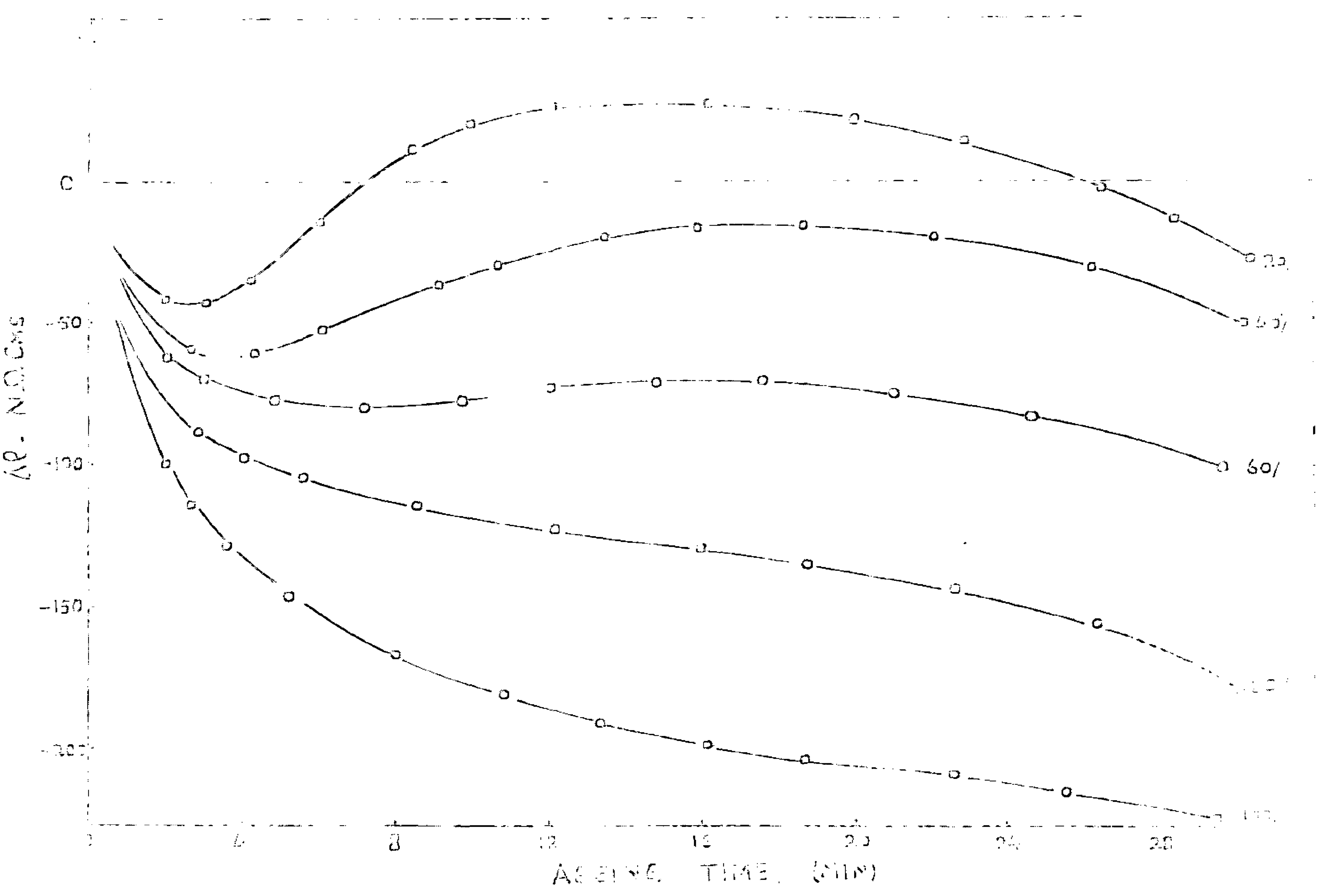

0
-50
-100
-150
4
8
60/

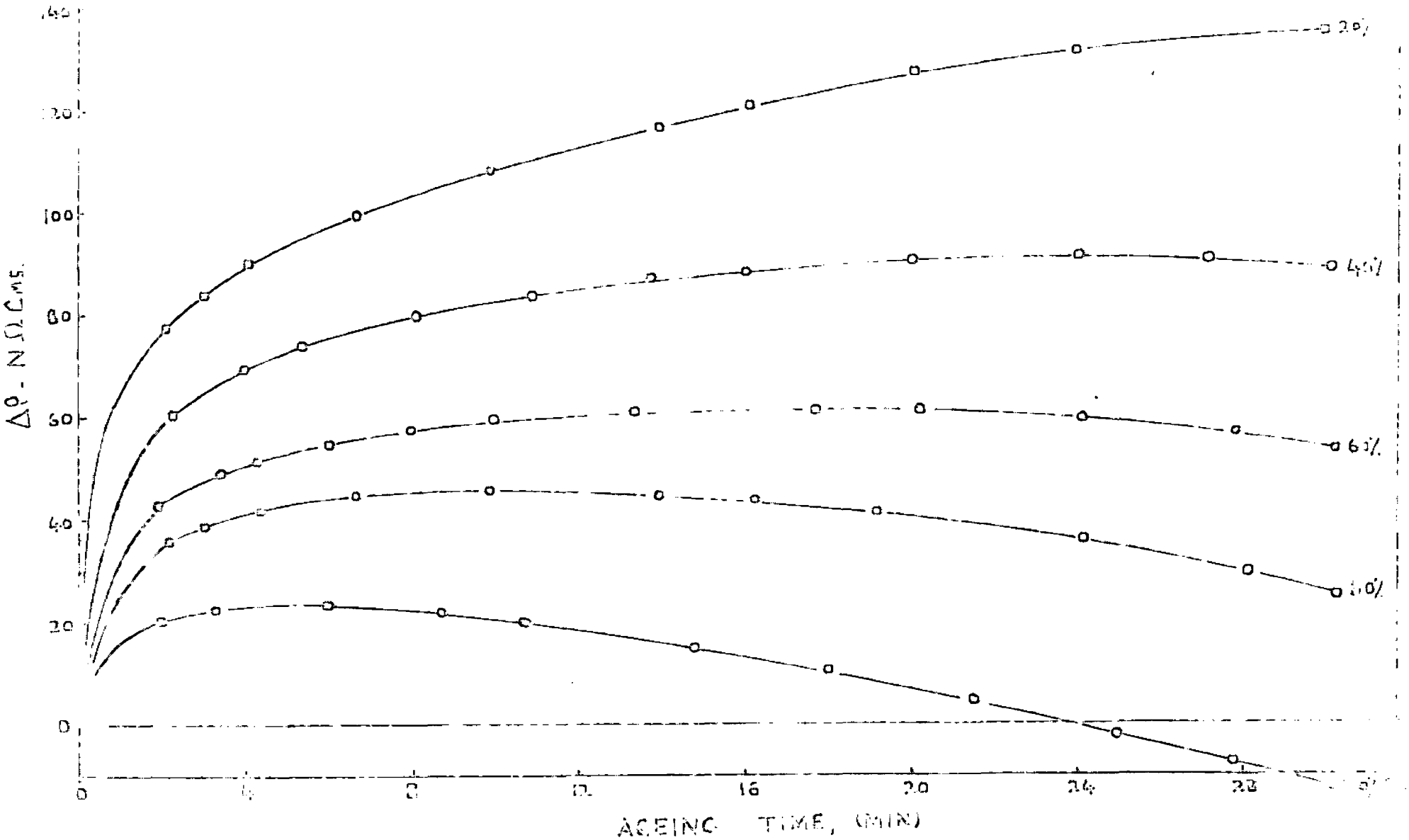
Δρ - NΩCMS.
120
100
80
60
40
20
0
0
8
12
16
20
24
28
ACEING TIME, (MIN)
2%
4%
6%
10%

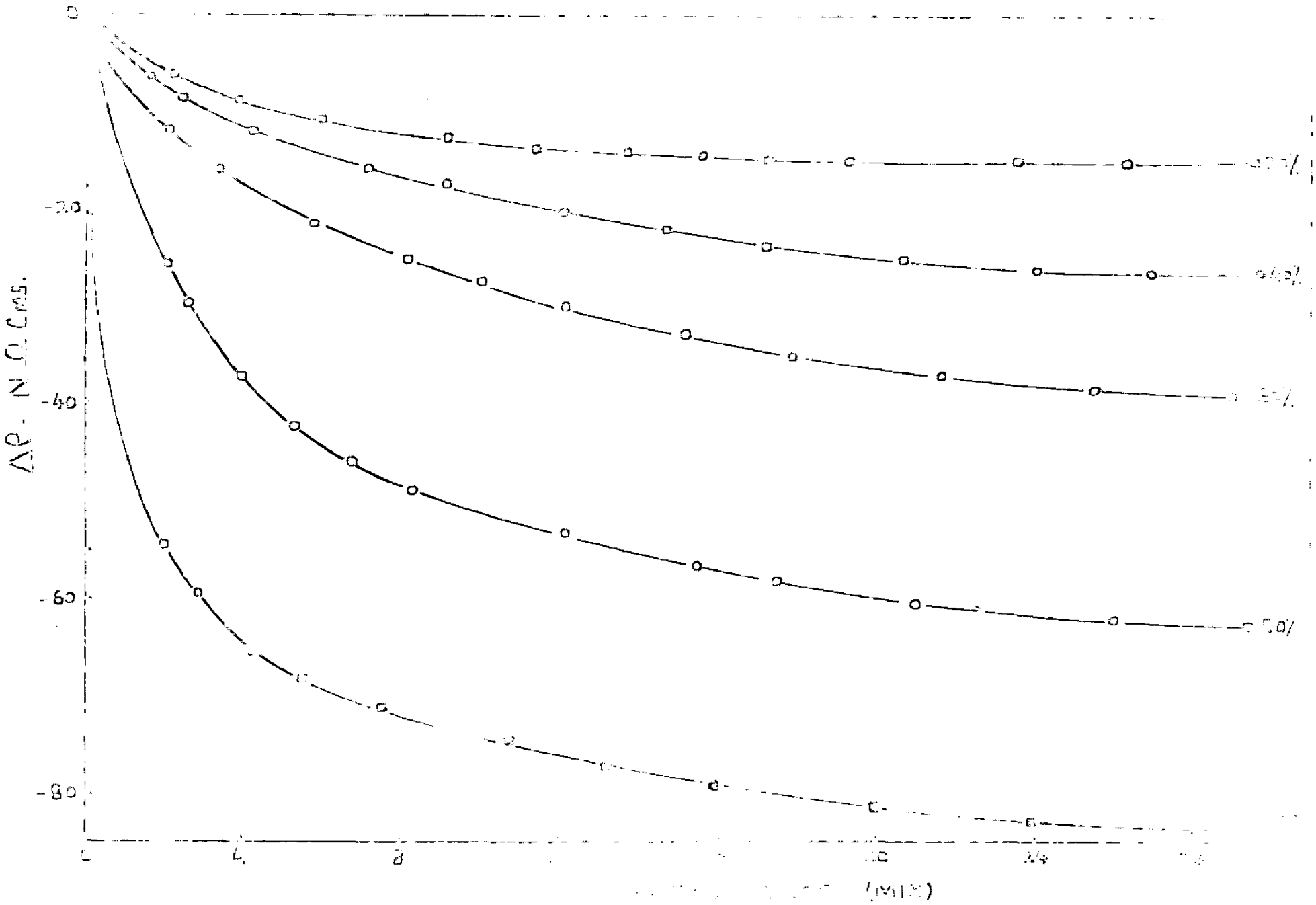
-20
-40
-60
-80
ΔP - N Ω CMS.
8
(MIN)

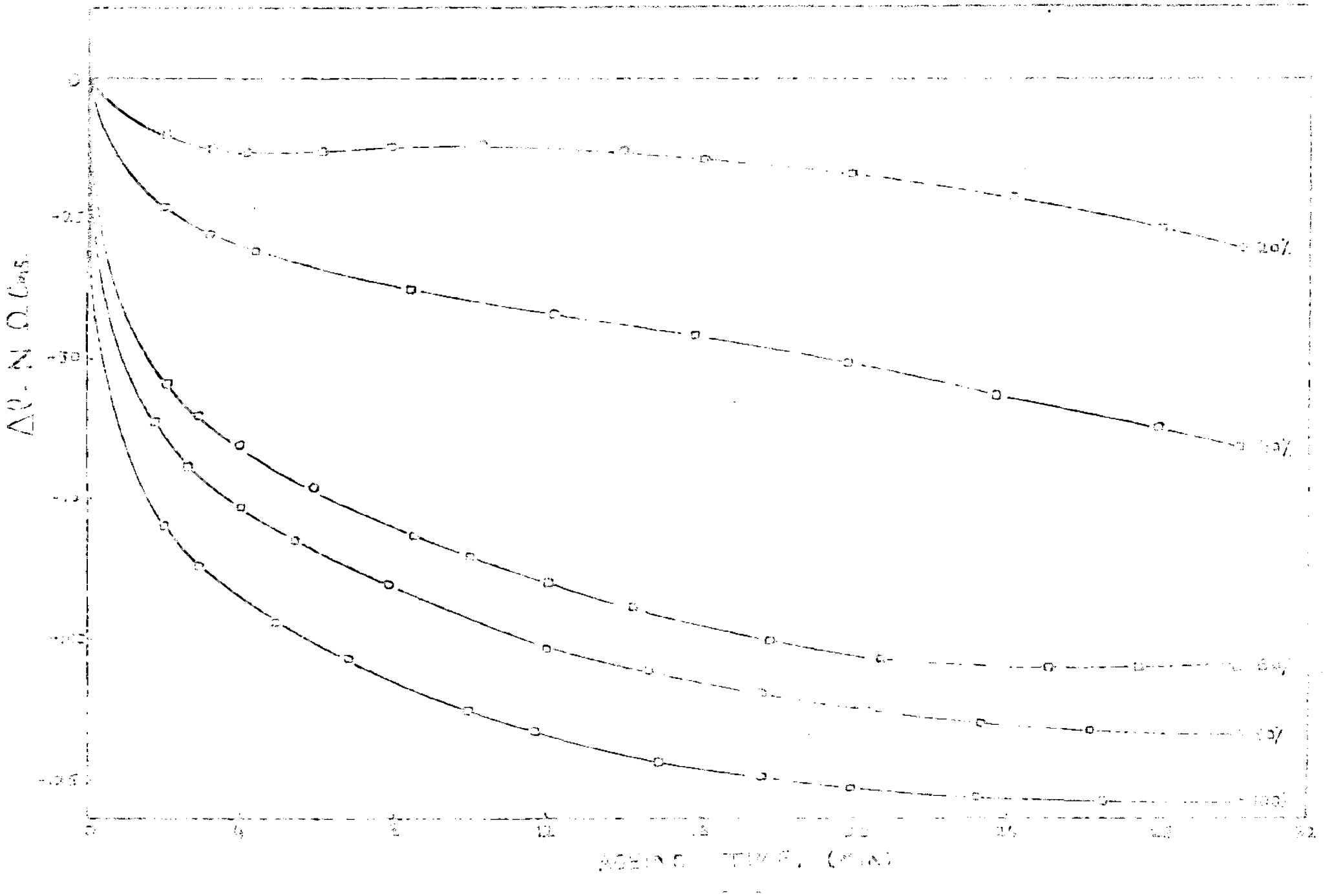

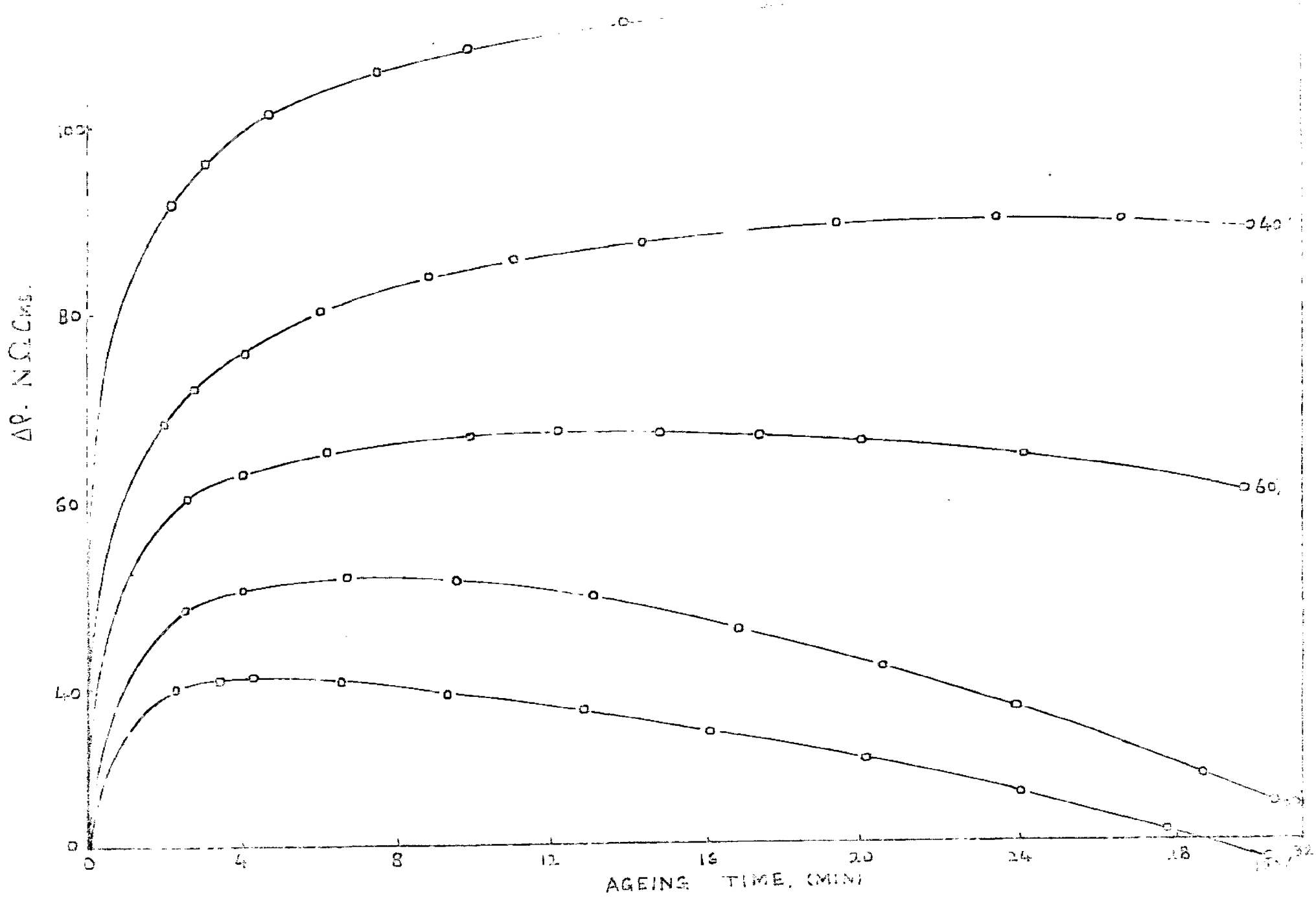
ΔP. N/Sq.Cms.
100
80
60
40
0
0
4
8
12
16
20
24
28
32
AGEING TIME, (MIN)
40
60

Fig 9.2?

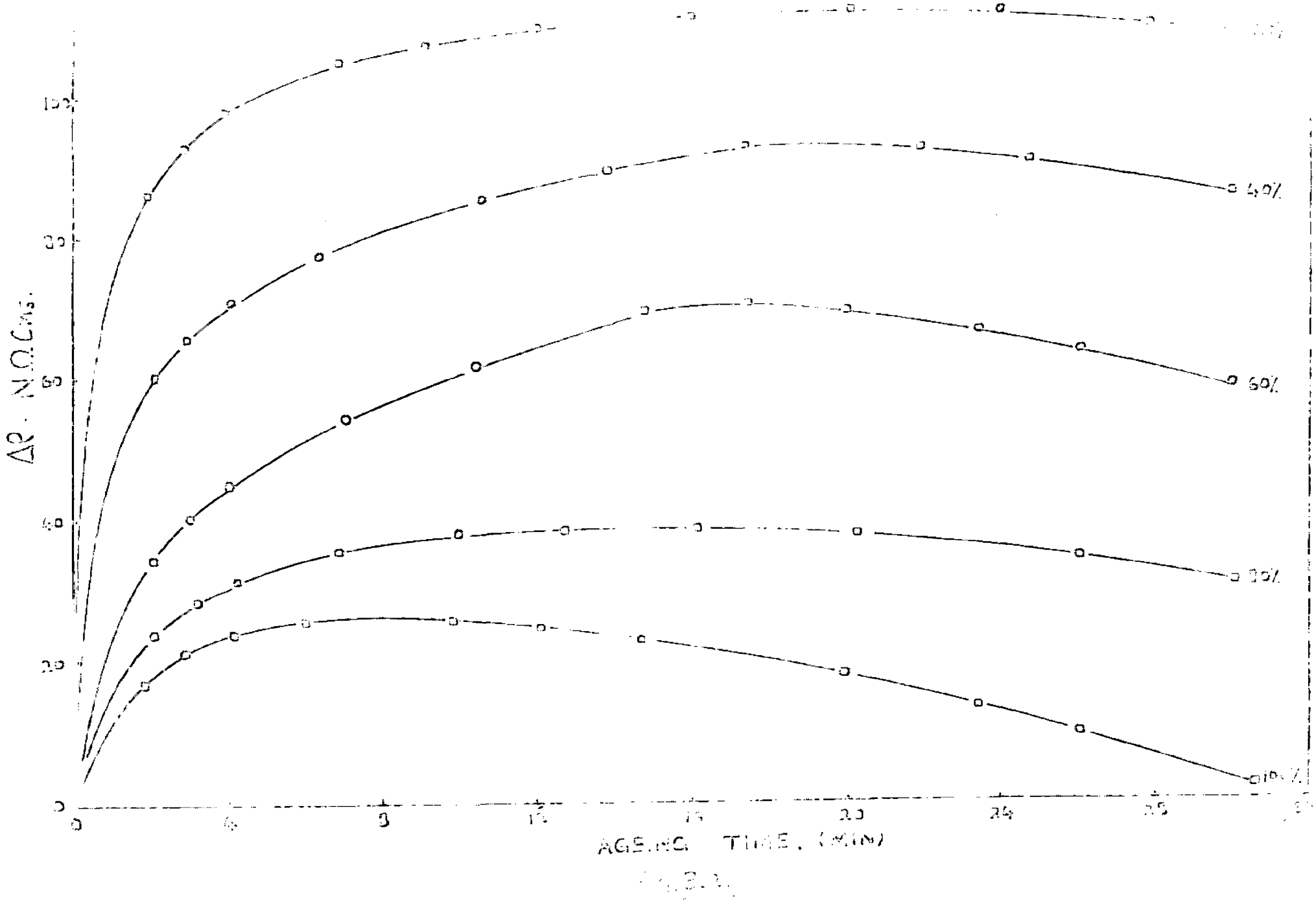
Δρ. NΩCms.
AGEING TIME. (MIN)
40%
60%

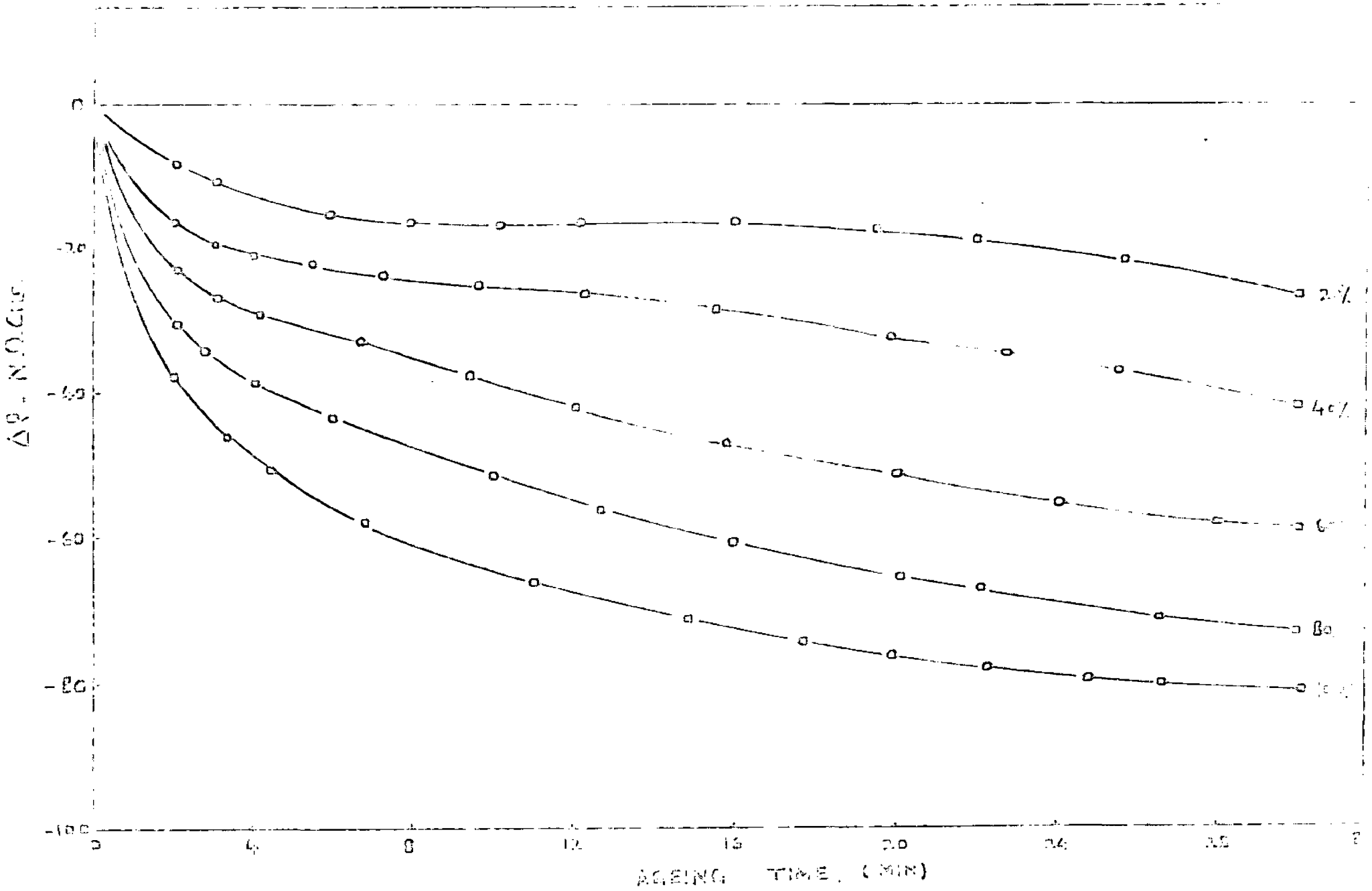

Fig 3.23

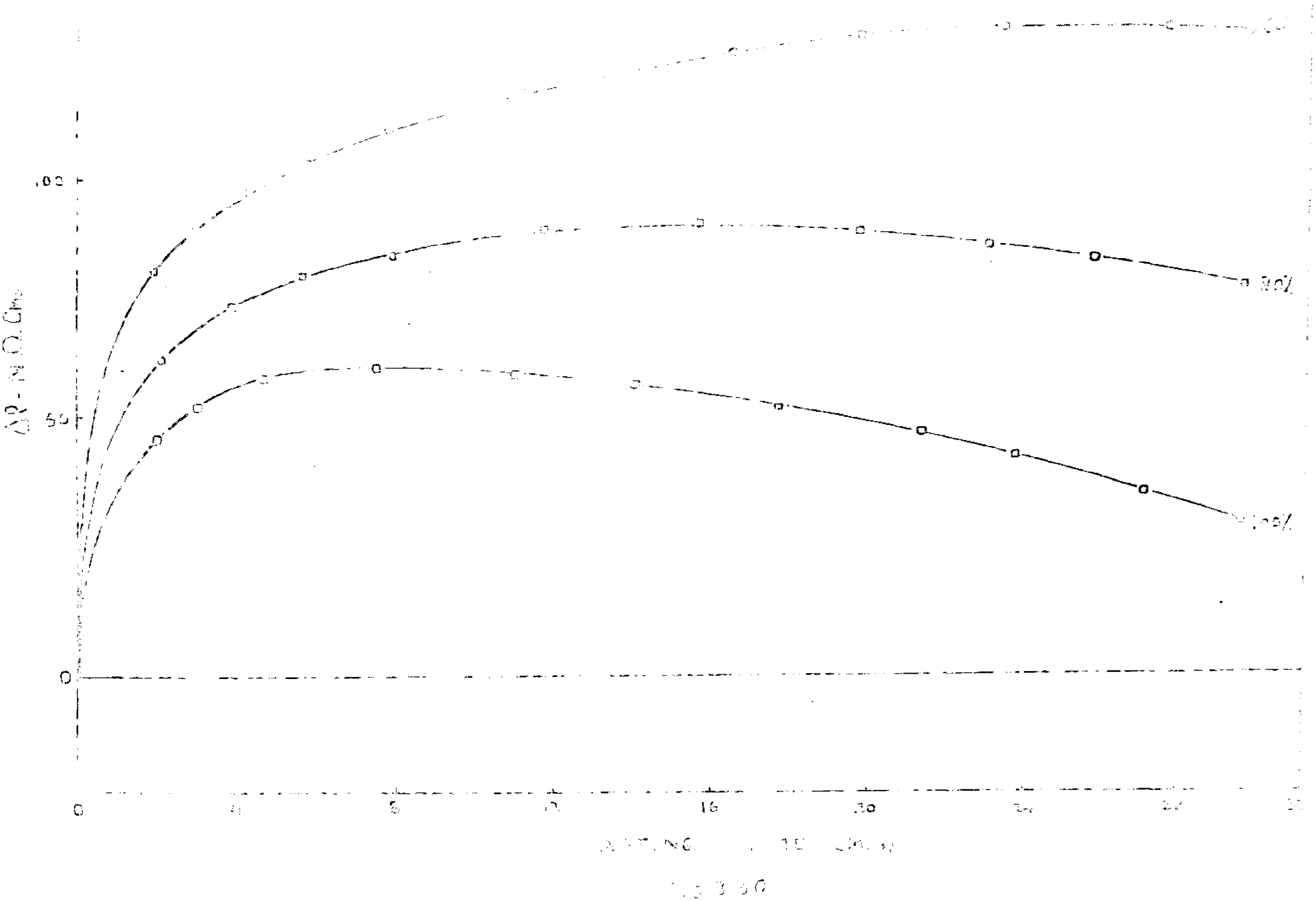
100
50
0
0
16
30

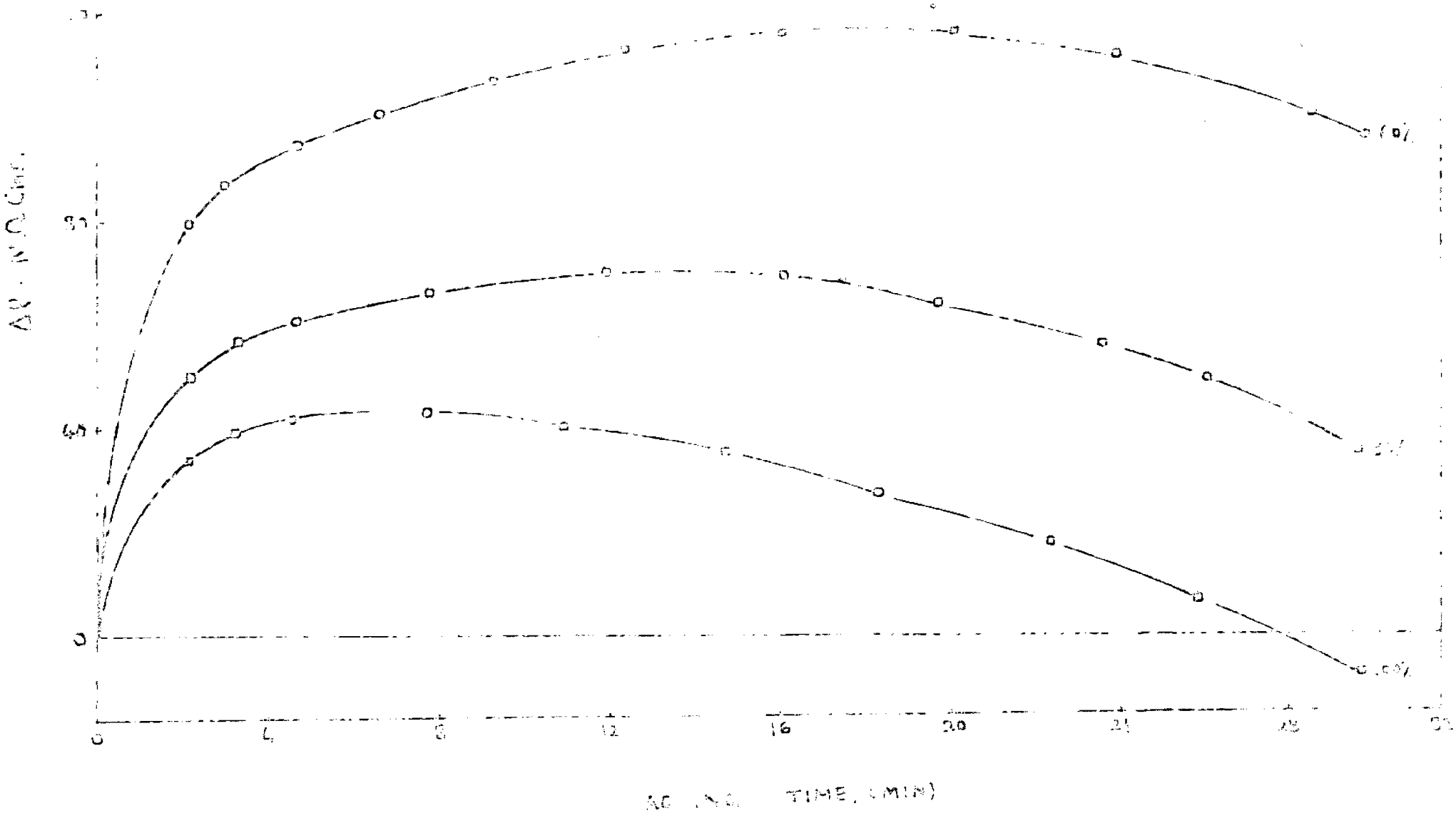
ΔP, IN. H2O (Gage)
0
4
8
12
16
20
24
28
32
TIME, (MIN)

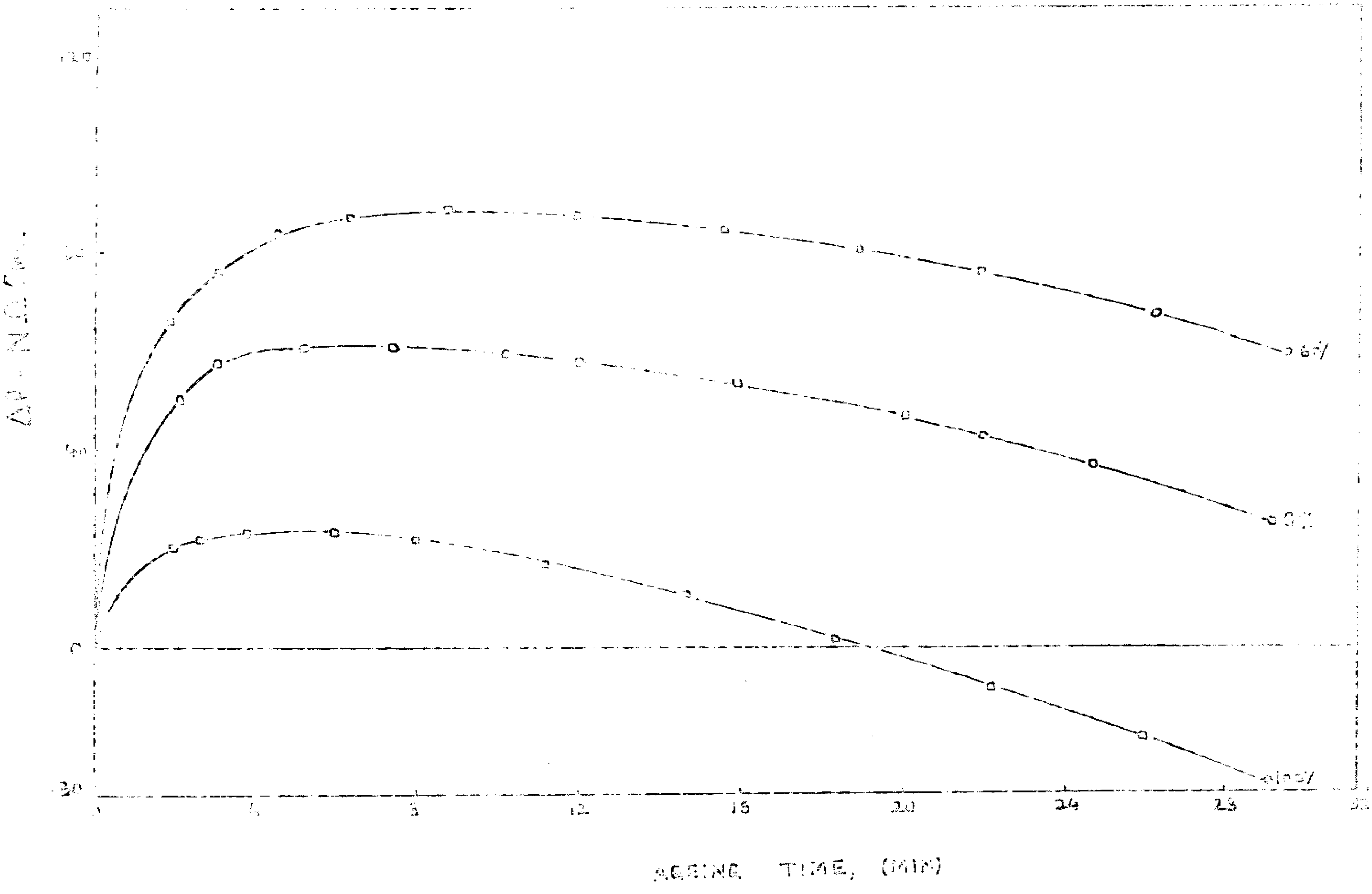

Fig. 3.32

D I S C U S S I O N

O F

R E S U L T S

4.0 Discussion of Results

Broadly speaking, the present work can be classified into two categories w.r.t. the ageing and re-ageing temperatures.

(A) Step ageing

(B) Partial reversion of G.P.zones

The alloys after homogenization and quenching were subjected to an ageing process at temperature T_A, for different lengths of time, given by five equal intervals of the resistivity peak, during primary ageing at T_A, and after the lapse of this time, called as pre-ageing time (t_{pA}), they were immediately subjected to a reageing operation at a temperature slightly above or below the ageing temperature T_A.

Now if, the reageing temperature was lower than the ageing temperature, the process is step ageing, and reageing temperature denoted as T_{RA}. And if the reageing temperature was above the ageing temperature, the process will result in the dissolution of a fraction of zones already formed at lower ageing temperature, with contemporary growth of the rest of the zones thermodynamically in equilibrium at the new reageing temperature. This process is termed as partial reversion of zones, and the re-ageing temperature denoted as T_R. Thus we conclude that the necessary conditions for for the two operations are :

(i) Step ageing if, $T_{RA} < T_A$

(ii) Partial reversion of zones if $T_R > T_A$.

The results obtained for these operations with various combinations of ageing and reageing temperatures in the present study were plotted on various figures as listed in Table III.

The results for step ageing, as well as for partial reversion of zones, are discussed on the basis of some fundamental established principles listed below:

(a) The average size of the zone (d_Z), reached after the lapse of a certain preageing time (t_{pA}) during ageing at T_A. The d_Z of the zones, gradually increases on ageing, and becomes practically constant, after a time almost equal to the average life time of vacancies, which in turn is influenced directly by the prevailing concentration of vacancies and their annihilation.

It has been assumed that by Mott's theory, the peak in resistivity is characterized by a critical scattering, at a critical zone size (d_C), which is approximately 10°A, thus the average size of zones is increasing or decreasing, through a peak in resistivity obtained at size d_C.

Further, it is clear that the time for reversion is directly related to the size of the zone, and thus to the preageing time (t_{pA}) with other conditions being similar. (Refer fig. 6.2 R.)

(b) There is an equilibrium number of zones (N_Z), having an average size 'd_T', which are in thermodynamic equilibrium at the ageing or reageing operational conditions.

This N_Z, is directly proportional to the degree of supersaturation, which is determined by the position of the metastable solvus line for G.P. zones. Thus the degree of supersaturation is directly related to the ageing temperature T_A. (or on T_{RA} or T_R for that matter), and hence, the N_Z also being directly dependent on T_A. Lower be the T_A, higher will be the supersaturation, and thus the N_Z value, and vice versa. In other words a lowering of T_A, will result in the growth of more number of zones, which are in thermodynamic equilibrium given by the T_{RA} or T_R, while raising the ageing temperature would result in dissolution of some of the zones, thus establishing a new number of zones determined by T_{RA} or T_R.

The development of a zone with average size (d_T) which is thermodynamically stable at a certain temperature, is influenced by the kinetics of the initial stages of ageing, and thus on T_H and T_A, which in turn controls the C_V, their annihilation, and the formation of secondary defects.

(c) As the ρ, of the alloy is a direct function of the number and size of the zones (thus their volume fraction), the height of the resistivity peak is directly dependent on the equilibrium number of zones, while its position is characterised by a critical scattering of electrons, at zone size d_C.

Now, N_Z is directly related to the T_A, the height of the resistivity peak is proportional to this N_Z value. In such a case,

the difference in the $\rho_{max.}$ at ageing and reageing temperatures is directly proportional to the difference in those temperatures. We summarise by saying, that peak heights of resistivity changes ($\Delta\rho$) versus reaging time, curves will be directly proportional to the <u>difference</u> ($T_A - T_{RA}$) <u>for step ageing</u> case and to the <u>difference</u> ($T_R - T_A$) <u>for partial reversion case</u>.

(d) The <u>slope</u> of the resistivity variation curves at instant t; ($d\rho / dt$), during reageing is a <u>kinetic term</u>, giving a hint about the rates of the process. Faster process will have greater slopes. Also a zero slope does not always means no reaction, but it may signify a balance in the two opposing effects contributing to the resistivity, as shall be discussed later.

(e) The ageing process is diffusion controlled, and hence, the migration of solute atoms, the concentration of vacancies and their annihilation (activational energies for formation and migration of vacancies) the interactions between the solute and the vacancies etc. are the factors governing the kinetics of the process. These factors govern the <u>slope</u> of the ageing curve, and also the <u>position</u> of the maximum.

The concentration of vacancies, & the preageing time, t_{PA}, is important for kinetics of the reageing process. With the lapse of t_{PA} the C_V is greatly reduced, and hence the <u>rates of the step ageing, as well as reversion</u> process is bound to be slower, with

its effects very clear during later stages of reageing, giving more or less horizontal curves. Explanations of the curves for various, t_{p_A} values (from 20 pct. to 100 pct. resistivity peak values), can be advanced in these terms. The times to attain resistivity peaks on step ageing process is much higher compared to that for ageing process.

(f) The variation in resistivity during the step ageing and specially during the reversion process, is a complex phenomenon and is the sum up of various factors contributing to the resistivity, as discussed below, taking the case of partial reversion:

i) In actual practice there is a distribution of zones of varying sizes in the vicinity of the average zone size, d_z. Thus, ρ is the sum up of the individual contributions of the zones of different sizes.

ii) There is a decrease in resistivity due to dissolution of a fraction of the zones lower than a temperature dependent critical size (d_T), which are thermodynamically unstable at reageing conditions. Thus a decrease in volume fraction of zones.

iii) An increase in resistivity, due to the growth of zones, with size above than those dissolving on reageing, as pointed out above. This gives rise in volume fraction of zones.

We conclude, that a net variation of resistivity during step ageing or reversion, will be the sum up of these factors. The individual contribution of these factors will determine the sum up curve, thus leading to an increase in ρ, if the factors contributing to the ρ increase over ride the factors contributing to the decrease in ρ, and vice versa. A horizontal portion of ageing curves may either signify the balance of the two opposing tendencies or a very slow reaction because a major part of vacancies has already been lost by that time because of lapse of t_{pA}.

Thus a complex phenomenon of step ageing or partial reversion can be comfortably explained in terms of above discussed and well established principles. In any of these operations, the tendency for the reaction is such as to obtain the new equilibrium state which is thermodynamically most stable under these conditions.

It will be more systematic to discuss the present results under two seperate headings of step ageing and partial reversion.

Step Ageing

Taking the case(similar to fig.1.10)where reageing is done at T_{RA}, after a specimen has been pre-aged at T_A, ($T_{RA} < T_A$), till peak in resistivity, we expect the following :

1) The average size of zones in the alloy pre-aged till peak (t_p) , at T_A has attained the critical scattering value, $d_c = 10^0 A$

Now reageing of this at a lower temperature T_{RA}, will result in further growth of these zones, thus contributing a decrease in ρ (curve B of fig. Q), which is actually the part of the ageing curve after the peak at T_A.

ii) An increase in ρ, due to increase in the equilibrium number of zones, which are expected to grow, due to lowering of the ageing temperature from T_A to T_{RA}, thus increasing the degree of supersaturation. This is shown by curve A of fig. Q, and represents the growth of new zones at reageing temperature.

iii) As the equilibrium number of zones is dependent on ageing temperature in this case the height of peak in curve A, is directly proportional to the difference in the equilibrium number of zones at T_{RA} minus those at T_A. Greater be the difference $(T_A - T_{RA})$, greater is the degree of supersaturation, and correspondingly the difference in the equilibrium number of zones, hence resulting in higher peaks for curve A.

iv) Times to peak in curve A is appreciably greater than compared to the time to peak for primary ageing at T_A, because of low C_V value, in the former case.

v) The net effect of these two factors, responsible for curve A and B, should be the curve expected on step ageing, which has been shown by curve C in fig. Q.

The sum up curve C, shows the peculiar nature of a rise, a flattened peak and finally a drop, corresponding to initially pre-dominating nature of curve A, while at later stages, the curve B pre-dominates.

vi) The reaction rates, as expected are much slower, because of considerable loss of vacancies during the pre-ageing stay time.

Now with this back ground, we shall take individual cases of step ageing, with their features and explanations.

Fig. 1.10 :- It may be observed that :

(i) For all values of t_{PA} from 20 pct. to 100 pct. there is an increase in resistivity, with least distinct peak in 20 pct. case. This is expected, because of the increase in volume fraction of zones, due to lower T_{RA}, compared to the T_A.

(ii) Rate of step ageing is faster in the case with lesser t_{PA}, because of high C_V left over with lesser pre-ageing.

(iii) A net increase in ρ, shows that the decrease of ρ, due to growth of zones, beyond size d_C, on re-ageing process is far less, than the increase due to growth of new number of zones.

(iv) The height of peak in 20 pct. case is greatest, because of maximum difference in the number of zones and the size of zones formed after 20 pct. pre-ageing time at 10^0C and those given by the peak at 0^0C.

Fig. 1.20 and 1.21 :- Basic arguments are similar as for fig.1.10 with a few new observations :

(i) Comparing the curves in fig.1.20 and 1.21, it is observed that the peaks are attained earlier, while reageing at $10^{0}C$, simply because of enhanced diffusion at $10^{0}C$, compared to that at $0^{0}C$.

(ii) A dropping of curves for 100 pct. case in later stages could be explained on the basis, that the zones which were previously growing have also attained resistivity critical size; d_c, by that time and they also contribute a decrease in resistivity. This also explains the appearance of earlier peaks in 100 pct. case compared to the 20 pct. cases in the same figure.

Fig. 1.30, 1.31 and 1.32 :- The nature of curves is similar to those obtained for step ageing in fig. 1.20. Here we note :

(i) In the case of fig. 1.32, the peaks are obtained earlier when we move from 100 pct. case towards 20 pct. case. This trend is also visible for curves in fig. 1.31 and 1.30. This is simply because of the earlier setting-in of the factors contributing to a decrease in ρ, in the case where the specimen has been already pre-aged so as to give high average zone size, prior to step-ageing. This is clear with the fact that the longer be the t_{p_A}, larger will be the average zone size prior to step-ageing.

(ii) A comparison of times to reach peak in 100 pct. cases, for

the figures 1.30, 1.31 and 1.32 show that peaks are earlier with higher re-ageing temperature, which is because enhanced diffusion with higher re-ageing temperature.

(iii) Slopes of the curves till lesser preageing time is steeper in each figure, and this is because of high concentration of vacancies with lesser preageing times.

(iv) Sloping down of curves with higher preageing times, is prominent in all these figures, which is still clear in figures with higher reageing temperatures. These could be explained on the quicker attainment and growth of zones, which had already attained since near to resistivity peak, when they are subjected to higher reageing temperatures.

(v) The crossing of zero reference line at an earlier time in 100 pct. case than in 80 pct. case, is due to larger prior zone size in 100 pct. case. A value lower than the zero reference line indicates that the zones have grown to such a size, where their contribution to resistivity is lesser than that just after preageing.

Effect of T_H:- Upto now the only variables were the ageing temperature and the reageing temperature with different preageing times. The nature of the curves obtained with different T_H values is similar to those obtained in figures with T_H = 300°C, already discussed above. For the effect of T_H , we shall, as an example

compare the figures 1.10, 2.10 and 3.10:

(i) For a certain pre-ageing time, for the above three cases, there is only a slightly higher peak with higher T_H value, but this effect is not very appreciable. This probably due to higher concentration of quench-in vacancies with higher T_H value.

(ii) For the initial rates of reageing in the above three cases, it can be observed that the rates of stepageing are faster in the case which has highest T_H. Again this is probably due to higher concentration of vacancies with higher T_H values.

The effect of T_H, can also be similarly explained while comparing the figures 1.30, 2.30 and 3.30.

Partial Reversion of Zones

Taking a case similar to figure 1.01, where an alloy has been aged at T_A and reaged at T_{RA}, $(T_R > T_A)$, we observe :

(i) A decrease in resistivity due to growth of those zones at T_R which had already attained a resistivity critical size at T_A. This has been shown by curve A of fig.R; and is actually, the part after the peak, of the ageing curve at $0^{\circ}C$.

(ii) A decrease in resistivity due to decreasing volume fraction of zones, because of equilibrium number of zones at T_R is much less than that at T_A, thus resulting in dissolution of a fraction

of zones. This is given by curve B of fig. R.

(iii) On prolonged reageing at T_R, there is possibility that the zones with size larger than those thermodynamically stable at T_R, may grow, thus contributing an increase in resistivity.

(iv) Thus the net sum of these factors will give the resultant, partial reversion curve 'C', which shows a gradual decrease in resistivity on reageing.

(v) As should be expected, the maximum drop in resistivity will be observed in the reversion operation in which the degree of supersaturation is greatly reduced, i.e. greater be the(T_R-T_A) value, greater the depth of reversion curves, as this is directly related to the ratio of the equilibrium number of zones given by the peaks of the ageing curves at T_R and T_A respectively.

(vi) One should expect the rates of reaction for lower t_{PA} to be faster because of high concentration of vacancies with lesser t_{PA}.

Now we shall discuss individual cases of reversion.

Fig. 1.01:- We observe following features in 100 pct. preageing:

(i) A decrease in resistivity due to growth of those zones at T_R which have already attained critical scattering size during preageing, till the peak in resistivity.

(ii) A decrease in resistivity due to dissolution of a fraction

---

of zones, because equilibrium number of zones at 10°C is lower than that at 0°C

Both of these factors contribute in decreasing the ρ, hence the sum up curve also shows a continuous decrease on reageing.

In 20 pct. preageing case, we observe a decrease followed by an increase and finally not very distinct peak, which is explained in following terms:

(i) Probably, before crossing the zero reference line, the dissolution of zones is the predominating reaction, resulting in a net decrease in resistivity.

(ii) After some time, the increase in volume fraction of zones, due to their growth at $10^{o}C$, overrules the decrease in volume fraction of the zones dissolving, thus giving a net increase.

It is seen that the greatest decrease is shown by the 100 pct. case, in which both the factors, discussed earlier, contribute a decrease in resistivity whereas in cases with lesser preageing stay, dissolution of already formed zones takes lesser time, and the curves cross zero line after some time, which is quicker for 20 pct. case compared to the 40 pct. case.

Fig. 1.02 and 1.03:- These are explainable on the similar lines as for fig.1.01 with additional features as:

(i) Comparing the curves for fig. 1.01, 1.02, and 1.03, it is observed that the magnitude of decrease in resistivity, is highest for reageing at $30^{o}C$, obviously because of higher difference in $(T_R - T_A)$, as we raise the reageing temperature from $10^{o}C$ to $30^{o}C$.

(ii) Further, the crossing of the zero line for curves with

lesser t_{PA}, is earlier, because of earlier superseeding of the factors contributing an increase in ρ. (i.e. growth of zones at T_R).

(iii) The peaks after the initial decrease, are observed earlier, with a rise in reageing temperature, because of increased diffusional properties with higher reageing temperatures.

Fig. 1.12 to 1.13 :- Here again curves are almost similar in nature to those in fig. 1.02. In the case of fig. 1.13 even with 20 pct. case, the initial decrease followed by an increase has been eliminated, because of the fact that the degree of supersaturation is lesser for reageing at 30°C compared to, reageing at 20°C.

Fig.1.23 :- Here the flatness of almost all the curves is probably due to loss of a considerable fraction of vacancies during t_{PA}, in the alloys preaged at a higher temperature i.e. 20°C, compared to the case of preageing at 10°C or 0°C. Here the flatness of the curves is more likely due to concentration of vacancy effect, rather than the balance of two opposing factors contributing to ρ :

Effect of T_H :- It may be observed that there is no major change with respect to the nature of curves, due to variations in T_H, if we compare the respective figures for reversion, with different T_H values e.g. comparing the figures 1.03, 2.03 and 3.03, it may be observed that :

(i) The rates of reageing are somewhat slower, in the cases, with lesser homogenization temperature. This effect is due to

the variation of concentration of quench-in vacancies.

(ii) Because of the higher concentration of quench-in vacancies with higher homogenization temperatures, thus resulting in faster reaction, it is observed, that almost each stage of the curves becomes more prominent. This will be clear, if we compare the curves for 20 pct. preageing time, in the figures 1.03,2.03 and 3.03.

It is concluded, that the explanations for various step-ageing and partial reversion of zones, employed in the present study, can be satisfactorily advanced in terms of the established principles enumerated in the beginning of the discussions.

Further, the discussions of the step-ageing processes in greater detail taking the case similar to fig. 1.10, makes clear all relevant features of such a process.

Similarly a detailed discussion of the partial reversion process, taking the case similar to fig.1.01, can be used for the understanding of the other reversion processes employed in the present study.

The apparent activational energies for the migration of vacancies E_{II}, were calculated, from the data of fig.1.0, 2.0 and 3.0 . The results are listed below:

Homogenization temperature (T_H°C)	Value of E_{II}
300°C	0.42 eV.
350°C	0.40 eV.
400°C	0.35 eV.

The increase in the E_{II} values, with increasing T_H, can be explained on the basis of the effects of T_H, on the concentration and role of vacancies. With increasing the homoginization temperature, the proportion of di-vacancies, which have a lower activational energy for migration, compared to that for a single vacancy increases. Hence, lesser proportion of single vacancies, with increasing homoginisation temperature is the probable cause for decrease in values of E_{II}.

5.0 CONCLUSIONS

There are many aspects of the ageing mechanism which are confirmed by the present study.

The role of quench-in vacancies appears to be the most important factor in governing the various aspects of ageing. The much slower rates during re-ageing are explainable in terms of the prevailing concentration of vacancies, the diffusional controlled processes of migration of solute atoms, and annihilation of vacancies at the temperature of ageing or re-ageing.

It has been possible to explain the results of the present work on the established understanding about the size of the zones, the dependence of their equilibrium number on the ageing temperature, and the observance of a peak in resistivity at a critical zone size.

Further, the results have been explained on the proposed theory that there is a temperature dependance of the size of the zones with respect to their thermodynamic stability at this temperature.

The apparant, activational energy, E_H for the migration of vacancies, was calculated to be, 0.42 eV, 0.40 eV and 0.35 eV for the homogenization temperatures, 300°C, 350°C and 400°C respectively.

6.0 SUGGESTIONS FOR FURTHER WORK

Keeping in view the significance of the present work, in better understanding of the pre-precipitation stage of ageing, a further advanced work is suggested on the following guidelines:-

1. Electrical resistivity studies should be supported by electron diffraction, X-ray intensity, and small angle X-ray diffraction studies for still better understanding of the [illegible], size, shape, number and distribution of clusters and zones.
2. The effect of solute concentration can be studied.
3. Similarly the effect of ternary additions (trace additions) can be undertaken.
4. The study can be extended to sub-zero temperatures, so as to make the processes slower, which can be more conveniently studied.
5. There is the unexplored aspect with respect to the determination of the activational energies of the reageing processes (step-ageing and reversion of zones) as has been hinted in Ref.(44).

7.0 REFERENCES

1. Wilm, A., Metallurgie, 8, (1911) 225.
2. Wilm, A., Metallurgie, 8, (1911) 650.
3. Merica, P.D., Walternberg, R.G., and Scott, H., Trans. Met. Soc. A.I.M.E., 64, (1921) 3.
4. Knno, S., Science Reports, Tohuku Imperial University, 11(1922) 269.
5. Frankach, U., and Schweizer.E., Z. Metallk, 14 (1922) 49.
6. Gaylor, M.L.V., and Preston, G.D., J. Inst. Metals, 41 (1929) 191.
7. Rosenhain, W., J. Inst. Metals, 44 (1930) 226.
8. Tammann, G., Z. Metallk, 22, (1930) 365.
9. Merica, P.D., Trans. Met. Soc. of A.I.M.E., 99 (1932) 131.
10. Jenkins, C.H.M., and Buckmall, E.M., J. Inst. Metals 57 (1935) 141.
11. De Sorbo, W., Treaftis, H.N. and Turnbull, D., Acta. Met. 6 (1958) 401.
12. Turnbull, D., Rosenbaum, H.S., and Treaftis, H.N., Acta. Met. 8 (1960) 277.
13. Guinier, A., Acta. Met. 3 (1955) 510.
14. Guinier, A., X-ray diffraction, W.H.Freeman, San-Francisco, 1963.
15. Gerold, V., Phys. Status Solidi, 1, (1961) 37.
16. Guinier, A., Ann. Physique, 12, (1939) 161.
17. Preston, G.P., Proc. Royal Society A 161, (1938) 526.
18. Borelius, G., Defects in Crystallin Solids, Physical Society p.169, (1955).
19. Borelius, G., Larsson, L.E., The mechanism of phase transformation in metals., J. Institute of Metals. p 285, (1956).
20. Herman, H., and Cohon, J.B., Nature, 191, (1961) 63.
21. Haberkron, H., and Gerold, V., Phys. Status Solidi, 15, (1966) 167.
22. Hirsch, P.B., and Kelly, A., Phil. Mag. 12, (1965) 881.
23. Harkness, S.D. and Hron, J.J., Trans. Met. Soc. A.I.M.E.

24. Nabarro,F.R.N., Proc. Roy. Soc. A52 (1940) 90.
25. Nabarro,F.R.N., ibid., A175 (1940) 519.
26. Mott, N.F., and Nabarro,F.R.N., Proc. Roy. Soc. 52 (1940) 86.
27. Baker, R.G., Bradon, D.G., and Nutting, J., Phil. Mag.[8] 4 (1959) 1339.
28. Turnbull,D., Solid State Physics, 3, (1956) 226.
29. Zener, C., Proc. of Int. Conf. on Physics of Metals. Amsterdam(1948),p 117.
30. Seitz,F.,L'Etat Solide, Inst. Int. Phys. Solray,(1952) 401.
31. Federighi,T., Acta. Met. 6, (1958) 379.
32. Lomer,W.M., Vacancies and other defects in Metals and Alloys J. Inst. of Metals, (1958) 79.
33. Pensari, C, and Federighi, T., Phil. Mag. [8] 3 (1958) 1223.
34. Hart, E.W., Acta. Met. 6, (1958) 553.
35. Federighi, T., and Thomas, G., Phil. Mag. [8] 7 (1962) 127.
36. Gerold, V., and Schweizer,W., Z. Metallk 52, (1961) 76.
37. Walker, C.B., and Guinier,A., Acta. Met. 1,(1953) 568.
38. Garf,R.,Comptes Rendus 249 (1959) 1110.
39. Friedel,J., Les Dislocations, Gauthoir Villars, 1956.
40. Brooks,H., Metal interfaces, Trans. Amer. Soc. of Metals. (1952) 20.
41. Guinier, A., Acta. Cryst. 5 (1952) 51.
42. Bradshaw, F.S., and Pearson,S., Phil. Mag.[8] 2 (1957) 94.
43. Webb, W.B., Acta. Met. 7, (1959) 748.
44. Pensari, C., and Federighi,T, Acta. Met. 8 (1960) 217.
45. Westmacott, K.H., Barnes, R.S., Hull,D., and Smallman,R.E., Phil. Mag.[8] 6 (1961) 929.
46. Mott, N.F., J.Inst. Metals, 60 (1937) 267.
47. Geisler,A.H., Phase transformations in solids,(1951) 387.
48. Pine, W.E., Acta. Met. 7 (1959) 228.
49. Labusch. Phys. Status. Solidi 3 (1963) 1661.
50. Matyas, Z., Phil. Mag.[7] 40 (1949) 324.
51. Woodles, ibid, [7] 40 (1950) 31.
52. Simeroka and Synock, Acta. Met. (1957) 223.
53. Fink,W.L., and Smith, D.W., Trans. A.I.M.E. 124 (1937) 162.
54. Garf,R. and Lenormand, Acad. Sci., Paris (1964) 3494.
55. Morta, Anantharaman, T.R., and Gerold,V., Phys.Status Solidi 8 (1965) 5.

56. Garwood, R.D., Davies, A.L., and Richards, G.L., J. Inst. Metals 88, (1959-60) 311 and 375.
57. Garf, R., Journal Physics, Paris 22 (1962) 819.
58. Geisler, A.H., Barrtt, C.S., and Hohl, R.F., Trans. A.I.M.E. 152 (1943) 201.
59. Baur, R., and Gerold, V., Z. Metallk, 52 (1961) 671.
60. Baur, R., and Gerold, V., Acta. Met., 10 (1962) 637.
61. Carpenter, A., and Garwood, R.D., J. Inst. Metals 94, (1966) 301.
62. Larsson and Lasek, ibid. , 95 (1967) 320.
63. Nicholson, R.B., and Kelly, A., Progress in Metal Phys. VOL.10, Edited by Bruce Chalmers.
64. Dash, J., and Fine, M.E., Acta. Met. 9 (1961) 149.
65. Katz, K.I. and Herman, H., Mat. Sc. Engg. 1, (1966) 162.
66. Borelius, G., J. Inst. Metals. 3 (1951) 477.
67. Johnson, A.A., Huges and Barton., ibid., 94 (1966) 186.
68. Strongin, B.G., Phys. Met. Metallography, 23(2), (1967) 55.
69. Vahi, R.P., and Anantharaman, T.R., Current Science, 28, (1969) 1.
70. Rao, K., Herman, H., and Parche, Mat. Sc. Engg., 1, (1966) 162.
71. Ellwood's, A., J. Inst. Metals. 80, (1951) 217.
72. Cohen, J.B., Trans. A.I.M.E., 242 (1968), 166.
73. Rudman and Hillard, H, Acta. Met. 15, (1967) 1023.
74. Gaylor, M.L.V., Jr. Inst. Metals, 28, (1922) 213.
75. Dehlinger, V., and Knapp, H., Z. Metallk, 43, (1952) 223.
76. Silcock, J.M., Heal, and Hardy, J. Inst. Metals. 82, (1953) 239.
77. Knobeevski, S.T., ibid., 69 (1943) 397.
78. Garf, R., ibid., 86, (1957-58) 534.
79. Borelius, G., Vootensk, Acad. Handl, 169, (1943) 177.
80. Richards and Garwood, R.D., J. Inst. of Metals, (1965) 393.
81. Perry, P., Acta. Met., (1966) 1143.
82. Asdente, M., Acta. Met. (1961) 587.
83. Entwisttle, and Perry., J. Inst. Metals (1966) 24.
84. Murakami, Kawano and Murakami, Acta. Met. (1969) 29.
85. Smugesky, Herman and Pollack, ibid., (1969) 883.
86. Wilkes, ibid., (1968) 863.
87. Larsen, Acta. Met. (1967) 55.
88. Herman, H., ibid., (1967) 154.

89. Horman,H., Cohon, J.B., ibid., (1963) 43 ,
90. Poderighi,T., and Ponsari,C., Acta. Met. (1969) 422.
91. Murakami, Kwano, and Murakami, Trans. A.I.M.E.(1969) 815.
92. Markons,S.D., Hron,J.J., Met. Trans.(1970) 43.
93. Lipsit, H., Metallurgical Transactions, (1971) 1739.
94. Ciach,R., Scripta Metallurgica, (1970) 39.
95. Raman,K.S., ibid., (1970) 197.
96. Bohn,G., and Gerold,V., ibid., (1970) 269.
97. Chatterjee,A. and Fabian,D.J., ibid., (1970) 285.
98. Ramchandran,V., and Srinivasan, N.K., ibid., (1967) 103.
99. Raman, K.S., ibid., (1971) 791.
100. K.Krishna Rao, Katz,V.I., and Herman,H., Met. Sc. Engg., 28, 1, (1966-67) 263.
101. Raman,K.S., Das,E.S.D. and Vasu,K.I., J. Met. Sc. (1970) 5.
102. Shee,S.K., Vghi,R.P., and Misra,S., J. Indian Institute of Metals, (1967) 148.
103. Kots,L.E., Rao, K.K., and Herman,H., ibid., (1966) 95.
104. Vahi,R.P., and Anantharaman,T.R., ibid., (1966) 41.
105. Vahi,R.P., and Anantharaman,T.R., ibid., (1971) 61.
106. Vahi,R.P., Kutumba Rao, V.U.P., and Anantharaman, ibid., (1970) 20.
107. Carpenter and Garwood,R.D., Met. Sc., Engg., 1 (1967) 202.
108. Hardy and Heal, Report on precipitation, Prog. Metal Phys.V-5.
109. Smith,G.C., Age Hardening of Metals, Prog. Metal Phys. V-1.
110. Kimura,H, Hasiguti,R.R., Acta. Met. 9 (1961) 1076.
111. Gould, R.V., J. Inst. Metals, (1971), 1.
112. Murakami, Kawano, and Murakami, ibid., (1971) 160.
113. Rao,K., and Herman,H., ibid., (1966) 180, 420.
114. Garf,R., ibid., (1950) 282.
115. Price and Kelly, ibid., (1950) 425.
116. Rao, and Herman, J. Inst. Metals , (1966) , V-94 , p320.
117. Herman,H., Metallurgical Transactions , (1971), 16.

NOTATIONS

T_H - Homogenisation Temperature

T_A - Ageing Temperature

T_{RA} - Re-ageing temperature for stop-ageing case

T_R - Re-ageing temperature for reversion case

t_p - Time required to reach peak in resistivity

t_{PA} - Pre-ageing time

E_M - Activational Energy for migration of vacancies

E_F - Activational Energy for formation of vacancies

D_S - Diffusion Coefficient of solute atom in solvent matrix

E_{S-V} - Interaction energy between solute and solvent

δ - Atomic mismatch between solute and solvent atoms.

C_V - Concentration of vacancies .

γ - Interfacial energy between zones and matrix

ρ - Electrical resistivity of alloy

$\rho_t(T)$ - Resistivity at instant t after quenching while ageing at T°C

G . modulus of rigidity